The Impact of Loss of Function Mutations of NHEJ Genes on Gene Targeting and DNA DSB Repair in Human Somatic Cells

A DISSERTATION
SUBMITTED TO THE FACULTY OF THE GRADUATE SCHOOL OF
UNIVERSITY OF MINNESOTA
BY

Farjana Jahan Fattah

IN PARTIAL FILFILMENT OF THE REQUIREMENTS FOR THE
DEGREE OF
DOCTER OF PHILOSOPHY

Eric A Hendrickson, PhD
Advisor

April 2009

Acknowledgements

First and foremost, I would like to express sincere gratitude to my supervisor, Dr. Eric Hendrickson for his guidance and support throughout my graduate student years in his laboratory. I truly appreciate his encouragement, which has been tremendous help at times of my struggles. It allowed me to pursue challenging and interesting scientific projects and to become a better scientist. I also thank him for his unlimited patience, his understanding of my struggles of being a mom during my PhD thesis.

I would like to thank all past and present members of Hendrickson laboratory with whom I have had the pleasure of working. Special thanks to Brian Ruis, Youngbao Wang, Natalie Lichter, Natalie Weisensel, Euhan Lee, Sehyun Oh, Junghun Kewon, Gautom Ghosh and Riaz Fattah for all their selfless assistance, stimulating discussions, advices, and friendship during my years in Hendrickson Laboratory.

My special thanks goes to all the past and present members of Bielinsky, Livingstone and Harris Laboratory.

I would also like to thank the members of my thesis committee, Dr. Dennis Livingston, Dr. Jeff Simon, Dr. Michael O'Connor and Dr. Duncan Clark for their critical reviews of my scientific progress and their helpful suggestions.

I thank everyone in the Department of Biochemistry, Molecular Biology and Biophysics, University of Minnesota for all their help over the years and Graduate shool for 'Doctoral Dissertation Fellowship'.

Finally, I would like to thank my husband, Riaz Fattah, for his endless support and encouragement during the difficult times of my graduate study and my son, Raiyan, for the happy days that he has provided me with. I would like to thank my family specially my parents, my in-laws, and my brother and sister-in-laws, who have supported and encouraged me during the course of my PhD.

Dedication

To my parents

ABSTRACT

Non-homologous end-joining (NHEJ) is the predominant repair pathway for DNA double-strand breaks (DSBs) in human cells. The core NHEJ pathway is composed of seven factors: Ku70, Ku86, DNA-PK_{cs}, Artemis, XRCC4, XLF and LIGIV. Mutation of any one of these NHEJ genes leads either to death, profound immune deficiencies, ionizing radiation sensitivity and/or cancer predisposition in human patients. We attempted to generate Ku70-null human somatic cells using a rAAV-based gene knockout strategy. Our data demonstrated that Ku70 is an essential gene in human somatic cells. More importantly, however, in $Ku70^{+/-}$ cells, the frequency of gene targeting was 5- to 10-fold higher than in wild type cells. RNA interference and short-hairpinned RNA strategies to deplete Ku70 phenocopied these results in wild-type cells and greatly accentuated them in $Ku70^{+/-}$ cell lines. Thus, Ku70 protein levels significantly influenced the frequency of rAAV-mediated gene targeting in human somatic cells.

XLF is the newly identified core factor for NHEJ. To characterize XLF function in human cells, we knocked out XLF gene in HCT116 cells. XLF deficient cells are highly sensitive to ionizing radiation and DNA damaging agent, and have intrinsic DNA DSB repair defects. In V(D)J recombination assay, we find that XLF deficient cells have dramatic defect to form both V(D)J coding and signal joints. The phenotypes of XLF deficiency were rescued by a WT XLF cDNA over-expression. We conclude that, in humans, XLF is essential for C-NHEJ mediated repair of DNA-DSBs.

Biochemical and genetic studies in mouse and hamster cells showed that DNA ends can also be joined via a backup pathway, especially when proteins responsible for NHEJ, are reduced or absent. In order to get insights in to backup NHEJ mechanism, we employed a reporter system based on the *in vivo* rejoining of cohesive and incompatible ends. We report here more than 10 to 20 fold reduction in NHEJ proficiency in DNA-PK_{cs}, XLF and LIGIV null human cells, which is characterized by an increase in microhomology use. Strikingly,

conditional knock-out of Ku86 did not result in defect in end-joining, while having an impact on repair fidelity.

TABLE OF CONTENTS

LIST OR TABLES

LIST OF FIGURES

CHAPTER I

INTRODUCTION

Among the many forms of damage that can cause chromosomal instability, DNA double-strand breaks (DSBs) seem to be the most dangerous and a single unrepaired DSB appears to be sufficient for inducing apoptosis (295). DSBs occur when the sugar backbones of both strands are broken close enough to disrupt Watson-Crick base pairing, resulting in the liberation of two dsDNA ends. Because the liberated ends can physically separate from each other & because there is no template with which to direct accurate repair, DSBs are among the most severe type of DNA damage and among the most difficult to repair. Ironically, these lesions occur with some frequency as they can arise exogenously from factors such as ionizing radiation (IR) exposure or endogenously from factors such as oxidative damage (17). In addition, DSBs can also arise during DNA replication; when a replication fork passes through a template that contains a single-stranded break, the break will be converted into a DSB on one of the sister chromatids (140, 145). DSBs also occur naturally as intermediates in several essential cellular processes. Notably, they are intermediates during recombination in meiosis (69), a process which is necessary for germ-cell development. In addition, DSBs are generated during the assembly of mature immunoglobulin (Ig) or T-cell receptor (Tcr) genes by V(D)J recombination and during Ig heavy chain (IgH) class switching. It is thus very clear that DSBs can occur by various means and at different stages of the cell cycle.

DSBs are particularly dangerous lesions if they occur during the replication of the genome and during the segregation of duplicated chromosomes into daughter cells. Proper genome duplication is hampered by DSBs, and if broken chromosomes are carried through mitosis, the acentric chromosome fragments will not partition evenly between daughter cells. Therefore, eukaryotes have developed several checkpoints to prevent cells from starting DNA

replication (the G1/S checkpoint), from progressing through with replication (the intra S checkpoint) or from proceeding into mitosis (the G2/M checkpoint), if they contain a DSB (3, 137, 139).

DNA DSB repair pathways

There are two main pathways for DNA DSB repair — homologous recombination (HR) and non-homologous end-joining (NHEJ). These pathways are largely distinct from one another and function in complementary ways to effect DSB repair (53, 75, 110, 168, 276, 317) Whereas HR ensures accurate DSB repair, NHEJ does not. The relative contribution of these two DSB-repair pathways is likely to differ depending on the stage of the cell cycle (75, 276). However, the pathways are not mutually exclusive because repair events that involve both pathways have been described (236). During HR, the damaged chromosome enters into synapsis with, and retrieves genetic information from, an undamaged DNA molecule with which it shares extensive sequence homology. In contrast, NHEJ, which brings about the ligation of two DNA molecules without the requirement for extensive sequence homology between the DNA ends, does not need synapsis of the broken DNA with an undamaged partner DNA molecule. Both pathways are highly conserved throughout eukaryotic evolution but their relative importance differs from one organism to another. Simple eukaryotes such as the yeasts *S. cerevisiae* and *S. pombe* rely mainly on HR to repair radiation-induced DNA DSBs. In contrast, in mammals the NHEJ pathway predominates in many stages of the cell cycle — particularly in G0 and G1 — although HR is also of importance, particularly during S- and G2-phases (131).

Homologous Recombination (HR)

The molecular basis and genetic requirements of HR were initially defined by studies in bacteria and yeast but it has become clear that this pathway is well

conserved in higher organisms. In brief, genetic analysis of *S. cerevisiae* identified a set of genes — *RAD50*, *RAD51*, *RAD52*, *RAD54*, *RAD55*, *RAD57*, *RAD59*, *MRE11* and *XRS2* — whose products play important roles in HR and whose defects lead to increased sensitivity to IR. Mammalian homologues of essentially all of these factors in the "RAD50 group" have now been described (311, 317). HR is complex and — based on analyses of HR under various biological circumstances and in different organisms — there are several models for precisely how HR takes place (53). An early event in yeast HR is believed to be the nucleolytic resection of the DNA DSB in the 5' to 3' direction. The efficiency of this reaction *in vivo* relies upon, and probably involves, a complex containing Rad50p, Mre11p and Xrs2p (NBS1 in humans). The ensuing 3'-single-stranded DNA tails are then bound by Rad51p in a process that is influenced by other proteins, including replication protein A (RPA), Rad52p and Rad54p. Notably, human RAD52 has been shown to preferentially bind to DNA DSBs, leading to the proposal that competition between it and Ku for DNA ends may determine which of the two DSB repair pathways is employed (294). The Rad51p nucleoprotein filament then interacts with an undamaged DNA molecule and, when a homologous region has been located, Rad51p catalyzes strand-exchange events in which the damaged molecule invades the other DNA duplex, displacing one strand as a D-loop. These events are influenced by the other members of the RAD50 group of proteins and by other factors such as RPA. The 3' terminus of the damaged DNA molecule is then extended by DNA polymerase that copies the missing information from the undamaged partner, and the ends are subsequently rejoined by DNA ligase I. Finally, after migration, the DNA crossovers (Holliday junctions) are resolved by cleavage and ligation to yield two intact DNA molecules. Although HR is generally accurate and non-mutagenic, an exception to this can occur when direct repeats flank the two DNA ends. In this case, HR by the pathway of single-strand annealing may lead to loss of one of the two direct repeats and the intervening DNA (110).

Although mammalian homologues exist for all of the known *S. cerevisiae* HR factors, the details of HR are likely to be considerably more complex in higher eukaryotes. One indication of this is the existence of several RAD51 paralogues, such as RAD51B, RAD51C and RAD51D, and other proteins with weaker homology to the catalytic domain of RAD51, such as XRCC2 and XRCC3 (311). At least some of these factors interact directly with RAD51 and their function appears to be to help in the assembly of the RAD51 nucleoprotein filament and/or in the selection of and interaction with the appropriate recombination substrate. Indeed, where analyzed, these factors have important roles in the HR process. Recent work has established strong links between HR and the breast cancer susceptibility proteins, BRCA1 and BRCA2, which do not appear to have direct homologues in yeast. Specifically, loss of function of either BRCA1 or BRCA2 in mammalian cells markedly reduces the efficiency of accurate homology-directed DNA repair (202, 203, 266, 318). Furthermore, mutation of BRCA2 stimulates error-prone homology-directed repair of DNA DSBs that have been generated between repeated sequences (287). It is not yet clear exactly how these effects are brought about but they may reflect the binding of BRCA1 and BRCA2 to RAD51. Indeed, BRCA2, through its BRCT motifs directly interacts with RAD51 thereby affecting both the nuclear localization and DNA binding properties of RAD51 (58) and permitting RAD51 to form foci at sites of DNA damage within the cell (42, 257, 329). The presence of BRCA1 in complexes involved in chromatin remodelling and/or the control of transcription (21, 256) raises the possibility that it may also affect HR by changing chromatin structure at the sites of DNA DSBs or that it could influence HR indirectly through its involvement in the transcriptional responses to DNA damage.

Loss of HR in vertebrate cells leads to an inability to successfully traverse S-phase, and this is probably due to an inability to restart replication at sites where DNA replication forks have collapsed as a consequence of encountering

endogenously generated lesions such as DNA single-stranded breaks. This model explains why the inactivation of genes such as *RAD51*, *BRCA1* and *BRCA2* leads to the death of vertebrate tissue culture cells and to early embryonic lethality in the mouse (171, 260, 267, 286). The inviability of vertebrate cells disrupted for *MRE11*, *RAD50* or *NBS1* may also be related to defects in HR (180, 319, 320, 336). Nevertheless, hypomorphic mutations or conditional alleles of the above genes have been described that allowed for cellular viability and, in some cases, the development of mice to maturity. For instance, mice bearing one truncation mutation of Brca2 are small and radiation sensitive and have an increased incidence of thymic lymphoma (51, 221). Cells bearing this or another truncation mutation were shown to be radiosensitive, to display high levels of spontaneous chromosomal rearrangements and/or to senesce prematurely in culture (198, 326). It should be noted, however, that HR can be involved in mechanisms of telomere maintenance (in mammals, called the alternative lengthening of telomeres (ALT) pathway) that do not rely on telomerase (72, 149). It is therefore possible that some of the phenotypic effects of loss of HR factors could reflect deficiencies in telomere metabolism. Confusingly, however, not all HR genes are essential. A good example of this is provided by *RAD54* mutant mice or chicken DT40 B-cells in which the *RAD54* gene has been homozygously disrupted. These animals and cells, respectively, are radiosensitive and have reduced rates of HR but are viable (74, 276). Furthermore, when these mutations are combined with deficiencies in Ku, this results in even greater radiosensitivity than either of the single mutants, thus providing strong support for the idea that HR and NHEJ act in complementary ways to repair radiation-induced DNA damage in vertebrates (75, 276). In addition, DT40 cells lacking RAD51B or mouse cells lacking *XRCC2 or XRCC3* are all viable and have reduced rates of HR and high levels of chromosomal aberrations and/or mis-segregation of chromosomes at mitosis (60, 103, 132, 174, 226, 275, 277). Homologous recombination thus clearly plays very

important roles in maintaining the genomic integrity in a variety of organisms.

Finally, recent data reveal links between the ATM- and ATR-dependent systems of DNA-damage signaling and the activation of the HR pathway. For example, work in the chicken DT40 system has shown genetically that ATM functions, at least in part, by affecting the HR pathway (200). Further evidence for such a link is provided by the findings that a subgroup of A-T patients do not have mutations in ATM but instead bear hypomorphic mutations in *MRE11* (272) and that hypomorphic defects in NBS1 cause the related human disorder, Nijmegen breakage syndrome (NBS) (36, 297). These diseases are characterized by radiosensitivity and defects in the intra-S-phase DNA-damage checkpoint. The latter appears to be dependent on the phosphorylation of NBS by ATM in response to DNA DSBs (89, 172, 315, 333); for a review see (225). In addition, it seems likely that the lethality associated with the disruption of ATR function in mice or DT40 cells is linked to the involvement of ATR in triggering HR as a mechanism to help the resolution of stalled DNA replication complexes. The *S. cerevisiae* Mre11p complex also functions in DNA-damage responses, including the S-phase checkpoint, thus suggesting a high degree of evolutionary conservation for its roles in DNA-damage signaling (55, 102, 289). Perhaps phosphorylation by ATM or ATR affects the ability of the vertebrate and yeast MRE11 complexes to process DSBs. Alternatively, or in addition, the effects of ATM and ATR and their yeast homologues on HR might reflect the ability of these kinases to phosphorylate histone H2AX and thus bring about changes in chromatin structure at the sites of DNA DSBs. It is also possible that ATM and ATR affect HR indirectly by influencing events such as cell-cycle progression or the control of deoxyribonucleotide synthesis.

Non-Homologous End Joining (NHEJ)

NHEJ seems to be the primary mechanism of DSB repair in mammalian

cells (168, 306). In contrast to HR, this pathway does not require homology and can rejoin broken DNA ends directly, end-to-end. Genetic studies, using radiosensitive, DSB-defective mammalian cell lines with mutations in genes that encode components of NHEJ have been useful in identifying many genes involved in the NHEJ DSB repair process (105, 129, 156, 234). In the last decade, significant advances have been made in our understanding of how DSBs are resolved by NHEJ. Seven different genes have been shown unequivocally to be required for NHEJ: Ku70, Ku86, DNA-PKcs, XRCC4, DNA ligase IV (LIGIV), Artemis and XLF/Cernunnos. Three of these molecules comprise the DNA-dependent protein kinase (DNA-PK) complex, a serine-threonine protein kinase that must be physically associated with dsDNA to be active (155); reviewed by (49). The complex contains two subunits. The 467 kDa catalytic subunit, DNA-PKcs, intrinsically possesses weak DNA-binding activity as well as protein kinase activity (116, 322). In the presence of the regulatory subunit, (the Ku heterodimer), however, DNA-PKcs is localized to dsDNA ends where its DNA binding is stabilized and its kinase activity greatly accentuated (98, 274). Ku binds to dsDNA ends in a sequence-independent manner and then translocates to internal sites (73). The second NHEJ factor, XRCC4 is a 37 kDa protein, which interacts with and catalytically stimulates the activity of LIGIV (99, 163, 195). The XRCC4-LIGIV complex carries out the final step of joining DNA ends in NHEJ (101). Artemis, which is a nuclease, was described in 2001 (201) and it may play an important role in DNA-end processing during NHEJ and specifically during V(D)J recombination (185). Finally, the XLF/Cernunnos factor, which was discovered recently, seems to act in a complex with XRCC4-LIGIV (4, 26) although its exact function is unknown.

The Ku Complex

The Ku complex, a heterodimer formed by Ku70 and Ku80 subunits, was originally identified as an autoantigen in the sera of patients suffering from

polymyositis-scleroderma overlap syndrome (193). Ku appears to perform multiple cellular functions. Its nuclear roles involve DNA repair, DNA replication, telomere maintenance, and regulation of transcription, whereas in the cytoplasm, Ku inhibits apoptosis by sequestering the Bax protein outside of mitochondria (48, 250). Unexpectedly, Ku has also been localized in the plasma membrane, where it participates in cell adhesion (142, 188, 204).

The Ku complex is best known for its role in NHEJ DNA repair. Ku has strong affinity for the ends of dsDNA that is relatively independent of their DNA sequence and structure. Ku can bind to blunt ends, to ends with 5'- and 3'- ss protrusions, or to hairpins (8, 73). Ku also binds to the heterologous DNA ends produced by IR (219). The crystal structure of the human Ku70/80 heterodimer provided an elegant explanation for its affinity to DNA ends (300). Ku70 and Ku80 proteins share a similar three-domain topology, consisting of an α/β-domain at the N terminus, a central β-barrel domain, and a helical C-terminal arm. The central domains of Ku70 and Ku80 form a double ring that encircles the DNA molecule. However, Ku makes no contacts with the DNA bases and only a few contacts with the sugar-phosphate backbone, which explains its sequence-independent mode of DNA interaction. Electrophoretic mobility shift assays, electron microscopy, and footprinting experiments reveal that multiple Ku molecules can bind a single linear DNA molecule *in vitro* (73), but that Ku does not efficiently interact with closed circular plasmids. This observation supports a model in which the initial binding of Ku to DNA occurs through a DNA end followed by translocation inwards. The ability of Ku to move inward from the DNA terminus might be important for an efficient NHEJ reaction, as it frees the DNA end for subsequent enzymatic processing.

The N-terminal α/β-domains and helical C termini of Ku70 and Ku80 lie at the periphery of the complex and do not significantly contribute to DNA interactions or heterodimer formation. Rather, these domains provide an

interface for binding other DNA repair proteins. Notably, Ku-like proteins capable of binding dsDNA ends have been found in bacteria and bacteriophages (54, 304). They share sequence similarity with the central domain of their eukaryotic counterparts, but lack the domains at the N and C termini. Thus, eukaryotic Ku70 and Ku80 proteins appear to have evolved from an ancestral prokaryotic *Ku* gene; the DNA end binding activity is the most conserved biochemical property of the Ku complex, whereas the N- and C-terminal interaction motifs have evolved presumably to enhance Ku's function in higher eukaryotes.

The efficiency and accuracy of NHEJ decreases dramatically in cells deficient in Ku, as demonstrated by assays utilizing repair of site-specific breaks produced either by transforming cells with a linearized plasmid (plasmid religation assay) or by induction of site-specific endonucleases such as HO or I-*Sce*I (chromosomal DSB assay) (24, 164). Ku participates in several steps of NHEJ and is implicated in alignment and synapsis of the DNA ends, ligation, suppression of exonuclease resection, and recruitment of additional factors that are important for processing of the DNA breaks. It is still debatable whether the association of Ku with broken DNA plays a structural role in NHEJ by directly stabilizing DNA ends and facilitating their synapsis, or whether it simply serves as a platform for loading other repair proteins. The role of Ku in DNA end synapsis was inferred from visualization of human Ku:DNA complexes by atomic force microscopy (37, 219) and supported by the observation that Ku is capable of bridging two DNA fragments in an *in vitro* pull-down assay (19, 231). However, an independent study suggested that DNA-PKcs, rather than Ku, mediates synapsis (63). This has been supported by recent structural work. Thus, Ku most likely facilitates the association of DNA ends indirectly, via its recruitment of DNA-PKcs, which directly promotes synapsis.

Another aspect of NHEJ where Ku's presence is obvious is in the protection of DSBs from excessive nucleolytic processing. Sequence analysis of

the fusion junctions derived from the cells lacking Ku (24, 164) or produced in a cell-free system using protein extracts depleted of Ku (79) revealed deletions encompassing up to hundreds of nucleotides around the break site. The propensity of the NHEJ reaction toward deletions in the absence of Ku strongly indicates that the Ku heterodimer stabilizes DNA ends and protects them from excessive nucleolytic degradation before ligation ensues. Nevertheless, only a few studies directly address the interplay between Ku and nucleolytic activities at intrachromosmal DSBs. A twofold increase in the rate of 5'- to 3'-end resection has been reported in budding yeast deficient for Ku when a DSB was induced in proliferating cells (153). The increased resection rate was suppressed by concomitant mutation in the *MRE11* gene, which encodes a known nuclease. On the other hand, the stability of the 5'-end was indistinguishable in wild-type and *ku*-deficient strains when a break was induced in cells arrested in G1 (86). These differences may be attributed to a variable availability of the nuclease activity during the cell cycle.

Besides its function in stabilizing DNA ends, Ku also directly facilitates break ligation. It has been reported that the LIGIV/XRCC4 complex is recruited to DNA ends via interaction with Ku (46, 211). Ku stimulates ligation under conditions where one or two molecules bind per DNA end whereas Ku is inhibitory at higher concentrations that would promote binding of multiple Ku heterodimers (147, 231). Further biochemical experiments demonstrated that recruitment of LIGIV/XRCC4 to the break results in inward translocation of Ku, freeing the DNA end for subsequent ligation (147). The ability of the LIGIV-XRCC4 to cause the translocation appears to be restricted by the presence of only a few internally bound Ku molecules.

A key function of Ku in NHEJ is to recruit and coordinate end-processing activities to make DNA ends amenable to ligation. Reconstitution of the NHEJ reaction *in vitro* demonstrated that Ku stimulates association of human α and β-

with DNA fragments (184). Polymerases α and β belong to the Pol X family, and are implicated in filling in gaps arising during alignment of DNA ends. Ku is also important for recruitment of Artemis, a structure-specific nuclease essential for processing coding joints during V(D)J recombination. Finally, Ku directly interacts with the Werner syndrome helicase and the Mre11 complex, both of which are implicated in nucleolytic processing of DNA ends (94, 158, 159, 218).

The LIGIV/XRCC4/XLF Complex

Three DNA ligases (LIGI, LIGIII, and LIGIV) are present in mammalian cells. Genetic studies in budding yeast (279, 307) and the mouse (84) revealed that the NHEJ ligase activity is provided exclusively by LIGIV. LIGIV forms a complex with the XRCC4 protein (orthologs in *S. cerevisiae* are called Lig4 and Lif1, respectively), which is also required for ligase activity (99, 123). Crystallographic analysis indicated that the stoichiometry of the human LIGIV/XRCC4 complex is 1:2 (263). Biochemical analysis of an *in vitro* reconstituted NHEJ reaction revealed that the LIGIV/XRCC4 complex possesses a unique ssDNA ligation activity that permits joining of one DNA strand across a gap in the opposite strand (184). While LIGIV is the major NHEJ ligase yeast *lig4* mutants are nevertheless still capable of plasmid religation, albeit with significantly reduced efficiency and accuracy (279). LIGIV-independent end-joining appears also to occur in higher eukaryotes; a knockout of LIGIV in a human cell line did not completely abolish V(D)J recombination (100). Furthermore, LIGIV deficiency does not prevent nonhomologous chromosomal integration of a *P* element and T-DNA in *Drosophila* and *Arabidopsis*, respectively (191, 291). It remains to be determined which ligase is responsible for the residual end-joining activity.

Two additional NHEJ factors associated with LIGIV/XRCC4 have been identified. Nej1 in *S. cerevisiae* is a haploid-specific protein whose expression is

repressed by the Mata1/_2 repressor (85, 138, 290). Nej1 interacts with Lif1, and *nej1_* mutants are deficient in plasmid religation and chromosomal DSB repair assays. Two independent studies have recently reported discovery of a novel human protein, Cernunnos/XLF, which interacts with the LIGIV/XRCC4 complex (4, 26). Cernunnos/XLF is predicted to share structural similarity with XRCC4. Patients carrying a mutation in the Cernunnos/XLF gene or cell lines in which the protein was depleted by RNAi display impaired NHEJ (331). A more detailed understanding of the molecular function of these NHEJ-associated proteins awaits further genetic and biochemical analyses.

DNA-PKcs/Artemis

In addition to the Ku heterodimer and XRCC4/LIGIV, the mammalian NHEJ core components consist of the DNA-dependent protein kinase catalytic subunit (DNA-PKcs) and Artemis. DNA-PKcs is a member of the phosphoinositide-3-kinase–related family, which also includes ataxia telangectasia-mutated (ATM) and ataxia telangectasia-related (ATR) DNA damage signaling proteins. The essential role of DNA-PKcs in DSB repair was demonstrated by studies of severe combined immune deficient (SCID) mice carrying a defective DNA-PKcs gene. SCID mice display aberrant V(D)J recombination and exhibit a radiosensitive phenotype (14, 49, 168). DNA-PKcs physically associates with the Ku heterodimer forming a catalytically active DNA-PK holoenzyme complex. Ku recruits DNA-PKcs to a DSB via a C-terminal domain on the Ku80 protein (76), leading to a rapid activation of DNA-PK in response to DNA damage. Activation of the kinase appears to require an additional direct interaction of DNA-PKcs with the DNA. Although DNA-PKcs can also bind to DNA termini and activate its kinase in the absence of Ku, this occurs at much lower efficiency (113).

The requirement for DNA-PKcs in NHEJ is well established, but little is known about its function in DSB rejoining or its *in vivo* phosphorylation targets. *In vitro* studies indicate a stimulatory role for DNA-PKcs in DNA synapsis (63) and ligation (20, 146). Ligation stimulation may be implemented via autophosphorylation of DNA-PKcs, resulting in remodeling of the DNA-end-bound DNA-PK complex (20, 40). In addition, DNA-PK phosphorylates histones H2AX and H1 (146, 220), and histone H1 phosphorylation by DNA-PK derepresses ligation of *in vitro* reconstituted nucleosomes by LIGIV (146). These observations indicate that DNA-PK may facilitate the NHEJ reaction by modifying the local chromatin environment to provide access of other DNA repair complexes to DSBs.

New insight into the role of DNA-PKcs in NHEJ has been gained from the identification of Artemis, a structure-specific nuclease important for processing DNA ends during V(D)J recombination (201, 240). Artemis is recruited to DNA ends by DNA-PK, which activates its endonuclease-hairpin opening activity and permits ligation of the coding ends (185). Increased sensitivity of Artemis-deficient cells to IR and a failure to rejoin 10% of radiation-induced DSBs suggests an additional NHEJ function outside of V(D)J recombination (235). However, the radiosensitive phenotype of both DNA-PKcs and Artemis-defective cells is significantly milder than cell lines deficient for Ku or XRCC4 (88, 239, 240). The different genetic requirements for repair radiation-induced DSBs or breaks occurring during V(D)J and class switch recombination indicate that, in contrast to the Ku70/80 heterodimer and LIGIV/XRCC4, DNA-PKcs/Artemis are important for only a subset of NHEJ reactions. The less stringent requirement for DNA-PKcs/Artemis in NHEJ is in accordance with the fact that orthologs of these genes have been found only in vertebrates and slime molds (126) but not in invertebrates, plants, or fungi.

The Mre11 Complex

The Mre11 complex consists of the evolutionary conserved Mre11 and Rad50 subunits and the less conserved Nbs1/Xrs2 protein (Alternately referred to as the MRN or MRX complex. Like Artemis, Mre11 is a structure-specific nuclease. Mre11 exhibits 3'- to 5'-dsDNA exonuclease and ssDNA and dsDNA endonuclease activities. The Rad50 protein is a member of the SMC (structural maintenance of chromosome) protein family, which also includes cohesin and condensin subunits. Rad50 forms a structural scaffold, containing C- and N-terminal ATPase domains that are connected by a long coiled-coil region separated in the middle by a flexible hinge. Scanning force microscopy revealed that the Rad50 protein folds back in the hinge region to bring together terminal ATPase domains. The whole structure is stabilized by antiparallel association of the coiled-coil regions (59). Dimerization of two Rad50 proteins is mediated by a zinc-finger-like hook in the hinge domain (125). One Nbs1/Xrs2 and two Mre11 molecules interact with the Rad50 dimer, forming a complex capable of binding and tethering DNA ends. The Mre11 complex plays a central role in DSB repair. It is involved in DNA damage detection and signaling, as well as in HR and NHEJ. MRN is among the first enzymatic complexes to arrive at a DSB, suggesting that it acts as a DSB sensor to initiate DNA damage signaling and repair through a pathway that includes activation of the ATM kinase (151, 173, 262). The Mre11 complex is also essential for early steps of meiotic recombination, where it mediates nucleolytic processing of 5'-DNA ends at meiotic breaks (208, 209).

The NHEJ function of the Mre11 complex has definitively been established only in budding yeast. Deletion of any component of the complex results in a 10- to 100-fold decrease in the efficiency of DNA end-joining assays (70). Biochemical analysis showed that the yeast Mre11 complex has a DNA end-bridging activity and facilitates joining of linear DNA molecules by Dnl4/Lif1 (45). Epistasis analysis suggests that Ku, Mre11, and Lig4/Lif1 complexes participate

in the same NHEJ pathway (24, 197, 218). This hypothesis is further supported by the observation that Ku augments the stimulatory role of the Mre11 in the Lig4-dependent ligation of DNA ends *in vitro* (45). Thus, in yeast, genetic and biochemical experiments indicate that the Mre11 complex acts in concert with Ku to promote efficient alignment of DNA ends and recruitment of LIGIV. Whether the same interactions occur in higher eukaryotes is still not known.

The Mre11 complex can also function — independently from Ku — in the end-joining mechanism that processes noncomplementary DNA ends (182). Characteristic features of this pathway include fusion products with deletions spanning up to 300 nucleotides and sequence microhomology at the fusion points. Accordingly, this mechanism has been dubbed microhomology-mediated end joining (MMEJ). The efficiency of the MMEJ pathway significantly decreases in cells lacking MRN or the Rad1/Rad10 3'-flap nuclease, although MMEJ does not require Ku heterodimer (182). MMEJ is not entirely dependent on LIGIV, indicating that its function can be substituted by another ligase, most likely Cdc9 (the yeast ligase I ortholog required for ligation of Okazaki fragments). A current model of MMEJ predicts that nucleolytic processing of 5'-ends of DSBs by Mre11 uncovers microhomology that can be utilized for annealing and alignment of DSBs. The resulting 3'-flaps are removed by Rad1/Rad10 endonuclease generating 3'-ends suitable for gap-filling reaction and ligation (182).

The role of MRN in NHEJ in other organisms is unclear. Repair of DSBs in higher eukaryotes frequently occurs by an MMEJ-like mechanism that generates microhomology at fusion junctions (232). The human MRN complex possesses exonuclease activity, which is stimulated by noncohesive DNA ends, but is inhibited when a 3'-end anneals to a homologous region of another DNA molecule. This enzymatic property of the Mre11 complex is consistent with its role in MMEJ (222). However, there is no strong *in vivo* evidence demonstrating

a significant contribution of the Mre11 complex to DNA end-joining repair outside of budding yeast (64, 187, 320).

Additional DNA End Processing Factors

DSBs that occur as a result of cellular metabolism or external genotoxic stress are most likely not amenable to direct ligation. Such ends may be formed by incompatible 3'- or 5'-end protrusions or contain unusual chemical structures that must be removed to restore 3'-OH or 5'-phosphate groups. Rejoining of such substrates usually requires nuclease and polymerase activities that trim incompatible sequences and fill in gaps. So far the only nuclease unequivocally identified to be required specifically for NHEJ is Artemis, although, as discussed above, MRN is likely also involved. Two nuclease complexes that cleave branched DNA structures have been shown to contribute to efficient DNA end-joining in budding yeast. As discussed above, the Rad1/Rad10 nuclease participates in MMEJ by removing 3'-flaps (182), whereas removal of the 5'-flap intermediates arising during NHEJ is dependent, at least in part, on Rad27 (the yeast homologue of FEN1) (316). However, both Rad1/Rad10 and Rad27 play a more general role in DNA repair; Rad27 is required for processing replication intermediates, whereas Rad1/Rad10 is also involved in base excision repair and HR. Another enzyme implicated in nuclease processing during NHEJ is the human Werner syndrome helicase (WRN). *In vitro* studies have shown that WRN is recruited to DNA ends via physical interaction with Ku. This interaction stimulates the 3' to 5' exonuclease activity of WRN (157, 158). It remains to be established whether WRN has a physiological function in NHEJ *in vivo*.

DNA polymerization and gap-filling activities during NHEJ are mediated mainly by members of the Pol X family of nonreplicative DNA polymerases. Genetic data implicate polymerase 4 (Pol4), the only member of the Pol X family in budding yeast, in the repair of the subclass of DSBs that require gap-filling and

flap-removing activities (57, 308). Biochemical analysis revealed that the DNA synthesis activity of Pol4 is stimulated by association with Lig4/Lif1, and that both protein complexes interact with Rad27. Together, these proteins coordinate processing and ligation of DNA ends with noncomplementary 5'-ends (283, 284). Four Pol X polymerases have been found in mammalian cells, of which three, Pol _, Pol _, and terminal deoxynucleotidyl transferase (TdT), are involved in NHEJ (184). The polymerases display distinct catalytic properties, which may allow efficient NHEJ at a wide spectrum of substrates. While TdT adds random nucleotides to DNA termini, both Pol α and Pol β can perform template-dependent gap-filling synthesis on mismatched ends. Similar to TdT and in contrast to Pol α, Pol β does not require alignment of the primer with the template DNA strand (210). Plants possess a single Pol X polymerase (most related to Pol α) (288), whereas *Caenorhabditis elegans* and *D. melanogaster* completely lack this class of polymerases (28) although they clearly perform NHEJ. Hence, expansion of the Pol X family in mammals may reflect their unique function in the rearrangement of genes encoding immunoglobulins and T-cell receptors.

Mechanism of C-NHEJ:

While the exact mechanism of C-NHEJ remains obscure, a reasonable model is predicted, described below:

Step 1: Ku binding:

Upon DNA damage the highly abundant Ku heterodimer, consisting of the DNA helicases Ku70 and Ku86 binds to open DNA ends (194). It has been estimated that the Ku protein is as abundant that if it were evenly distributed in the cell, single molecules would be only 4-6 diameters apart from each other (168). This way the Ku protein ensures a quick detection of DSBs and protects the open DNA ends from nucleolytic attack (68). Structural data shows that Ku heterodimer forms a ring and encloses the dsDNA like a bead on a thread (300). Because purified Ku binds DNA in vitro, it is plausible to think that, additional

loading factors may not be needed in vivo (300). Ku70 and Ku86 proteins are very unstable if they are not part of heterodimer. Therefore, decreased Ku70 protein expression automatically leads to decreased Ku86 protein expression and vice versa (6) (161).

Step 2: DNA-PK$_{cs}$ autophosphorylation

After the Ku protein associates with DNA, it recruits DNA-PK$_{cs}$ to the damaged site. Upon DNA binding DNA-PK$_{cs}$ changes its conformation, which triggers its kinase activity and leads to autophosphorylation (22), (237). This autophosphorylation seems to occur in trans and implies that DNA-PK$_{cs}$ molecules are bound to both DNA ends in proximity (237).

Several DNA-PK$_{cs}$ atuophosphorylation sites have been identified to date and current models suggest that existence of at least three distinct functional clusters of such sites. The first cluster, also termed ABCDE, includes the potential autophosphorylation sites T2609 (A), T2920 / S2624 (B), T2638 (C), T 2609 (D) and S 2612 (E) (67). In vivo, phosphorylation of the T2609 site is essential for both cell survival and DSB repair after IR (Chen et al., 2002). Also, DNA-PK$_{cs}$ pT2609 co-localizes at DNA damage foci with the DSB repair proteins H2AX and 53BP1. In reconstitution experiments with DNA-PK$_{cs}$ deficient hamster cells, expression of DNA-PK$_{cs}$ mutated in all ABCDE sites lead to increased radiation sensitivity and decreased NHEJ activity. Experiments reconstituting NHEJ activity in vitro showed that DNA bound DNA-PK$_{cs}$ can control access of other factors to the open DNA strand (233). This function of DNA-PK$_{cs}$ seemed to be regulated by phosphorylation in the ABCDE cluster (233). In Summary, the ABCDE cluster is important for the end joining activity of DNA-PK$_{cs}$.

Hypothetically, another cluster of autophosphorylation sites is responsible for kinase disassembly, because mutations in the ABCDE cluster do not abolish such activity (192). Recently, another autophosphorylation site, upstream of the ABCDE cluster has been identified at S2056. DNA-PK$_{cs}$ autophosphorylation at S2056 is independent of ATM and is important for NHEJ efficiency. Interestingly,

S2056 phosphorylation occurs in irradiated cells mainly in G1 but not in S phase. Moreover, in response to replication-associated DSBs, phosphorylation of S2056 was increased and further seemed to be dependent on DNA-polymerase α or δ activity.

Step III: DNA damage response

The cellular DNA damage response ensures that apart from the activation of DNA repair pathways the cell reacts appropriately to the insult (335). For this, the cell cycle is halted at checkpoints, and in the case of extensive damage, apoptosis is induced. One of the first responses to DNA damage is phosphorylation of the DNA damage response protein ATM at S1981 (12). Presumably triggered by changes in chromatin atructure, ATM dimmers autophosphorylate in trans and monomerize. This event further increases ATM kinase activity and ATM then targets checkpoint proteins like p^{53}, NBS1 and Chk2, which halt the cell cycle at G1, S or G2, respectively (1), (12). Interestingly, ATM also participates in the actual DNA repair process by phosphorylating H2AX together with DNA-PK_{cs} (273). Phosphorylated H2AX (γ-H2AX) is a marker for damaged DNA regions, and it has been suggested that γ-H2AX concentrates DNA repair proteins and prepares the chromatin for subsequent DNA repair events (80). Recently, it was shown that ATM can also phosphorylate DNA-PK_{cs} at T2609.

Step IV: DNA end processing

Depending on the underlying cause, DSB can look very differently. For this reason they require specific end processing before the final DNA ligation reaction can occur (168). Several factors have been implicated in this process:
DNA breaks caused by IR are either blunt or staggered with either 5’ or 3’ overhanging ends.These ends can be processed by the MRN complex consisting of the endonuclease Mre11, Rad50 and NBS1 (292). The nucleolytic resection

activity of MRN complex also has been implicated in the HR pathway of DSB repair (305). More extensive DNA processing may require that the DNA is unwound by DNA helicases. For example, the Warner helicase interacts with DNA-PK_{cs}, is regulated by DNA-PK_{cs} phosphorylation and might participate in DNA end processing (157), (323)..

The formation of DSB at stalled replication forks requires DNA polymerase activity and several DNA polymerase like α and δ has been implicated in this reaction (228). But also DNA damage due to IR exposure might require DNA polymerase activity, and it was shown that DNA polymerase μ forms acomplex with Ku and XRCC4/ Ligase IV and co-localize with γ-H2AX foci (186).

During V(D)J rearrangement the recombination activating proteins 1 and 2 (RAG 1 and 2) cause DSB with hairpins (189), (252). These hairpins have to be opened first in order to ligate both DNA strands together and to complete the reaggangement of the immunoglobin variable region (253). After a bilong quest for the elusive factor, it was found that in complex with DNA-PK_{cs} the exonuclease Artimis acquires also endonuclease activity and is therefore able to open these hairpin structure (185). In agreement with this role, loss of function mutations in Artimis or DNA-PK_{cs} result in a SCID phenotype with no T or B cells (254), (185), (214).

In order to ligate open DNA ends together, DNA ligases require a 3' end phosphate group. If this phosphate group is lost by the DNA damage or end processing, the polynucleotide kinase (PNK) can phosphorylate the 3' end and allow DNA ligation.

Step IV: DNA end ligation

The DNA ligation step of NHEL is carried out by the XRCC4/XLF/Ligase IV complex (99). It has been suggested that two molecules of XRCC4 are associated with one molecule of Ligase I. While XRCC4 is the structural protein

that may hold the open DNA ends together, Ligase IV provides the catalytic activity to close the gap (100).. Both proteins are phosphoproteins, for Ligase IV it was shown that it is a phosphorylation target of DNA-PK_{cs}, while XRCC4 phosphorylation depends on other protein kinases.

Step VI: Dissociation of the DNA-PK complex

This NHEJ step is the least understood step. Assuming that the Ku heterodimer stays on the DNA until the final ligation step, the question is how it gets unloaded from the DNA. The first possibility is that the dimmer can be separated by an additional factor, presumably at the expanse of ATP.In the alternative case, Ku could be cleaved by a protease (68). In fact, a Ku70 derived polypeptide that binds and inhibits the proapoptotic factor BAX has been recently identified. However, the search for the responsible protease has so far been unsuccessful. recently, it has been suggested that ubiquitination of Ku86 might play a role for Ku unloading form the break site (229).

For DNA-PK_{cs} it is clear that hyperphosphorylation leads to its dissociation from Ku and DNA. However, it is not clear which DNA-PK_{cs} phosphorylations sites in particular are responsible for this event, and they are yet to be identified. It is also unclear if phosphorylated DNA-PK_{cs} gets dephosphorylated and can be reused, or if phosphorylated DNA-PK_{cs} is to be degraded. Even though there is some evidence that dephosphorylation occurs, the corresponding phosphatase has been elusive so far (66).

Disease with DBS repair deficiencies:

Human diseases can occur when components of the DNA DSB pathway are dysfunctional. Deficiencies in repairing DSB lead particularly to pronounced clinical radiosensitivity. Most of these diseases show similar in vitro cellular phenotypes, such as sensitivity to ionizing radiation and other DSB-inducing

chemicals, cell cycle checkpoint defects or a high frequency of chromosomal breaks and rearrangements.

Ataxia telengiectasia:

Ataxia telengiectasia (A-T, a rare autosomal recessive syndrome resulting from mutations in the ATM kinase is a prime example of the consequences of an inappropriate response to DNA DSBs. A-T is a multisystem disorder that includes telangiectasia (dilated blood vessels, usually ocular), immunodeficiency and proneness to malignancies particularly lymphoma and leukemia. However, the most prominent clinical manifestation of A-T is the progressive ataxia characterized by the loss of Purkinje and granular cells in the cerebellum, confining A-T patients to the wheelchair generally by age of 10 or younger. At cellular level, ATM deficiency is manifested by increased sensitivity to ionizing radiation and other agents that yield DNA DSBs but little or no hypersensitivity to other forms of DNA damage.

Ataxia telengiectasia-like disorder:

Ataxia telengiectasia-like disorder (ATLD) shows similar features to those of A-T including neurodegeneration. ATLD results from hypomorphic mutations of MRE11 that lead to attenuated levels of all three component of MRN complex. Although an increase incident of tumors is not reported in ATLD, small number of individuals with this syndrome leaves this an open question. MRE11 is a member of the Mre11- Rad50- Nbs1 (MRN) protein complex. MRN and its individual components are involved in response to cellular damage induced by ionizing radiation and radiomimetic chemicals, including complexing with chromatin and with other damage response proteins, formation of radiation-induced foci, and induction of different cell cycle checkpoints.

Nijmegen breakage syndrome:

Nijmegen breakage syndrome (NBS) is a rare autosomal recessive disorder characterized by microcephaly, immunodefficiency, and in increased incidence of hematopoietic malignancies. NBS results from hypomorphic mutation of another MRN component, Nbs1 (65). Nbs1 is located on human chromosome 8q21 and codes for a protein product called nibrin, Nbs1 or p95. Over 90% of patients are homozygous for a founder mutation: a deletion of five base pairs which leads to a frame shift and protein truncation. The protein Nbs1 is suspected to be involved in the cellular response to DNA damage caused by ionizing radiation, thus accounting for the radiosensitivity of NBS.

The phosphorylation of Nbs1 by ATM would indicate that ATM acts upstream of the MRN complex. Consistent with this were the suggestions that ATM could be activated in the absence of fully functional Nbs1 protein. In contrast, the regulation of some ATM target proteins, e. g. Smc1 requires the MRN complex as well as ATM. Mbs1 may, therefore, be both substrate for ATM and mediator of ATM function. Recent studies that indicate a requirement of the MRN complex for proper ATM activation suggests that the relationship between ATM and the MRN complex in the DNA damage response is yet to be fully determined.

It has been proved that a small increased fraction of unrejoined double strand breaks and. More significantly, increased chromosome breaks in non cycling Nbs1 cell at 24 h after irradiation (93). One of the Nbs1 lines examined (347BR) was atypical in showing a nearly normal checkpoint response. In contrast to the mild checkpoint defect, 347BR displayed marked γ-ray sensitivity similar to that shown by other Nbs1 lines. Thus the γ-ray sensitivity correlates with the repair defect rather than impaired checkpoint control. Taken together, the results provide direct evidence for a repair defect in NBS cells and are inconsistent with the suggestion that the radiosensitivity is attributed only to impaired checkpoint arrest. 347BR also displays elevated spontaneous damage

that cannot be attributed to impaired G2-M arrest, suggesting a function of Nbs1 in decreasing or limiting the impact of spontaneous arising double strand breaks.

DNA-PK$_{cs}$:

Recently the van Gent laboratory has described the first human RS-SCID patient, with a missence mutation in DNA-PKcs (293). The mutation L3062, did not affect the kinase activity or DNA end-binding capacity of DNA-PKcs itself. But the presence of long P-nucleotide stretches in the immunoglobulin coding joints indicated that the mutation caused insufficient Artimis activation. They also found that the overall end-joining activity was also compromised, suggesting an Artemis-independent DNA repair function of DNA-PK$_{cs}$. Most importantly, this study suggests that residual DNA-PK$_{cs}$ activity is indispensable in humans. On the other hand, recently a study from our group also demonstrated that DNA-PK$_{cs}$ is not essential for human somatic cells, though deletion of this gene leads to severe proliferation defects, genomic instability and shortening of telomere length (245).

LIGIV syndrome:

Hypomorphic mutations of Ligase IV that attenuate LIGIV activity lead to LIGIV syndrome whereby individuals display similar phenotypes to NBS such as unusual facial features, growth retardation and microcephaly (216). Ligase IV is important in NHEJ and V(D)J recombination. Ligase IV syndrome patients display immunodeficiency. Cells from these individuals are radiosensitive and defective in NHEJ repair of DNA DSBs. Immunodeficiency also occurs in individuals with mutations in the XRCC binding protein, XLF/Cernunnos and a similar neuropathology to LIG4 syndrome is present (26).

In a previous in vitro study, a DNA ligase IV-null human pre_B cell line and human cell lines with hypomorphic mutations in Ligase IV have been shown to be significantly impaired in the frequency and fidelity of end joining (265). Analysis of the null line demonstrated the existence of an error-prone DNA Ligase IV-

independent rejoining mechanism in mammalian cells. Analysis of lines with hypomorphic mutations demonstrates that residual DNA Liogase IV activity, which is sufficient to promote efficient end joining, nevertheless can result in decreased fidelity of rejoining. Thus, DNA Ligase IV is an important factor influencing the fidelity of end joining in vivo. The Ligase IV defective cell lines also showed impaired end joining in an in vitro assay using cell-free extracts (265). Finally, they demonstrate that the ability of DNA ligase IV along with XRCC4 to protect DNA ends may contribute to the ability of DNA Ligase IV to promote accurate rejoining in vivo.

It has been shown that DNA Ligase IV deficient (180BR) human cells have a pronounced repair defect after ionizing radiation doses between 10 and 80 Gy by pulse field gel electrophoresis (PFGE). At higher doses, the mutation in 180BR cells leads to more severe repair defect, indicating that mutated DNA Ligase IV protein can handle a small but not an excessive number of DSBs. The DSB repair of the Ligase IV null pre-B cells N114P2 with targeted disruption of both Ligase IV alleles is significantly impaired in comparison with the time course of the DNA Ligase IV-deficient primary fibroblasts. The difference is most pronounced for repair times of 8 and 24 h in N114P2 cells compaired with 180BR cells, more than twice as many unrepaired DSBs.

Artemis:

Mutations in the Artemis protein in humans result in hypersensitivity to DNA double-strand break-inducing agents and absence of B- and T-lymphocytes (radiosensitive severe combined immune deficiency (201). Artemis cleaves DNA hairpin intermediates during V(D)J recombination in an ATM-independent manner (185). However, it mediates the repair of a fraction (10%) of DSBs incurred after ionizing radiation in an ATM-independent manner (Riballo et al., 2004). Current models suggest that Artemis functions to process the neds of otherwise non-ligatable DSBs prior to logation by core NHEJ factors (176). The

mechanism of Artemis activation in vivo is unclear, although Artemis is rapidly hyperphosphorylayted in an ATM-dependent manner after exposure to DSB-inducing agents. ATM and other PIKKs, including DNA-PK_{cs}, preferentially phosphorylate serine or threonine followed by glutamate (S/TQ) motifs. Artemis contains 10 such sites, of which eight are located in the C-terminal 200 amino acids. Artemis cDNA mutated in seven of these sites was able to complement the radiosensitivity of Artemis-deficient cells. Despite this, other studies have suggested that phosphorylation of Artemis by DNA-PK_{cs} leads to endonuclease activation (185), (184), (183).

In previous study, the major DNA-PK and ATM phosphorylation sites within Artemis (S503, S516 and S645) was identified under physiological relevant ionic conditions, and showed that ATM-dependent Artemis phosphorylation at S645 occures in vivo (95). ATM cannot substitute for DNA-PK to suppor Artemis activity in vitro, supporting the in vivo dependency upon DNA-PK_{cs}.

Given the existence of the NHEJ-deficient patients described above, it is surprising that patients with mutations for Ku70, Ku86 or XRCC4 have not yet been described. In mice, the functional inactivation of XRCC4 results in lethality (88), and if the essential feature of this gene is conserved in humans, this would perforce explain its absence in patients. Similarly, although Ku70 and Ku86 knockout mice are viable and a plethora of Ku-null cell lines have been described previously (330), no spontaneous whole animal model defective in either Ku subunit have been ever reported. Moreover, the functional inactivation via gene targeting of Ku70 (77) or Ku86 (161) results in nonviable human somatic cells. Extrapolation of these observations concerning Ku to humans suggests that the human Ku subunits are essential, and this explains the absence of Ku-deficient patients.

Interaction between HR and NHEJ:

It has been proposed that HR and NHEJ are not necessarily independent, since coordination action of both pathways is invoked by cell in order to repair a DSB with minimal error (236), (247). Thus both HR and NHEJ repair pathways are required to maintain genomic integrity, even in the absence of a specific genotoxic insult. Several studies in hamster cells have suggested that when NHEJ is impaired, HR seems to increase and vice versa (236), (5). Furthermore, cells obtained from DNA-PKcs- deficient SCID mice that are impaired in NHEJ and V(D)J recombination show more efficient levels of HR (227). There is a reported interaction between ATM and DNA breaks at the site of V(D)J recombination, suggesting that ATM also plays a role in NHEJ and V(D)J recombination. Altogether, different types of DSB repair are intricately linked together in a dynamic fashion with cell cycle regulation, but with sufficient flexibility to allow for redundancy and backups should one factor or type of repair fail.

Back-Up (Ku-independent) NHEJ:

NHEJ appears to consist of at least two sub-pathways: the main end-joining pathway described above (C-NHEJ) and one interchangeably referred to as MMEJ (microhomology-mediated end joining), A-NHEJ (alternative-NHEJ) or B-NHEJ (backup-NHEJ) (hereafter referred to as B-NHEJ) mediated by signature microhomologies. Thus, mammalian cell lines defective for Ku, DNA-PKcs, LIGIV and XRCC4 are still proficient for some NHEJ, but the majority of the repair products carry significant microhomlogy at the repair junction (215), (190).

The genes and mechanism required for the B-NHEJ are poorly defined, but there are some interesting clues. First, MRE11, the 3’ > 5’ exonuclease, required for HR, has enzymatic properties consistent with it also plays a role in B-NHEJ repair (222). Similarly, chromosomal translocations and DNA repair events in yeast cells deficient in MRE11 often lack microhomology at their junctions (23), (41). More recent work from a number of laboratories (11 (Guirouilh-Barbat, 2004

#965), (108), (302) has also implicated a trio of genes (PARP-1: XRCC1: LIGIII; poly (ADP-ribose) polymerase-1: XRCC1: DNA ligase III) that were previously best understood for their roles in base excision repair (32) PARP-1, XRCC1 and LIGIII physically interact and exist as a complex within cells (31), (32). PARP-1 is a highly abundant nuclear protein that binds rapidly to DNA DSBs and catalyzes the transfer of ADP-ribose from its substrate NAD^+ to variety of DNA repair factors, albeit mainly to itself (312). PARP-1 has its well-documented role in ssDNA repair (312). Whereas its potential role in DSB repair has only recently been appreciated (310). Murine knockouts of PARP-1 are viable (303) although they show defects in chromosome stability, especially when crossed into p53-deficient (281). The genetic analysis of PARP-1 has been complicated by the presence of one clear homolog, PARP-2, whose functional redundancy with PARP-1 is not understood. LIGIII is one of the three eukaryotic ligases and, like PARP-1, it has a well documented role in ssDNA repair. LIGIII encodes four isoforms that differ at their C-termini and their cellular localization (nuclear or mitochondrial), but LIGIIIα, which is constitutively bound to XRCC1, appears to be the biologically more important isoform. Murine knockouts of LIGIII are not viable (230). XRCC1 does not contain any obvious motifs, but appears to serve as a scaffold into which other proteins bind. In addition, it acts as a stability factor for LIGIII as loss of XRCC1 expression is accompanied by reduced LIGIII level (175). Murine knockouts of XRCC1 are not viable (278).

While the evidence for a biological role for B-NHEJ is repairing IR-induced DSBs is weak, the evidence for a significant role in V(D)J and class recombination seems unequivocal (52), (321).

V(D)J recombination, CSR and SHM:

Mutations that affect DNA DSB repair frequently also affect the pathways responsible for site-specific and general recombination (170). This overlap of recombination and DSB repair pathways is presumed to result from the

postulated role of double-stranded ends as structural intermediates in many types of recombination and repair (120). In mammals, the generation of the immune system requires a somatic site-specific re-arrangement process termed V(D)J recombination (223). In progenitor cells, large clusters of isolated V, D and J elements are extracted from these clusters and enzymatically assembled to generate a functional V(D)J element that will ultimately partially encode an Ig or TcR protein, respectively. V(D)J recombination is conceptually broken down into lymphoid-specific and general steps. The upstream lymphoid site-specificity of this event is mediated by *cis*-acting RSSs (recombination signal sequences) that consist of conserved heptamer and nonamer elements separated by a spacer of defined length (12 or 23 nucleotides) but of with no sequence conservation (124). A RSS flanks the 3'- side of every V element, both sides of D elements and 5'-side of every J element, which promotes the ordered (D joins only to J and V joins only to DJ) assembly of Igs and TcRs. A pair of RSSs are recognized by RAG-1: RAG-2 (recombination activating genes 1 and 2, respectively) recombinase and bought together into a synaptic complex. The RAG-1: RAG-1 recombinase introduces single-stranded nicks adjacent to the RSS and the V, D or J element to which it is bound. Subsequent interstrand trans-esterification reactions results in hairpinned V, D or J coding ends and blunt RSSs. RAG-1: RAG-2 are necessary and sufficient for all of these lymphoid-specific upstream events and mutation of either gene causes primary immune defficiencys (199). Additional downstream general events that are carried out by the NHEJ branch of the DSB reapir pathway are, however, required to rejoin the RSSs (termed signal joint formation) and coding ends (termed coding joint formation) back together. In particular, the hairpinned coding ends are eventually nicked back open by DNA-Pk_{cs}:Artemis complex (185), processed with nucleotide additions and/or deletions and then joined together by LIGIV:XRCC4:XLF complex. The RSS ends are generally joined into a signal joint by the LIGIV:XRCC4:XLF complex without any additional processing. Again, mutations which disrupt NHEJ result in a novel form

of primary immuno deficiency denoted RS-SCID (radiation sensitive-SCID) due to the manifested defects in DNA DSB repair and V(D)J recombination.

Following productive V(D)J recombination in B-cells, functional Igs can undergo the additional process called CSR and SHM that enhance either the effector function or the affinity of the antibody, respectively (96). CSR is a somatic DNA recombination process initiated or by another recombinase AID (activation induced deaminase) in which the constant region isotype domain downstream of a productive V(D)J recombination event is altered. In SMH, point mutations that result in amino acid changes are introduced into the V(D)J portion of a functional Ig gene. Amino acid changes that increase the affinity of an Ig for its antigen can then be selected for in the periphery. Mechanistically, CSR and SHM occur by AID- induced deaminations of cytosine residues to uracils, which are subsequently removed from the DNA by UNG (uracil nucleotide gycosylase) to leave a nick in the DNA. In the case of CSR it is believed that 2 closely-spaced nicks on opposing strands generates a DSB whereas in case of SMH, the nicks are probably repaired with relaxed specificity to permit incorporations of non-cytosine residues (96). Since DSBs are generated during CSR it is not surprising that this process is also mediated by NHEJ. Intriguingly, however, mutations in C-NHEJ genes, which ablate V(D)J recombination, have a reduced impact on CSR (38). This is due to the ability of CSR to utilize factors from the B-NHEJ sub-pathway (215). Given these mechanistic constraints it is not surprising that mutations of AID, UNG, C-NHEJ or B-NHEJ factors results in immuno deficiency.

AAV and rAAV:

AAV is a human parvovirus that has both lytic and latent lifecycle reviewed by (205), (298). The lytic part of the AAV life cycle, during which AAV is replicated, requires the presence of a helper virus, generally adenovirus or herpes virus. Thus, AAV has only been detected in individuals undergoing the symptoms of an adenoviral (9) or herpes simplex virus (27) infection. Approximately 85% of the human population is seropositive for AAV and there is

no pathology nor disease attributed to an AAV infection (205). During a latent infection, AAV integrates stably into the human genome, preferentially, but not exclusively, at a site (AAVS-1; AAV integration site-1) on chromosome 19q13.4 (249). It was characteristic of site-specific integration that first drew the attention of gene therapy field to AAV, since the use of AAV as a gene delivery vector wouldn't have the serious problem of random insertional mutagenesis attendant with other viral vector delivery system (111), reviewed by (212).

AAV is a single-stranded DNA virus of 4.68 kb. Either strand of a latently integrated AAV DNA can be packaged (241) and both are equally infectous. Multiple serotypes of the virus are known and although only the AAV-2 serotype is routinely utilized in the laboratory, work is underway to expand the utility of the other serotypes. AAV encodes two genes, Rep (replication) and Cap (capsid). Rep is required for viral replication, needed for viral integration and can potentiate viral gene expression. Rep protein mediates AAVS1 integration by binding to Rep binding sites within the AAVS1 and AAV ITRs (inverted terminal repeats). Rep nicks at the TRS (terminal resolution site) within the AAVS1 and the ITRs and at least the former nick is absolutely required for targeted integration (325). Cap encodes the viral capsid proteins, of which 3 isoforms, VP1, VP2 and VP3, exits (130). The Rep and Cap genes are flanked by identical ITRs of 145 bp that form T-Shaped hairpins, due to three palindromic sequences residing within the ITRs (181). The ITRs are essentially the only *cis*-acting sequences necessary foe viral replication, packaging and integration. This fact greatly facilitated the development of rAAV first as a gene delivery and later as a gene-targeting vector. Thus, if Rep and Cap are provided in *trans*, then the internal 4.39 kb of AAV can consist of recombinant DNA of the investigator's choosing (81). Similarly, the adenoviral gene products E1A, E1B, E4, E2A and VA are required for AAV replication (205). Originally, these were provided by co-infecting with live adenovorus, which, of course, precluded the use of the

resulting AAV stock for gene therapy experiment for gene therapy experiments. This significant detriment was overcome once again simply by providing recombinant adenoviral functions in *trans*. In Summary, AAV has been known to the research community for some 4 decades and the lifecycle of the virus is quite well understood. The virus was subsequently conscripted in the 1980s by investigators who were interested in viral vectors for use in gene therapy and clinical trials using AAV are well underway (reviewed by (Mueller, 2008 #1047). Recombinant molecular biological methodologies were then used to develop a rAAV system for the production of virus stocks that could productively infect every human (and many other mammalian) cell line tested to date.

This story took an unexpected and surprising turn in 1998, when Russell and Hirata demonstrated that rAAV vectors could be used for gene targeting (246). Impressively, they used rAAV not just to inactivate genes, but to introduce defined modifications into homologous chromosomal sequences at high frequency. They demonstrated this first with a NEO (neomycin phosphotransferase) reporter construct, but also showed that they could modify an endogenous locus (HPRT; hypoxanthine phosphoribosyl transferase) with very similar efficiency (246). In the intervening 8 years, the Russel laboratoty and many others have confirmed and extended these original observations. Thus, 18 endogenous loci have been inactivated in a wide variety of human cell lines, ranging from investigator favorites like HCT116 and NALM-6 to normal diploid fibroblast or stem cell lines. The most spectacular use of rAAV to date was the correction of a dominant negative mutation in the COL1A1 genein stem cells derived from patients afflicted with osteogenesis imperfecta (39). Overall, 234 rAAV-mediated, correctly-targeted events have been recorded from a total of 6,305 viral integrations. This is an overall targeting frequency of 3.7%, which is far better than the traditional transfection-based approaches.

Why rAAV works so well for gene targeting is not clear. *A priori*, the viru, because of its ITRs, has at least 145 nt of non-homology at either end of the

donor DNA and this is generally a serious, if not insurmountable, deterrent to homologous integration (82). Moreover, because the drug selection cassettes that are usually present on a targeting are ~2 kb length, this restricts the left and right homology arms to ~1.0 kb apiece, such that the resulting recombinant virus can be packaged properly. This length of homology for the arms is extremely short in comparison to traditional approaches using transfection of linear dsDNA, where arms of at least 3 to 8 kb are standard. That rAAV gene targeting does work, however, is indisputable. Since invasion of a single-stranded donar DNA into the recipient chromosome is an essential feature of gene targeting, it is possible that rAAV – a ssDNA virus – directly becomes a HR intermediate and many modles cartoon the single-stranded viral DNA as the strand invader (298). The large stimulation in gene targeting, however, that accompanies the introduction of DSB at the target locus and the recent demonstration that transduction is correlated with the conversion of viral ssDNA to dsDNA suggest more classical models of gene targeting using either on or two ends of linear dsDNA (148). Needless to say, a fuller understanding of the mechanism of rAAV integration and a better ability to manipulate it should facilitate clinical trials. Moreover, research into other features, such as cell cycle and transcriptional effects, the impact of chromatin structure and promoterless selection schemes, etc. are also likely critical parameters and it is an almost certainly that the current rAAV gene targeting efficacy can be substantially optimized.

CHAPTER II

Ku70, an Essential Gene, Modulates the Frequency of rAAV-Mediated Gene Targeting in Human Somatic Cells

Introduction

Somatic gene targeting is defined as the intentional modification of a genetic locus in a living cell (1). This technology has two general applications of interest and importance. One is the inactivation of genes ("knockouts"), a process in which the two wild-type alleles of a gene are sequentially inactivated in order to determine the loss-of-function phenotype(s) of that particular gene. The second application is the clinically more relevant process of gene therapy, which, in a strict sense, involves correcting a preexisting mutated allele of a gene back to wild-type ("knock-ins") in order to alleviate some pathological phenotype associated with the mutation. Importantly, while these two processes are conceptually reciprocal opposites of one another, they are mechanistically identical — as both require a form of DNA double-strand break (DSB) repair termed homologous recombination (HR).

In HR (2), the ends of the donor dsDNA are resected to yield 3'-ssDNA overhangs, which are targets bound by RAD51 and RAD52. RAD51 is a potent strand exchange protein and together with RAD54 (3), an ATPase that remodels chromatin, it facilitates crossover of the incoming donor DNA with its cognate chromosomal homologous sequences. This gene targeting event generates a complex structure that is identical to the linearized plasmid "ends-out" recombination intermediates that have been defined in yeast (4). Resolution of this structure requires the action of helicases, polymerases, resolvases and ligases in a complicated process that has not yet been rigorously defined (2). Importantly, human cells express all of the HR gene products needed to carry out gene targeting (1). These events occur, however, only at a low frequency due to the preferred usage of a competing pathway of DNA DSB repair, nonhomologous end joining (NHEJ).

NHEJ, is an evolutionarily conserved process that joins nonhomologous DNA molecules together (5). In their seminal work on gene targeting, Capecchi and co-workers showed that although somatic mammalian cells can integrate a

linear duplex DNA into corresponding homologous chromosomal sequences using HR, the frequency with which recombination into nonhomologous sequences occurred via NHEJ was at least 1000-fold greater (6). While not all the details of NHEJ have been elucidated, much is known about the process. First, the heterodimeric Ku (Ku86:Ku70) protein binds onto the ends of the donor DNA and prevents the nucleolytic degradation that would otherwise shunt the DNA into the HR pathway (see above; (5)). The binding of Ku to the ends of the DNA then recruits and activates the DNA-dependent protein kinase complex catalytic subunit (DNA-PK_{cs}). This DNA:protein complex is then brought into contact with a chromosome into which a DSB is introduced by a mechanism that is poorly understood although it correlates frequently with chromosomal palindromic sequences (7). Regardless, the chromosomal ends are probably also occupied by Ku and DNA-PK_{cs} and this facilitates the formation of a synaptic complex with the donor DNA (8). Once DNA-PK_{cs} is properly assembled at the broken ends, it, in turn, recruits additional factors such as the nuclease, Artemis, to trim the ends and a DNA ligase complex consisting of DNA ligase IV (LIGIV):X-ray cross complementing group 4:XRCC-4-like factor, to seal the break(s) (5). In summary, humans are different from bacteria and lower eukaryotes in that DSB repair proceeds primarily through a NHEJ recombinational pathway. Moreover, NHEJ must be overcome in order to facilitate gene targeting and this can only occur when the incoming DNA is shunted into the HR pathway.

Adeno-associated virus (AAV) is a nonpathogenic parvovirus — with a natural tropism for human cells — that is dependent upon a helper virus (usually adenovirus and hence the name) for a productive infection (9). In the intervening decade since it was demonstrated that recombinant AAV (rAAV) could be used as a vector for gene targeting in human cells (10), this methodology has gained wide acceptance (1). Seventeen different genes have been modified (generally knocked-out) in a plethora of immortalized and normal diploid human tissue

culture lines ((1) and unpublished data). Moreover, human adult stem cell lines derived from osteogenesis imperfecta patients afflicted with a dominant negative mutation in the COL1A1 gene have been corrected (a knock-in) with rAAV vectors (11). Lastly, over 20 clinical gene therapy trials utilizing rAAV are currently in progress. There are, however, reports of potential difficulties with the clinical use of rAAV vectors. In particular, a recent report found that in a mouse model for lysosomal storage disease mucopolysaccharidosis VII, the random integration of rAAV was associated with a high incidence of hepatocellular carcinoma ((12); reviewed in (13)). Thus, a better understanding of the mechanism of rAAV-mediated gene targeting and the factors that influence the frequency with which it correctly targets (presumably HR-mediated) versus those that influence its random integration (presumably NHEJ-mediated) clearly seems warranted.

Our laboratory has shown that the NHEJ gene Ku86 is essential in human somatic cells using classic gene targeting methodologies (14). To extend these studies to Ku70, we have utilized a rAAV vector approach. As expected, these experiments demonstrated that Ku70 is also essential. Surprisingly, however, the frequency of correct gene targeting increased 5- to 10-fold in Ku70 heterozygous ($Ku70^{+/-}$) cells. RNA interference and short-hairpinned RNA strategies to deplete Ku70 phenocopied these results in wild-type cells and greatly accentuated them in $Ku70^{+/-}$ cell lines. To support the generality of these findings, we extended them to an additional two loci, the chemokine (C-C motif) receptor 5 (CCR5) gene and LIGIV, and observed similar effects. Thus, Ku70 protein levels influenced the frequency of correct rAAV-mediated gene targeting in human somatic cells. Our data demonstrate that gene-targeting frequencies can be significantly improved by impairing the NHEJ pathway and we propose that Ku70-depletion can be used to facilitate both knockout and gene therapy approaches.

Results

Use of Gene Targeting to Generate Ku70-Null HCT116 Cells.

We have generated, using rAAV-based methodology, a $Ku70^{+/-}$ HCT116 cell line ((15); Fig. 1B). HCT116 is a human colon carcinoma cell line that is diploid, has a stable karyotype and is wild type for almost all the DNA DSB repair, checkpoint and chromosome stability genes that have been examined ((1); Fig. 1A). $Ku70^{+/-}$ HCT116 cells showed haploinsufficient deficits as they grew slower, were more sensitive to ionizing radiation and had shortened telomeres in comparison to the parental cell line (15). These phenotypes were not unexpected as heterozygous Ku86 ($Ku86^{+/-}$) HCT116 cells had similar haploinsufficiencies (14, 16). Since we had also subsequently shown that human Ku86 null ($Ku86^{-/-}$) cell lines were not viable, we wanted to extend this observation to human Ku70-deficient cells. To experimentally achieve this goal, one of the $Ku70^{+/-}$ clones (#53; Figs. 1B and 2A) was transiently exposed to Cre recombinase. Cre should excise the internal neomycin selection cassette, which is flanked by loxP sites, within the integrated targeting vector (Fig. 1B). Forty-eight single cell clones were picked, duplicated into media containing or lacking G418 and G418-sensitive clones were identified. Correct excision of the neomycin gene was confirmed by the generation of a diagnostic ~350 bp PCR product with the primer set 70 Cre F and 70 Cre R (Fig. 1C; Fig. 2A, 53-39 lane). Seven such clones were obtained in this fashion and one of them, #53-39, was used for a second round of gene targeting with the original targeting vector containing the neomycin selection cassette. Productive infection of #53-39 cells should produce three potential outcomes: 1) random targeting (the majority of the events), 2) correct targeting, but of the already inactivated allele from the first round of targeting (*i.e.*, “retargeting”; Fig. 1D), or 3) correct targeting of the remaining functional allele to generate the desired null clone (Fig. 1E). Several diagnostic PCR strategies were utilized to distinguish these events (Fig. 1). In two separate screens (elaborated in detail below) a total of 27 correctly targeted clones were obtained. Strikingly, all 27 clones were

retargeted. This conclusion was substantiated by the fact that although all of the clones were correctly targeted (Fig. 1D; Fig. 2B top & data not shown), they still retained exon 4 sequences (Fig. 2B, bottom & data not shown). Moreover, all 27 of the clones still expressed Ku70 protein at levels that were ~50% of that observed in the parental cell line (Fig. 2C and data not shown). The large disequilibrium in gene targeting in which 27/27 clones were re-targeted and no null clones were obtained strongly suggests that Ku70, like Ku86, is an essential gene in human somatic cells.

Diminished Ku70 Protein Levels Increase the Gene-Targeting Frequency of the Ku70 Locus in HCT116 Cells.

The above results, while important, were rather expected. One surprising finding, however, was observed. Our initial frequency for obtaining $Ku70^{+/-}$ cell lines was 0.69% — 3 correctly targeted clones identified from 437 G418-resistant, internal control PCR-positive, clones screened ((15); Table 1). In the first attempt to obtain a null clone, 4 correctly targeted clones (all retargeted) were identified from a total of 97 G418-resistant colonies, for a targeting frequency of 4.12% (Table 1). This represented a 6-fold (4.12/0.69 = 5.97) increase in the gene targeting frequency in $Ku70^{+/-}$ cells. To investigate whether the reduced Ku70 expression level was facilitating a higher frequency of correct targeting, we attempted to phenocopy this effect. Thus, the parental HCT116 cell line ($Ku70^{+/+}$) was utilized to stably express a short hairpin RNA (shRNA) — obtained from the MISSION™ TRC-Hs 1.0 (human) lentiviral shRNA library (17) — targeting Ku70. Five different shRNA sequences (#608, #609, #610, #611 and #612) were tested for their ability to knockdown the level of Ku70 in HCT116 cells. Among these five sequences, #609 and #610 reduced Ku70 expression the best — to about ~10% of that observed in the parental line (Fig. 3A). The cell line expressing the shRNA sequence #610 ($Ku70^{shRNA}$) was used for Ku70 gene targeting and 2 of 65 total clones were correctly targeted (Table 1). This

represented a 4.6-fold increase over the parental HCT116 line. Next, we utilized the siGENOME SMARTPool on the parental HCT116 cells to silence Ku70 expression to ~20% of that observed in the control transfected population (Fig. 3B). These cells ($Ku70^{siRNA}$) had a 8.4-fold increase in gene targeting (10/173; 5.78%; Table 1). To extend this line of experimentation to its logical conclusion, siRNA was used in an attempt to further knockdown Ku70 protein expression in 53-39 $Ku70^{+/-}$ cells that already contained reduced levels of Ku70 due to genetic ablation. Thus, 53-39 $Ku70^{+/-}$ cells were transfected twice at 24 hr intervals with the siGENOME SMARTPool for Ku70. A significant reduction in Ku70 protein levels as assessed by Western analysis 48 hr following the first siRNA treatment was observed (Fig. 3B, 53-39 + siRNA). 53-39 $Ku70^{siRNA}$ cells expressed ~5% the Ku70 protein when compared to the parental cells. Moreover, the Ku86 protein level in 53-39 $Ku70^{siRNA}$ cells was also decreased confirming previous observations suggesting that the stability of Ku70 and Ku86 are coordinately linked (5, 14). Impressively, 23 correctly targeted (all retargeted) clones were recovered from 111 G418-resistant clones screened, for a targeting frequency of 20.72% (Table 1). This represented a 30-fold increase in gene targeting compared to the parental line. It is important to note that this was a minimum frequency since a statistically equal number (*i.e.*, 23) of null clones were presumably not recovered because Ku70 is essential. *In toto*, these results demonstrated that lowering the expression level of Ku70 significantly increased the gene targeting frequency at the Ku70 locus in HCT116 cells.

Diminished Ku70 Protein Levels Increase the Gene-Targeting Frequency at Other Loci in HCT116 Cells.

To investigate the generality of the enhancement of gene targeting by Ku70 depletion, the gene targeting frequency at another locus, chemokine (C-C motif) receptor 5 (CCR5), was determined. CCR5 is a cell surface co-receptor for the human immune deficiency virus and has no known role in DNA repair (18).

Moreover, a rAAV targeting vector for CCR5 and methodologies for identifying correct targeting events had already been well-established by the laboratory of Bert Vogelstein (19). Using this vector and these methodologies, we determined that the targeting frequency for the parental cell line was 1.06% (Table 2). In four independent Ku70-reduced backgrounds we observed a significant increase in the correct gene targeting frequency (Table 2). This included $Ku70^{shRNA}$ cells (5.2%; a 4.5-fold increase), $Ku70^{siRNA}$ cells (5.3%; a 4.6-fold increase), 53-39 ($Ku70^{+/-}$) cells (6.6%; a 5.8-fold increase) and 53-39^{siRNA} cells (9.9%; a 8.6-fold increase). Thus, without exception and regardless of which technique was utilized, a reduction of Ku70 expression increased the frequency of gene targeting 4- to 9-fold at the CCR5 locus.

Finally, the effect of Ku70 depletion on gene targeting frequency at the LIGIV locus was analyzed. Recently, our laboratory has generated $LigIV^{+/-}$ cell lines in a HCT116 background using a rAAV-mediated knockout approach (Oh, S. and Hendrickson, E. A., manuscript in preparation) by deleting part of exon 3 of this locus. Two correctly targeted LIGIV cell lines were identified from 176 drug resistant clones screens, for a targeting frequency of 1.13% (Table 3). When these studies were repeated in the $Ku70^{+/-}$ clone 53-39, 6 correctly targeted LIGIV cell lines from 148 drug-resistant clones were identified. This corresponds to a 4.05% targeting frequency and a 3.6-fold increase in gene targeting in comparison to the parental line.

In summary, multiple targeting experiments at 3 different loci (Ku70, CCR5 and LIGIV) demonstrated that a reduction in Ku70 expression facilitates correct gene targeting in human somatic cells.

Diminished Ku70 Protein Levels Do Not Decrease the Frequency of rAAV Random Integration.

An explanation of the above results is that in the presence of reduced levels of Ku70, the number of correct gene targeting events increases. An alternative

possibility is that the absolute number of correct targeting events remains constant, but that the number of random integration events is decreased. To experimentally test this latter possibility, the frequency of random integration events was measured. Equal numbers of the parental cells (WT HCT116), parental cells expressing shRNA (WT + shRNA), $Ku70^{+/-}$ cells (53-39) and $Ku70^{+/-}$ cells expressing shRNA (53-39 + shRNA) were independently infected with three different concentrations of two different rAAV viral stocks. Two to three weeks later, the total number of drug-resistant colonies was scored. There was no statistically significant difference between any of the cell lines for either virus at any concentration (Supplementary Fig.1). Thus, we conclude that a reduction in Ku70 in human somatic cells does not result in a reduction of random integration of rAAV gene targeting vectors.

Discussion

Ku70 is Essential in Human Somatic Cells.

The Ku heterodimer is a well-conserved protein(s), with homologs known to exist in every species from bacteria to humans (5). In all organisms examined, mutations in either Ku subunit result in the expected deficits in DNA DSB repair, DNA recombination and sensitivities to DNA damaging agents. Importantly, in all organisms — with one glaring exception — Ku is nonetheless dispensable for viability. Intriguingly, humans appear to be unique in that Ku has evolved into an essential gene. This hypothesis is supported by the lack of documentation for even a single patient with a mutation in either Ku subunit. Moreover, the targeted disruption of both alleles of the Ku86 gene in human HCT116 somatic cells was lethal (14). The reason why Ku should be uniquely essential in humans is not clear although a role in telomere maintenance seems likely (16). Here, we corroborate the hypothesis that Ku is essential in humans by demonstrating that Ku70-null cells are not viable. This conclusion was based upon 27 recovered second round targeting events, which occurred solely on the already inactive allele (Fig. 2 and Table 1). There is overwhelming evidence to support the view that targeting vectors target the paternal & maternal alleles without bias. In an experiment designed to disrupt b-catenin, 11 second round targeting events occurred on the functional allele and 15 on the inactive allele (20). Similarly, in two independent studies involving Ki-*ras*, 4 from 7 (21) and 9 from 15 (22) targeting events occurred on the functional allele. Moreover, in rAAV-mediated targeting studies, 10 from 19 targeting events for COL1A1 occurred on the wild-type allele and 9 of 19 on the mutant allele (11). Because of this lack of bias in the targeting methodology, the striking disequilibrium of 27 out of 27 retargeting events is strong evidence for the essential nature of Ku70 in HCT116 cells. A direct demonstration of the essential nature of Ku70 awaits the construction of a cell line expressing a conditionally-null Ku70 allele.

Reduced Ku70 Expression Augments the Frequency of Correct Gene Targeting in Human Somatic Cells.

Attempts to target the second allele of the Ku70 locus demonstrated that the gene targeting frequency was higher in $Ku70^{+/-}$ cells compared to the parental cell line. The interpretation of this result — that a reduction in Ku protein levels increases the frequency of gene targeting — was confirmed by two independent methodologies: that of transient RNA interference and the stable use of short-hairpinned RNAs (Table 1) and was confirmed at additional loci (Tables 2 and 3). It should be noted, however, that there wasn't always a linear relationship between the levels of Ku70 protein in a cell line and the frequency of gene targeting. Thus, the $Ku70^{shRNA}$ cells expressed less Ku70 protein than the $Ku70^{+/-}$ cells, but had a lower — and not the predicted higher — frequency of gene targeting (Tables 1 and 2). This was probably due to the much slower growth of the $Ku70^{shRNA}$ cells (our unpublished observations), which may have a deleterious effect on gene targeting since rAAV preferentially transduces actively dividing cells (23). Similarly, the $Ku70^{siRNA}$ cells expressed less Ku70 protein than the $Ku70^{+/-}$ cells, but the two cell lines often had about the same frequency of gene targeting (Tables 1 and 2). This was likely due to the fact that the $Ku70^{siRNA}$ cells represented a heterogeneous population of cells with some cells being effectively transfected and other cells not, which presumably translated itself into heterogeneous targeting frequencies. These technical qualifiers notwithstanding, a reduction in Ku70 protein expression was without exception always associated with an increase in the frequency of correct gene targeting.

The demonstration that Ku can regulate gene targeting is very well documented in fungal systems. Thus, deletion of *Neurospora crassa* Ku70 and Ku86 genes resulted in higher gene targeting frequencies (100% in the mutants as compared to 20% in wild type cells) (24). This observation was then utilized in a robotics-driven, whole genome approach to expedite the functional inactivation

of 103 transcription factor genes (25) demonstrating the potent utility of Ku-reduced strains. Moreover, there has been a spate of reports of highly efficient correct gene targeting in Ku–deletion strains of 5 different species of *Aspergillus* (*e.g., Aspergillus niger* (26)), as well as *Sordaria macrospora* (27), and *Cryptococcus neoformans* (28), demonstrating that Ku-deficient strains are useful for gene targeting in filamentous fungi. Furthermore, the disruption of yKu70 (29) or *Kl*KU80 (30) also increased the frequency of gene targeting in the budding yeasts *Saccharomyces cerevisiae* and *Kluyveromyces lactis*, respectively. Thus, in fungi, where Ku is not essential, there is an exceptionally good correlation between reduced Ku expression and increased gene targeting.

An extrapolation of these observations to higher eukaryotes, however, has been lacking. Thus, deletion of Ku70 in chicken DT40 cells (31) and Ku70 (32) or Ku86 (33) in mouse cells did not result in an increase in gene-targeting frequencies. The discrepancy between human and chicken somatic cells can be reconciled given that DT40 cells are known to employ HR at high frequency (34). An explanation for the difference between human and mouse cells, however, is less obvious, albeit consistent with the more stringent requirement for Ku/NHEJ in human cells (this work; (14)). One possibility may be that mouse embryonic stem or fibroblast cells — the cells in which the mouse targeting experiments were carried out — may, like DT40 cells, carry out HR at a higher frequency than human somatic cells. Another possibility is that there are locus specific effects as, to date, only a single X-linked locus (the hypoxanthine phosphoribosyl transferase) locus has been examined in the mouse (32, 33). In summary, additional experiments are needed before it can be determined whether or not the observations reported here for human somatic cells are evolutionarily conserved.

There are multiple indirect mechanisms whereby Ku could regulate gene targeting such as by modulating the conversion of single-stranded viral DNA into double-stranded DNA. This process would be required if the gene replacement

aspect of rAAV gene targeting requires two independent crossover events (and thus two independent 3'-ends on the donor DNA). Hendrie and Russell, however, have argued (albeit circumstantially) that rAAV-mediated gene targeting is more likely mediated by viral single-stranded, rather than double-stranded, DNA (35). If this hypothesis is true, then we would instead favor a direct "competition" model that has been suggested by many laboratories (*e.g.*, (36)) whereby Ku and Rad52 compete for the viral DNA ends and shunt the virus into either NHEJ or HR pathways, respectively. This model is consistent with the demonstration that both Ku and Rad52 physically bind to rAAV ITRs during a viral infection (37). In this model, a reduction in Ku posits that Rad52 will statistically stand a better chance of binding the hairpin-shaped viral inverted terminal repeats (ITRs) and funnel the DNA into the HR pathway. In a wild-type cell, however, where Ku is more abundant than Rad52, the presence of normal amounts of Ku would favor random integration mediated by NHEJ. Mechanistically, the most likely role for Ku in rAAV random integration is to recruit DNA-PK_{cs} to the viral ITRs. DNA-PK_{cs}, would, in turn, recruit and activate the nuclease Artemis, which nicks open the viral ITR hairpins (38) facilitating integration of the virus. The observation that the vast majority of random rAAV integration events that have been sequenced have a viral endpoint that maps to the viral ITRs supports this interpretation (39). The competition model is not consistent with the conclusion that DNA-PK actually inhibits rAAV integration in mouse muscle (40) nor with a report that shRNA-mediated silencing of DNA-PK_{cs} gene expression in human MO59K somatic cells had no effect on rAAV-mediated gene targeting (41). However, in preliminary studies with HCT116 cell lines containing functional inactivation of either one or both DNA-PK_{cs} alleles we have repeatedly seen large increases in the correct gene targeting frequency that are comparable to those reported here for Ku-reduced cell lines (our unpublished data) supporting both a role for DNA-PK_{cs} in viral ITR nicking (38) and the competition model.

Other investigators have suggested that in addition to Ku and Rad52 competing for DNA ends that Ku may also actively suppress HR (42). We favor this hypothesis because it provides at least a partial explanation for the finding that the frequency of random integrations was not lower in a Ku-reduced background (Supplemental Fig. 1). Thus, if HR not only has less competition for the viral ends in the absence of Ku, but is also more active, it may facilitate viral integrations at chromosomal sites that are quasi homologous to the viral ITRs. Another potential explanation for the lack of an effect of a Ku deficiency on overall integrations is the recent description of an alternative (Ku-independent) NHEJ pathway (A-NHEJ; reviewed in (43)). In contrast to the classical, Ku-dependent NHEJ, which works on virtually all DNA DSBs, A-NHEJ seems to only work on a subset of these and/or in specialized pathways since it can participate in the repair of switch recombination-induced DSBs, but not ionizing radiation-induced DSBs (43). If A-NHEJ can also work in the pathway of gene targeting to facilitate random integrations, this might explain why the frequency of correct gene targeting goes up (Tables 1, 2 and 3) even when the frequency of random targeting does not change (Supplemental Fig. 1). In any case, it is important to emphasize that it has long been known that additional pathways for chromosomal DNA integration are quite active in DNA-PK defective cells (44) .

Regardless of the precise mechanism by which Ku regulates rAAV integration, we have demonstrated that a reduction in the levels of Ku70 in HCT116 human somatic cells greatly elevates the frequency of correct gene targeting. These observations have significant practical implications for basic researchers interested in gene disruption strategies and for clinical researchers interested in gene therapy.

Methods

Cell Culture. The human colon cancer cell line HCT116 was obtained from ATCC and maintained in McCoy's 5A media containing 10% FBS, 2 mM L-glutamine, 100 U/ml penicillin and 100 U/ml streptomycin. The cells were grown at 37°C in a humidified incubator with 5% CO_2. Cell lines harboring the targeting vector were grown in 1 mg/ml G418.

Silencing of Ku70. The pLKO.1-puromycin-based lentiviral vectors containing sequence-verified shRNA targeting Ku70 (XRCC6; GenBank accession number NM_001469) were obtained from the MISSION™ TRC-Hs 1.0 (Human) shRNA library through Sigma-Aldrich {TRCN0000039608, (#608); TRCN0000039609, (#609); TRCN0000039610, (#610); TRCN0000039611, (#611); TRCN0000039612, (#612)}. For the RNAi experiments, pre-designed, double-stranded siRNAs (SMARTPool) targeting human Ku70 were purchased from Dharmacon.

Targeting Vector Construction, Packaging and Infection. The targeting vectors, Ku70-Neo and LIGIV-Neo, were constructed utilizing the rAAV system as described elsewhere ((15); Oh, S. *et al*., unpublished data). The CCR5-Neo targeting vector has been described (19). All virus packaging and infections were performed as described (19).

Isolation of Genomic DNA and Genomic PCR. Genomic DNA for PCR screening was isolated using phenol extraction followed by ethanol precipitation. Ku70 and LIGIV targeting events were identified by PCR using the conditions described elsewhere (19). After Cre-treatment, the loss of Neo sequences was confirmed using 70 Cre F, 5'-CTGAGCACTTATGGAGCTTCCATTTAGTGGTAAG-3' and 70 Cre R, 5'-GAAGGCGGAGGTTGCAGTGAGCCAAGATTGTGCCAC-3' (Fig. 1C). For the

second round of Ku70 targeting, the Neo F2 (5'-GTGGCCGAGGAGCAGGACTGAATAAC-3') forward primer was used instead of the RarmF primer (Fig. 1D). Lastly, confirmation of the retention of exon 4 in retargeted clones was confirmed by PCR using Ku70 Ex4 F1, 5'-CAAGACATGATGGGCCACGGATC-3' and Ku70 3,4 R1 primers (Fig 1A). CCR5 targeting events were identified by PCR using the primers and conditions described elsewhere (19).

Cre-mediated Excision of the Neo Marker. Correctly targeted clones were transiently transfected by electroporation with pML-Cre to remove the Neo cassette. Cells were then grown in complete medium and plated 48 hr later at limiting dilution in 96-well plates. Single clones were picked 2 to 3 weeks later and transferred to 24-well plates. Each expanded clone from the 24-well plate was then duplicated into two 24-well plates: either without or with G418 (1 mg/ml). After a week, G418-sensitive clones were screened by PCR to confirm the loss of the Neo sequence (Fig. 1C).

Antibodies and Immunoblotting. Ku70 and Ku86 (Santa Cruz) and α-tubulin (Covance) antibodies were used for detection. Proteins were subjected to electrophoresis on a 4-20% gradient gel (Bio-Rad), electroblotted and detected as described (15).

Acknowledgements

The authors are indebted to Dr. B. Vogelstein (J. Hopkins University) and the many members of his laboratory who were extremely generous with their reagents and advice. The authors are also indebted to Brian Ruis (U. of Minnesota) for his technical help in establishing and using the rAAV gene targeting system. We would like to thank Dr. A.-K. Bielinsky for her helpful comments on the manuscript. These studies were supported in part by National Institutes of Health grants GM 069576 and HL079559 to EAH.

Fig 1. Experimental strategy and screening protocols for disruption of the Ku70 locus in human somatic cells. (A) A cartoons of the relevant portion (large rectangles = exons 3 and 4) of the human Ku70 genomic locus (horizontal line = genomic DNA) in the parental wild-type cells. The black arrows demarcate the indicated PCR primers. (B) The Ku70 locus in $Ku70^{+/-}$ (clone #53) cells. One of the endogenous alleles has been replaced by homologous genomic sequence (horizontal gray bars), LoxP sites (filled triangles) and the neomycin (Neo) resistance gene (rectangle). Additional PCR primers (black arrows) are indicated. (C) The Ku70 locus in $Ku70^{+/-}$ (clone #53-39) cells following Cre treatment. All symbols are as in (B). Additional PCR primers (black arrows) are also indicated. (D) The Ku70 locus in $Ku70^{+/-}$ (clone #53-39) cells following retargeting to the already inactive allele. All symbols are as in (B). Additional PCR primers (black arrows) are also indicated. (E) The Ku70 locus in $Ku70^{+/-}$ (clone #53-39) cells following correct second round targeting to the functional allele to generate the null cell line. All symbols are as in (B).

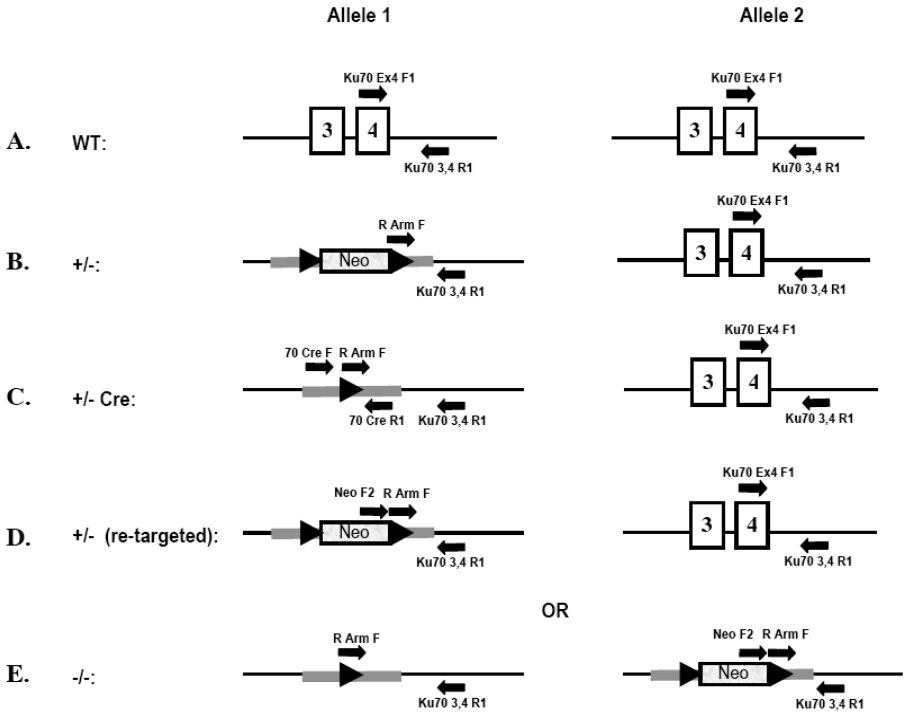
Allele 1
Allele 2
A.
WT:
Ku70 Ex4 F1
3
4
Ku70 3,4 R1
B.
+/-:
R Arm F
Neo
C.
+/- Cre:
70 Cre F
70 Cre R1
D.
+/- (re-targeted):
Neo F2
OR
E.
-/-:

Fig 2. Disruption of the Ku70 locus in HCT116 cells by gene targeting. (A) PCR characterization of the $Ku70^{+/-}$ clones #53 and #53-39. Ethidium bromide (EtBr)-stained agarose gels are shown. Left panel — from left to right the lanes are: molecular weight (MW) markers, genomic DNA isolated from wild-type cells and genomic DNA derived from clone #53 cells. The PCR reaction utilized the primers RArmF and Ku70 3,4 R1 (Fig. 1) and the diagnostic ~1.6 kb band was observed only in clone #53. Right panel — from left to right the lanes are: MW markers, genomic DNA isolated from clone #53 cells and genomic DNA derived from clone #53-39 cells. The PCR reaction utilized the primer set 70 Cre F and 70 Cre R and the diagnostic ~350 bp PCR product was observed only in clone #53-39. (B) Identification of correctly targeted clones following the second round of gene targeting. EtBr-stained agarose gels are shown. Top and Bottom panels — from left to right the lanes are: MW markers, and then genomic DNA isolated from the indicated cell lines. The PCR reaction for the top panel utilized the primer set Neo F2 and Ku70 3,4 R1 (Fig. 1) and the diagnostic ~1.6 kb band was observed only in those clones that were correctly targeted and contained the Neo gene. The PCR reaction for the bottom panel utilized the primer set Ku70 Ex4 F1 and Ku70 3,4 R1 (Fig. 1) and the diagnostic ~1.6 kb band, which indicated the retention of at least one copy of exon 4 was observed in all the clones. (C) All correctly targeted clones still express Ku70 protein, albeit at reduced levels. Whole cell extract of the indicated cell lines was subjected to immunoblot analyses to detect Ku70 (Top), and tubulin (Bottom) protein levels.

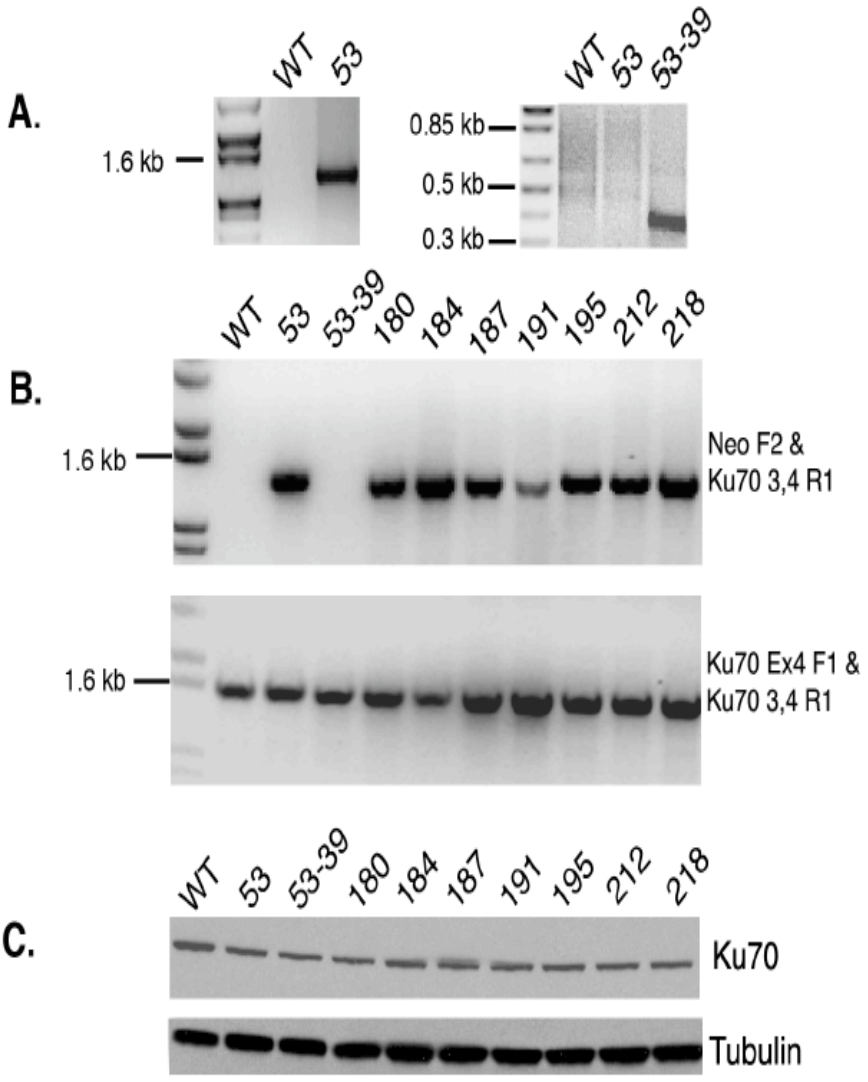
A.
WT
53
1.6 kb
WT
53
53-39
0.85 kb
0.5 kb
0.3 kb
B.
WT
53
53-39
180
184
187
191
195
212
218
1.6 kb
Neo F2 &
Ku70 3,4 R1
1.6 kb
Ku70 Ex4 F1 &
Ku70 3,4 R1
C.
WT
53
53-39
180
184
187
191
195
212
218
Ku70
Tubulin

Fig 3. Disruption of Ku70 gene expression by RNA interference technologies. (A) Stable cells lines generated using shRNA expression show reduced expression of Ku. Wild-type HCT116 cells were infected with lentiviruses carrying short-hairpin sequences (#609, # 610 or both #609 and #610). Whole cell extracts from stable puromycin resistant clones were subjected to immunoblot analyses using extracts from wild-type (WT) and clone #53-39 as controls. The extracts were probed sequentially for Ku70 expression and then Ku86 and tubulin. For the gene targeting experiments described in the manuscript, the #610 shRNA-treated stable line was used. A phosphoimager quantitation of this blot is shown below the figure. (B) Transient depletion of Ku70 protein expression. Wild-type (WT) and $Ku70^{+/-}$ 53-39 cells were transfected with a Ku70 siGENOME SMARTpool. All cells were transfected two times at 24 hr intervals and then harvested 72 hr after the first siRNA treatment. A knockdown of gene expression was measured by immunoblotting with the indicated antibodies. A phosphoimager quantitation of this blot is shown below the figure.

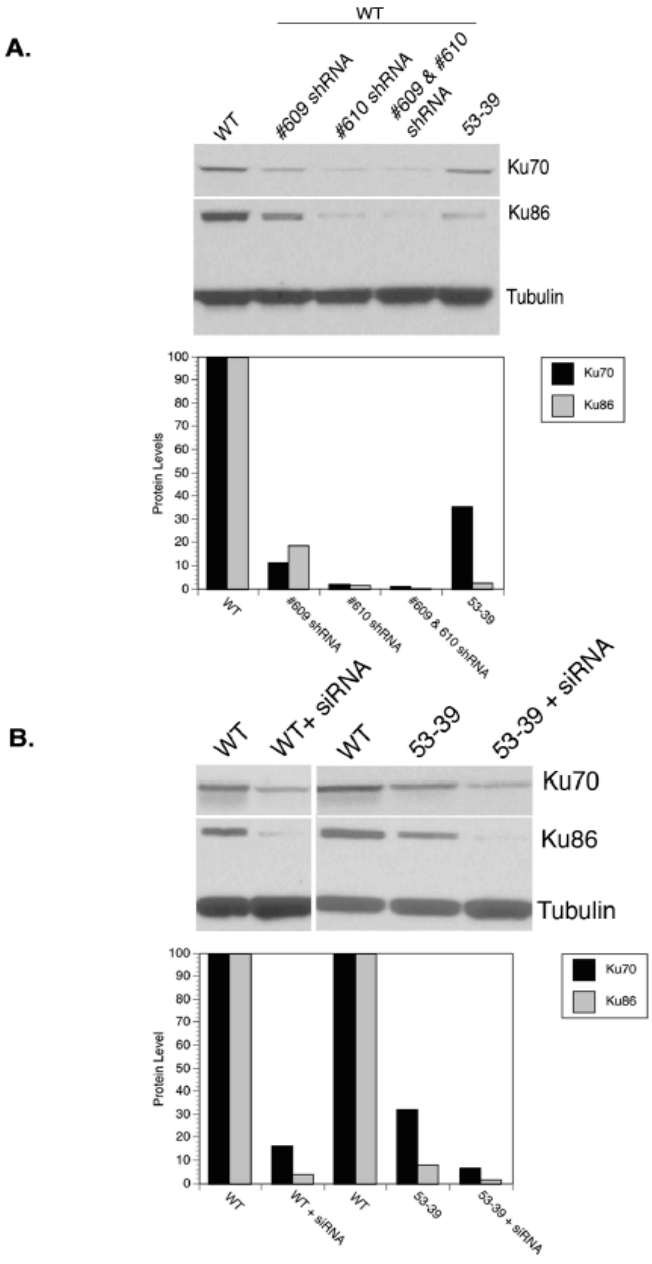
A.
WT
WT
#609 shRNA
#610 shRNA
#609 & #610 shRNA
53-39
Ku70
Ku86
Tubulin
Protein Levels
100
90
80
70
60
50
40
30
20
10
0
Ku70
Ku86
WT
#609 shRNA
#610 shRNA
#609 & 610 shRNA
53-39
B.
WT
WT+ siRNA
WT
53-39
53-39 + siRNA
Ku70
Ku86
Tubulin
Protein Level
100
90
80
70
60
50
40
30
20
10
0
Ku70
Ku86
WT
WT + siRNA
WT
53-39
53-39 + siRNA

Supplemental Fig. 1. A reduction in Ku70 protein levels does not affect random integration. WT HCT116, WT HCT116 treated with shRNA, $Ku70^{+/-}$ (53-39), and $Ku70^{+/-}$ (53-39) cells treated with shRNA were tested for their ability to be infected by either Ku70 rAAV (A) or CCR5 rAAV (B) viruses at different multiplicity of infections (shaded bars). Each experiment was performed twice and the average +/- the standard deviation is shown.

A. **Random Integration of Ku70 rAAV**

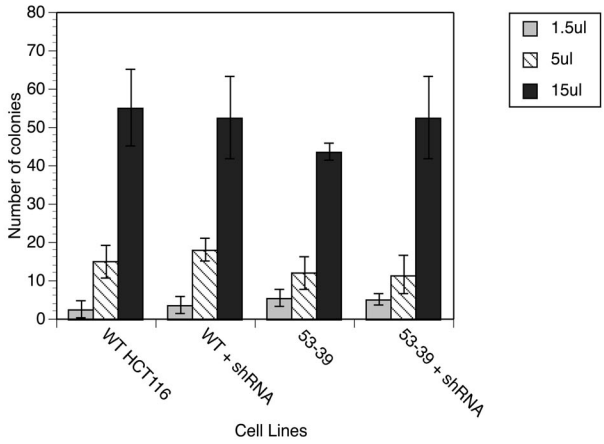

B. **Random Integration of CCR5 rAAV**

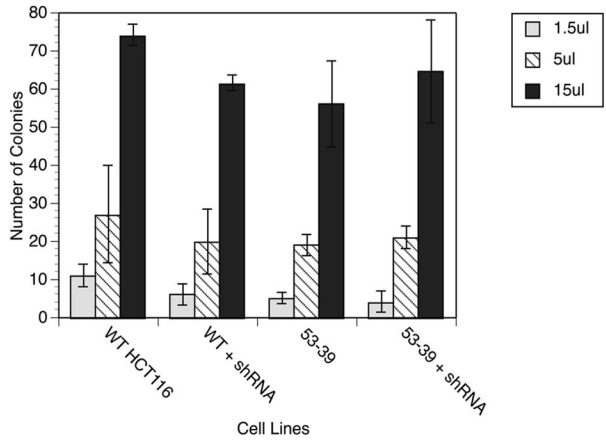

Table 1. Summary of gene targeting frequencies at the Ku70 locus

Cell line	# of colonies screened[a]	# of correctly targeted clones[b]	Targeting frequency[c]	Fold increase[b]
WT HCT116	437	3	0.69	1.0
WT HCT116 + Ku70 siRNA	173	10	5.78	8.4
WT HCT116 + Ku70 shRNA	65	2	3.08	4.4
53-39 ($Ku70^{+/-}$)	97	4	4.12	6.0
53-39 ($Ku70^{+/-}$) + Ku70 siRNA	111	23	20.72	30.0

[a]Drug resistant clones that were also positive for the internal control PCR.

[b]Drug resistant clones that showed correct targeting by PCR.

[c]Targeting frequency is the number of correctly targeted colonies per 100 drug-resistant colonies screened.

[d]The WT targeting frequency is set at 1. The fold increase = the targeting frequency in a specific cell line / targeting frequency in the WT background (0.69).

Table 2. Summary of gene targeting frequencies at the CCR5 locus

Cell line	# of colonies screened[a]	# of correctly targeted clones[b]	Targeting frequency[c]	Fold increase[b]
WT HCT116	262	3	1.15	1.0
WT HCT116 + Ku70 siRNA	150	8	5.33	4.6
WT HCT116 + Ku70 shRNA	96	5	5.20	4.5
53-39 ($Ku70^{+/-}$)	105	7	6.66	5.8
53-39 ($Ku70^{+/-}$) + Ku70 siRNA	152	15	9.86	8.6

[a]Drug resistant clones that were also positive for the internal control PCR.

[b]Drug resistant clones that showed correct targeting by PCR.

[c]Targeting frequency is the number of correctly targeted colonies per 100 drug-resistant colonies screened.

[d]The WT targeting frequency is set at 1. The fold increase = the targeting frequency in a specific cell line / targeting frequency in the WT background (1.15).

Table 3. Summary of gene targeting frequencies at the LIGIV locus

Cell line	# of colonies screened[a]	# of correctly targeted clones[b]	Targeting frequency[c]	Fold increase[b]
WT HCT116	176	2	1.13	1.0
53-39 ($Ku70^{+/-}$)	148	6	4.05	3.5

[a]Drug resistant clones that were also positive for the internal control PCR.

[b]Drug resistant clones that showed correct targeting by PCR.

[c]Targeting frequency is the number of correctly targeted colonies per 100 drug-resistant colonies screened.

[d]The WT targeting frequency is set at 1. The fold increase = the targeting frequency in a specific cell line / targeting frequency in the WT background (1.13).

CHAPTER III

XLF is Necessary for Cell Proliferation, Non-homologous End Joining and V(D)J Recombination in Human Somatic Cells

Introduction

DNA DSBs (double-strand-breaks) are the most cytotoxic form of DNA damage. They can occur by exogenous agents such as IR (ionizing radiation), topoisomerase inhibitors, radiomimetic drugs (e.g. bleomycin), and by cellular processes such as V(D)J recombination, class switch recombination, stalled replication forks and reactions that generate reactive oxygen species (30).

In mammalian cells there are two major pathways for the repair of IR-induced DSBs, namely non-homologous end joining (NHEJ) and homologous recombination (HR) (118); (176). HR is an accurate form of repair, which requires an undamaged sister chromatid to act as a DNA template and functions only after DNA replication (118); (25). In contrast, NHEJ is active throughout the cell cycle (244) and is considered the major pathway for the repair of IR-induced DSBs in human cells (25). In its simplest sense, NHEJ entails straightforward ligation of DNA ends. However, since the DNA ends formed by IR are complex and frequently contain non-ligatable end groups and other types of DNA damage, successful repair of DNA lesions by NHEJ must require processing of the ends prior to ligation. This can lead to loss of nucleotides from either side of the breaks, making NHEJ essentially error prone. In addition to HR and NHEJ, there is also increasing evidence for the existence of alternative end-joining pathway that directly ligate DNA ends in the absence of NHEJ (310), (309); (302), (11), (321). However, whether these pathways functions in normal cells or only when NHEJ is deficient is not clear.

There are seven well-characterized C-NHEJ factors (Ku70/Ku86 heterodimer, DNA-PK_{cs} (DNA-dependent protein kinase catalytic subunit), Artemis, XRCC4 (X-ray-complementation Chinese hamster gene 4), DNA ligase IV (LIGIV) (71), and another XLF/Cernunnos (thereafter XLF), that was discovered more recently (26), (4). Processing enzymes, such as DNA polymerase μ and λ, PNK (polynucleotide kinase) and WRN (Werner's syndrome helicase) also play a role in NHEJ, at least at a subset of DNA ends (166), (167).

The heterodimeric Ku protein (Ku86 and Ku70), binds DSBs, where among other functions, it recruits downstream C-NHEJ factors. DNA bound Ku forms a complex with and activates the DNA-dependent catalytic subunit, DNA-PK_{cs}, which subsequently activates the endonuclease activity of Artemis (95), (185), (201). The Artemis endonuclease processes a subset of DNA ends to prepare them for end joining (240). Finally Ligase IV (LIGIV), in association with XRCC4, performs the end ligation reaction. Ligase IV alone is capable of joining DNA as a purified protein (238)) so the role of XRCC4 appears to be regulatory, perhaps through a structural contribution to the repair complex.

In mammals, the generation of the immune system requires a somatic site-specific rearrangement process termed V(D)J recombination (223), (268). In progenitor cells, large clusters of isolated V (variable), D (diversity) and J (joining) elements reside along the chromosome. During B- and T-cell development, individual V, D, and J elements are extracted from these clusters and are enzymetically assembled to generate a functional V(D)J element that will ultimately partially encode an Ig or TcR receptor protein, respectively. V(D)J recombination is initiated by the recombination activating genes 1 and 2 (RAG1 and RAG2 endonucleases), which introduces DSBs between participating V, D or J coding sequences and flanking recombination signal (RS) sequences. RAG-mediated cleavage produces two blunt 5'-phosphorylated RS ends and two covalently sealed (hairpin) coding ends. Subsequently, C-NHEJ repairs the RS ends and coding ends to form RS and coding joint, respectively (71). Core C-NHEJ factors are required for both coding and RS joins, while DNA-PK_{cs} and Artemis are usually not required for blunt ligation of RS ends, but are instead required for coding joint formation due to their role in opening and processing hairpin intermediates (71)

XLF is the most recent member of the NHEJ core factor. The human XLF gene is located on chromosome 2q35 (4). Human XLF mRNA is ubiquitously expressed and encodes a nuclear protein of 299 amino acids with a theoretical

molecular weight of 33 kD (4), (26), (33). The amino acid sequence of XLF is conserved to a low degree from yeast to human (121), (7), (160), *NEJ1,* being the yeast homolog of XLF (121). Several inherited mutations of XLF have been identified in human patients (4), (26). Most recently, a balanced translocation that interrupts the XLF gene, has been identified in a fetal autopsy samples and suggested to be associated with polymicrogyria (PMG) (35).

XLF is similar in structure to XRCC4 (4), (162), (7), interacts with XRCC4 and is required for NHEJ and V(D)J recombination (4), (26), (258). In vitro, XLF stimulates the activity of DNA ligase IV towards non-compatible DNA ends, suggesting that XLF may only regulate the activity of XRCC4-Ligase IV under a subset of conditions (104), (162), (179), (282), (121). Like XRCC4, XLF also interacts with DNA. This interaction is highly dependent on the length of the DNA molecule and is enhanced by Ku (324), (179). Surprisingly, given the ability of XLF to interact with XRCC4, XRCC4 was not required for the recruitment of XLF to sites of DNA damage in vivo ((Yano, 2008 #851). However, the presence of XRCC4 did result in XLF being retained to the DSB through interaction with DNA-bound Ku. Like XRCC4, XLF is phosphorylated *in vitro* at c-terminal sites by DNA-PK and is phosphorylated by both ATM and DNA-PK *in vivo*; though phosphorylation is not required for NHEJ and its function remains unclear (328).

In mice, deficiency of any of the six well-characterized C-NHEJ factors results in increased cellular ionizing radiation (IR) sensitivity, genomic instability and severe combined immunodeficiency (SCID) due to the inability to complete V(D)J recombination (71). Moreover, targeted disruption of XRCC4 (88) and LIGIV (13), (84) in mice also results in embryonic lethality because of neuronal degeneration caused by p53-induced apoptosis (84), (88). Human somatic cells deficient for LIGIV show IR sensitivity and V(D)J recombination defect (100), (261). Moreover, mutations in LIGIV in human patients result in cancer predisposition and immuno-deficiencies (112). Most recently the van Gent laboratory in Amsterdam has described a patient with a misssense mutation in

DNA-PK_{cs} that results in radiosensitivity and inhibits Artemis activation (293). Artemis mutations in humans lead to SCID (201). In contrast, XLF mutations in humans lead to microcephaly and a combined immunodeficiency that is less severe than that associated with Artemis mutation (26), (4). XLF deficient human fibroblasts (26), (4) and mouse ES cells (331) are IR sensitive and have severe DSB repair defects, including severely impaired V(D)J recombination defect. However, surprisingly the mouse generated from $XLF^{\Delta/\Delta}$ ES cells are alive unlike other member of ligase IV complex, i.e. XRCC4 or LIGIV (160). This data suggests that, during embryonic development, XLF can be compensated by other factor/s. Detailed analyses demonstrated that the V(D)J recombination activities in the lymphocytes of the XLF knockout mouse are very similar to those of the wild type cells, although the ES cells exhibit impaired V(D)J recombination. These observations suggest the presence of a lymphocyte-specific compensation mechanism for XLF function. It is likely that similar compensation exists in human lymphocytes, because the XLF defective patients showed less severe immunodeficiency compared to the other NHEJ-deficient disorders. The precise mechanism of the lymphocyte-specific compensation of XLF is an important question that needs to be elucidated.

To explore the requirement for XLF expression in human somatic cells in more detail, we attempted to disrupt, via gene targeting, the XLF gene in the human adenocarcinoma somatic tissue culture cell line HCT116. While HCT116 is an immortalized and transformed cell line, it is diploid, has a stable karyotype, and is wild type for most DNA repair, DNA checkpoint, and chromosome stability genes (119). We describe here the isolation and characterization of HCT116 cell lines that are heterozygous and null for XLF expression. Our data demonstrate that XLF is not an essential gene in human somatic cells. We have used biochemical and cellular approaches to dissect the role of XLF in NHEJ in human cell. Our findings provide evidence that XLF is an essential core NHEJ factor in

human cell. In the absence of XLF cells showed pronounced growth defects and were severely defective for DSB repair as well as V(D)J recombination.

Materials and Methods

Cell culture:

Human wild type HCT116 cells were cultured in McCoy's 5A media containing 10% fetal calf serum, 100 U/ml penicillin and 50 U/ml streptomycin. The media was also supplemented with L-glutamine. The cells were incubated at 37°C in a humidified incubator with 5% CO_2. All cell lines derived from correct targeting were grown in the presence of 1 mg/ml G418. Cells stably infected with pBABE-Puro constructs are selected with 200 μg/ml of Puromycin.

Targeting vector construction

The targeting vectors were constructed utilizing the system described elsewhere (141). Briefly, the right and left homology arms of the XLF targeting were constructed by PCR from HCT116 genomic DNA. The primers used to construct the left homology arm for XLF were XLF4F1, 5'-ATACATACGCGGCCGCTGATCTTCAAGGGTCTTTACCTTCTGTTG-3' and XLF4R1, 5'-AAGTTATCCGCGGTGGAGCTCCAGCTTTTGTTCCCTTTAGAGATATCAATTAGCCAAAAGACT-3'. The right homology arm was constructed using the primers XLF4F2, 5'-TATGGTACCCAATTCGCCCTATAGTGAGTCGTATTACTTCGAGGTAAGAGGACATTCTTGGAG-3' and XLF4R2, 5'-ATACATACGCGGCCGCAACAGAACAGGGCTACTTAGGAAAGAGGA-3'. The arms were used in a fusion PCR reaction, together with a 4-kb *PvuI* restriction enzyme fragment containing the drug selection marker. The fusion PCR product was gel purified and ligated to the pAAV backbone using *NotI* restriction enzyme sites to construct the final targeting vector

Packaging and isolating virus

The targeting vector (8.0 μg) was mixed with pAAV-RC and pHelper plasmids (8.0 μg of each) from the AAV Helper-Free System (Stratagene) and was transfected into AAV 293 cells (Invitrogen) using Lipofectamine 2000 (Invitrogen).

Virus was isolated from the AAV 293 cells 48 hr after transfection using a freeze-thaw method (141)

Infections

HCT116 was grown to ~70-80% confluence in 6-well tissue culture plates. Fresh media (1.5 ml) was added to the cells 3 hr prior to addition of the virus. The required volume of the virus was added drop-wise to the plates. After a 2 hr incubation at 37°C, another 1.5 ml of media was added to the plates. After a further 48 hr incubation, the cells were transferred to 96-well plates and placed under selection (1 mg/ml G418) to obtain single colonies.

Isolation of genomic DNA and Southern hybridizations

Chromosomal DNA was prepared, digested, subjected to electrophoresis and then transferred to a nitrocellulose membrane as described (154). The membrane was hybridized with probe 'a' to detect correct targeting of the XLF targeting vector. The probe corresponds to ~550 bp and was made by PCR with the primers XLF5'ProbeF1, 5'-ATGAGTCTGGCTTGCACATGTTATG-3' and XLF5'ProbeR1, 5'-CATTCTGTGACTAAGGGAAGTTATCAGAC-3'. The PCR product was electrophoresed on a 1% agarose gel and gel purified prior to use. Probe '*zeo'* is an internal probe, 416bp in length, and was obtained by digesting the selection cassette with the restriction enzymes *AflIII* and *ApaLI*. The Prime-It ®II kit (Stratagene) was used to radiolabel the Southern probe with (^{32}P)-α-dATP.

Isolation of genomic DNA and genomic PCR

Genomic DNA for PCR screening was isolated using the PUREGENE® DNA Purification Kit (Qiagen). Cells were harvested from confluent wells from a 24-well culture dish. DNA was dissolved in a final volume of 50 μl, 1 μl of which was used in each PCR reaction. For XLF targeting events, PCR was carried out at both the 5' and 3' sides of the targeted locus. For the 5'-end Correct targeting was determined using LarmR, 5'- GCTCCAGCTTTTGTTCCCTTTAG and XLF-F1, 5'-GTTGTGTGTAGAGTGCGTTGGCTTATA-3'. For the 3'-end, the control PCR was carried out using the primer set RArmF, 5'-

CGCCCTATAGTGAGTCGTATTAC-3' and XLF4R2. For the 3'-end, PCR to screen for correctly targeted clones was performed using RArmF and XLF-R1, 5'-CAACCACACACACAAGCCACCTAACAC-3'.

RT-PCR analysis

Total RNA was isolated from cells using an RNeasy kit (Qiagen). Reverse transcription PCRs (RT-PCrs) were performed using Qiagen LongRange two-step RT-PCR kit. Briefly, 2μg of total RNA was used as a template for the first-strand cDNA synthesis primed by an XLF-specific reverse primer (Cer 7/8 R).

The resulting cDNA were than used in a PCR with three different sets of primers:

(i) Cer F1 (5'- TTT CGG TTC GCG CGA GCG GG -3') and Cer7R (5'-AGA CCA GTT GTT CTG GCT GG -3')

(ii) Cer F1 and CerR2 (5'- GGG AAG GAC TAG CTA GCA TGC AGT -3')

(iii) Cer F2 (5'- TTG ATT CGT CCT CTG ATG GG -3') and Cer7R

Expression Constructs

For creation of stable XLF complemented cell line, full-length XLF cDNA was cloned in pBABE-Puro (4). For pCherry expression constructs WT XLF full-length cDNA was cloned into pCherry (Clonetech) expression vector. The point mutations in XLF CDNA were introduced by site-directed mutagenesis. Primers sequences are available upon request.

Whole cell extract preparation

Cells were trypsinized and washed twice with PBS. For whole cell extraction, cells were boiled in lysis buffer (10 mM HEPES p^H 7.5, 5 mM $MgCl_2$, 1mM PMSF, 1X protease inhibitor cocktail (Roche) for 5 min. The samples were then digested with DNaseI (0.1 U/μl; Gibco) for 10 min at 37°C. The samples were finally boiled in 5X SDS buffer (0.225 M Tris-HCl, pH 6.8, 50% (v/v) glycerol, 5% SDS, 0.05% bromophenol blue, 0.14 M β-mercaptoethanol).

Immunoblotting

For immunoblot detection, proteins were subjected to electrophoresis on a 4-20% gradient gel (Bio-Rad), electroblotted onto a nitrocellulose membrane and

detected as described (114). Polyclonal rabbit antibody anti-XLF raised against the region between amino acids 250 and 299 was from Bethyl Laboratories. Anti XRCC4 (AHP 387) and Anti DNA Ligase IV (AHP 554) were purchased from Serotec. Anti-α-tubulin antibody was obtained from Covance. Anti-GFP antibody (JL-8) was from Clonetech.

Cell proliferation assay

To obtain a growth curve, 3 x 10^4 HCT116 cells, respectively, were plated out in each well of a 6-well plate in duplicate. Cell numbers were determined using a hemacytometer everyday thereafter starting at day 4 utilizing growth media without selection.

X-ray survival assay

For HCT116 cell lines, 300 cells were seeded into each well of a 6-well tissue culture plate about 10-12 hr before irradiation. Cells were then X irradiated using ^{137}Cs source at different doses. After irradiation, HCT116 cells were allowed to grow for 10-14 days before the colonies were fixed, stained, counted and cell survival percentage was calculated.

Etoposide sensitivity assay

300 cells were seeded into each well of a 6-well tissue culture dish in duplicate 16 h prior to drug treatment. Etoposide (Sigma) was dissolved in dimethyl sulfoxide (DMSO) to give a 10 mM stock solution and subsequently diluted in medium. Cells were incubated in etoposide containing medium for 12 days at 37°C, and then fixed and stained with crystal violet.

End-joining assay, transfection and FACS analysis

The *in vivo* end-joining reporter plasmid pEGFP-Pem1-Ad2 has been described previously (259). The plasmid was digested with *Hind*III or *I-Sce*I (NEB) for 8 to 12h to generate different types of DNA ends. Supercoiled pEGFP-Pem1 plasmid was used to optimize the transfection and analysis conditions. The pCherry plasmid (Clontech) was co-transfected with either linearized pEGFP-Pem1-Ad2 or with supercoiled pEGFP-Pem1 as a control of transfection efficiency. Cells

were split a day before transfection and were 60 to 70% confluent during transfection. All the plasmids were transfected using Lipofectamine 2000 (Invitrogen) according to manufacture's instructions. Green (EGFP) and red (Cherry) fluorescence were measured by flow cytometry 24h later (Wang M, NAR, 2006). For FACS analysis cells were harvested, washed in 1X PBS and fixed using 2% paraformaldehyde. FACS analysis was done on FACSCalibur instrument (BD Biosciences). For HCT116 cell line a red-versus-green standard curve was derived with varying amount of cherry and green (pEGFP-Pem1) plasmid to avoid measurements near the plateau region. The values of repaired events is a ratio of cells that are double positive for red and green fluorescence over total cells that are only positive for red fluorescence. This ratio normalizes the repair events to the transfection controls. In the summary chart, the value from the mutants is a percent repair of wild type cells. . Data was plotted using FLowJo 8.5.2 software.

Dik van Gent assay

The Dik van Gent assay was performed as described previously (299). In brief, 2.5 ug of *EcoR*V (NEB) and *Afe*I (NEB) digested plasmid pDVG94 were transfected into cells of 60% confluency, in 6 well plates, using lipofectamine 2000 (Invitrogen) according to manufacture's instruction. The transfection efficiency of wild type HCT116 and other mutant lines were determined using the plasmid pEGFP-Pem1 described above. 48h after transfection, plasmid DNA was recovered using modified Qiagen miniprep protocol. Repaired pDVG94 plasmid was PCR amplified using the primer DAR5 (γ-32P)-ATP labeled) and FM30 (299). The PCR product was digested with *BstX*I (NEB). Restriction fragments were separated along with undigested PCR product in a 6% polyacrylamide gel in TBE buffer. The gel was dried and exposed to film. The bands representing the undigested PCR product (180 bp) or cut (120 bp) and uncut (180 bp) PCR product after *BstX*I digestion were quantified using ImageQuant software and compared.

V(D)J recombination assay

Extrachromosomal V(D)J recombination assays were carried out using pGG 49, 51(91), (90) as substrate plasmids to monitor signal joint (138) and coding joint (CJ) formation, respectively. Briefly, 3 μg of pGG 49, 51, 52 plasmids were transfected with 8 μg each of RAG-1 and RAG-2 (217) into 10^6 exponentially growing cells using Lipofectamine 2000 (Invitrogen). Cells were then incubated for 48 hr at 37°C prior to recovery of the plasmid by a modified Qiagen^R miniprep protocol. Isolated plasmids were treated with the restriction enzyme *DpnI* (to remove un-replicated plasmids), transfected into chemically competent Top10 cells (Invitrogen) and then plated on ampicillin (100 μg/ml) or ampicillin (100 μg/ml) and choloramphenical (22 μg/ml) plates. DAC colonies (DAC= DpnI-treated-amp^R-cam^R) represent V(D)J recombination events, whereas DA colonies (DA= DpnI-treated-amp^R) are a measure of total plasmids recovered from each transfection. The percentage of SJ or CJ formation is calculated by dividing DAC by DA counts.

Telomere Fish

Cells were treated with colecemid at 100 μg/ml for 3 hr. The cells were trypsinized and then harvested by centrifugation. Metaphase spreads were prepared according to the manufacturer's instruction (Dako, Inc.) A Cy3-PNA probe was hybridized according to the protocol supplied by Dako, Inc. except that the sample was denatured at 85 to 90°C for 8 min and then incubated in humidified chamber overnight at 37°C. The images were captured and processed with FluoView 1000 software using an Olympus IX2 Inverted Confocal Microscope.

Immuno Staining:

The indicated cell lines were grown on 4-well chamber slide. Next day the cells were transfected with 2 μg of pCherry plasmid carrying WT or mutant XLF cDNA. 24 hr after transfection cells were harvested and fixed with 4% paraformaldehyde for 30 min and permeabilized with 0.2% TritionX-100 in

PBS for 5 min at room temperature. DAPI was used to stain the nucleus. Images were captured with Zeiss Axiovert 2 Upright Microscope.

Cytogenetic analysis

G-banding cytogenetic analyses were performed in the Cytogenetics Core Laboratory at the University of Minnesota as described previously (206)

Results

Generation of heterozygous XLF $^{+/-}$ HCT116 cell lines:

To characterize the function of XLF in human cells, we utilized recombinant AAV (rAAV) mediated gene targeting strategy (141), (245) to replace exon 4 of the XLF locus in a well-characterized diploid human colon carcinoma cell line, HCT116, with a LoxP-flanked copy of the NEO (neomycin phosphotransferase) drug resistant marker (Fig. 1). XLF, also known as Cernunnos, is a 37-kDa protein encoded by 8 exons on chromosome 2 (Fig 1A). Exon 4 was chosen for two reasons. First, any expression of the first 3 exons should yield a greatly truncated protein missing its XRCC4 and LIGIV interaction domains (7), (162) and secondly, any splicing over the mutated sequence should generate an out-of-frame protein. Five correctly targeted clones that were identified using PCR strategies were obtained from screening 201 NEO-resistant clones for a targeting frequency of 2.1%.

The targeting vector contained ~900bp long left and right homology arms flanking a neomycin-resistant selection cassette (Fig 1B). The left homology arm for the XLF targeting vector has sequences 5' to exon 4 and the right homology arm has sequences 3' to exon 4 (Fig1B). The 2.8-kb selection cassette has PGK promoter, the neomycin resistance gene (Neo), the FM promoter, and the zeocin resistance gene (Zeo)(Fig 1B). Two LoxP sites flank the selection cassette. Correct targeting of the endogenous genomic XLF locus deletes exon 4, resulting in a G418 resistant cell line. The removal of exon 4 should functionally inactivate XLF, since the hypothetical splicing from exon 3 to exon 5 results in an out-of-frame mRNA. Genomic DNA was isolated form G418-resistant colonies and was subjected to diagnostic PCR analysis to screen for correctly targeted clones. A control PCR, carried out using the primers RArmF and XLF 4R2 (Fig. 2A), was used to confirm the presence of the vector sequence in all G418-resistant clones (Fig. 2B, Vector Control), while primers XLF 4F2 and XLF R1 (Fig. 2A) were used to check the quality of isolated DNA and to confirm the presence of DNA in the

parental cell line (Fig. 2B, DNA Quality Control). Experimental screening PCR was also carried out, using the following two sets of PCR primers: XLF F1 and LArmR for the 5' PCR and RArmF and XLF R1 for the 3' PCR (Fig. 2A). LArmR and RArmF correspond to sequences unique to the targeting vector, while XLF F1 and XLF R1 reside externally in the 5' and 3' flanking regions, respectively (Fig 2B). The correct targeting events in 2 of the clones - XLF #27 and XLF #72 - are shown in Fig. 2A. This is confirmed by the 5' flanking PCR strategy, where all the clones showed the expected ~1.5 kb PCR band (Fig. 2B, 5' PCR), and by the 3' flanking PCR strategy, where the correct targeting events resulted in the production of ~1.45 kb bands (Fig. 2B, 3' PCR). The PCR bands resulting from correct targeting events were absent from two randomly targeted clones (XLF #38 and XLF #47) as well as from the parental HCT116 cell line (Fig. 2B).

Generation of homozygous XLF $^{-/-}$ HCT116 cell lines:

In order to construct a XLF $^{-/-}$ HCT116 cell line, the XLF $^{+/-}$ cell line XLF #27 were transiently exposed to Cre recombinase (pGKCre). Cre should excise the internal Neo cassette, which is flanked by LoxP sites, within the integrated targeting vector which leads to clones being rendered sensitive to G418 (Fig.1B). 48 single-cell cones were picked and duplicated into medium either containing or lacking G418, and five G418-sensitive clones were identified. Correct excision of the neomycin gene was confirmed by the generation of a diagnostic PCR product (data not shown). One (242cre3) of several such clones obtained in this fashion was used for a second round of gene targeting with the original targeting vector containing the Neo cassette. Productive infection should produce one of the three potential outcomes: (i) random targeting (the vast majority of the events), (ii) correct targeting, but of the already inactivated allele from the first round of targeting (i.e., "retargeting"); or (iii) correct targeting of the remaining allele to generate the desired null clone. Initially, 6 correctly targeted clones from 290 G418 resistant, internal-control-PCR-positive clones (targeting frequency of

2.1%) were identified using the primers NeoF2 and XLF R1 (Fig. 3A & B (primer pair Neo F2 and XLF R1), and data not shown). A diagnostic PCR strategy was then utilized to distinguish retargeting from null events (Fig. 3). 4 out of 6 clones were retargeted. The conclusion was drawn by the fact that although 4 clones were correctly targeted (data not shown), they still retained exon 4 whereas two clones (61 and #320 (data not shown) lacked exon 4 (Fig. 3B). Two sets of primers were used to confirm the absence of exon 4 in XLF null clones: (i) primers set: Ex4F1 and XLF R2 which should produce a ~1300 bp PCR and if exon 4 is present and (ii) Ex4 F2 and XLF R2 which should give a ~1200 bp band if exon 4 is not deleted. These two sets of primers confirmed that clone #101 did not have exon 4 sequences as the PCR product using genomic DNA from #101 did not produce the expected bands.

Southern hybridization was used to confirm the targeting events. Genomic DNA was isolated and digested with the restriction enzymes *BamH1* and *NheI* for 5' probe and *BamHI* only for 'Zeo' probe. Southern blot analysis was then performed using 5' probe (Sup Fig. 1B; 5' probe) or a probe corresponding to the vector sequence (Sup Fig. 1C; 'Zeo' probe). For the 5' Southern analysis, the appearance of a novel ~6-kb band caused by the presence of the targeting vector, confirmed that a correct targeting event has occurred in clone #27 ($XLF^{+/-}$) and in #101 ($XLF^{-/-}$) (Sup Fig. 1A & B). The ~6-kb band was absent, as expected, form the parental HCT116 cell line (WT), where only the endogenous ~2.4-kb band was observed (Sup Fig. 1A & B). In clone #27Cre3 the 6-kb band was shifted due to the Cre-mediated excision of Neo cassette. In clone #101 the 6-kb band reappeared due to the targeting of second allele with the targeting vector carrying the Neo cassette. When the genomic DNA from the indicated lines were digested with *BamHI* alone and probed with Zeo (Sup Fig. 1A & C) both clones #27 ($XLF^{+/-}$) and in #101 ($XLF^{-/-}$) had the single 6-kb band corresponding to the correct insertion of the targeting vector. The ~6-kb band was absent, as expected, form the parental HCT116 cell line (WT).

To confirm that no full length XLF mRNA was being produced in the XLF-null cells, total mRNA was isolated and first strand cDNA was generated using a primer (cer7/8R1) that spans exon 7 and 8 sequences, which ensures that only mRNA, and not genomic DNA, is amplified (Supp. Fig.2A). The cDNA was then subjected to PCR using primers (Cer F1 and Cer 7R) complementary to sequences located in exon 1 and exon 7, respectively (Supp Fig.2A). A 855 bp PCR product corresponding to the region encompassing exons 1 to 7 was produced from mRNA isolated from the parental cell line (HCT116 WT), a randomly targeted clone (201) and XLF $^{+/-}$ cell line (242) but was absent from the XLF $^{-/-}$ (61) (Supp.Fig. 2B), demonstrating that XLF $^{-/-}$ did not produce detectable full length XLF mRNA. A truncated 716-bp-band (Supp.Fig. 2B), that corresponds to the loss of exon 4 from the XLF genomic locus was detected. Since skipping exon 4 generates a frame-shift within the XLF open reading frame that quickly results in a stop codon, which is then destabilized by non-sense mediated decay, this analysis predicted that no functional full-length XLF protein would be produced in

XLF$^{-/-}$ cells. Primer pair Cer F1 and Cer R2 (residing in exon 3) was used to detect the mRNA upstream of exon 4. A predicted 459-bp PCR band is present in all the cell lines tested (WT, #27, #101, #38) demonstrating that deletion of exon 4 did not abolish the production of mRNA upstream of exon 4 (Supp. Fig. 2B). On the other hand, primers Cer F2 (residing in exon 4) and Cer 7R resulted a 382-bp PCR band in all the cells line tested except XLF$^{-/-}$ (61) (Supp.Fig. 2B), demonstrating the successful homozygous deletion of exon 4 from the XLF genomic locus.

Primary Characterization:

The removal of exon 4 (Fig. 1A) in the XLF locus should result in no XLF protein production due to a frame-shift event within the XLF open reading frame. The expression levels of the wild-type and the XLF $^{+/-}$ and XLF $^{-/-}$ cell lines were

determined by immunoblot analysis using a rabbit polyclonal XLF antibody raised against the C-terminus of XLF (Fig 4). The XLF $^{+/-}$ clones (242 and #72) expressed XLF at a level of ~50% (with the α-tubulin as a loading control) of that observed for the parental cells (Fig. 4), while the XLF $^{-/-}$ cells contained no detectable wild-type or truncated protein (Fig. 4). The complete absence of XLF protein in the XLF $^{-/-}$ cell line suggested that deletion of exon 4 from XLF genomic locus resulted cell lines deficient for XLF expression. XLF forms a complex with XRCC4 and DNA LIGIV. To check whether XLF deficiency had affected the expression or stability of XRCC4 or DNA LIGIV, the same immunoblot was stripped and blotted sequentially with antibodies against XRCC4 and LigIV. Absence of XLF protein had no significant effect on XRCC4 or LIGIV protein levels (Fig.4). So we concluded that, XLF is dispensable for the stability of both XRCC4 and Ligase IV.

In summary, based upon the molecular characterizations (Fig. 2, 3 and Supp Fig. 1), the RT-PCR (Supp Fig. 2), and the immunoblot analysis (Fig. 4), we concluded that the

XLF$^{-/-}$ cell lines are deficient for XLF protein expression.

Complementation of the NHEJ defects of XLF deficient HCT116 cells:

We next stably complemented one of the XLF$^{-/-}$ cell lines (61) with either a wild type cDNA or cDNA containing L115A or L179A mutations. L115A and L179A are not naturally occurring patient mutations (26), (4), but Andres et al., (Andres et al, 2006) using purified proteins and an in vitro DNA rejoining assay claimed that they defined critical XLF residues needed for XRCC4 interaction and LIGIV activity, respectively. The mutant proteins were expressed at a level comparable to that in a wild-type cell line (Fig. 7).

XLF deficient cells are impaired for cell proliferation:

Patients cell lines carrying muations in XLF open reading frame has growth defects (26). So we hypothesized that deletion of XLF gene should results in growth defects in cultured human somatic cells. To test our hypothesis, equal numbers of cells from all the cell lines were plated out in duplicate on day 0 and then the cell numbers were determined beginning 3 days thereafter for 7 days. Both the $XLF^{+/-}$ clones (242 and #72) and both $XLF^{-/-}$ clones (61 and #320) showed a significantly reduced rate of growth compared to that of the parental HCT116 cells (Fig. 5). The doubling time of the $XLF^{+/-}$ clones (242 and #72) were 24.0 h, which was slightly longer than that of the parental line, at 22.8 h. The $XLF^{-/-}$ clones (61 and #320), in contrast, showed much more severe growth defects, with a doubling time of 18.0 h. Thus $XLF^{+/-}$ cells are haploinsufficient and $XLF^{-/-}$ cells lines are severely defective for cell proliferation.

XLF deficient cells are impaired for repairing DSBs:

Patients cell lines harboring XLF mutations are sensitive to DNA damaging agents (Buck et al., 2006). Mouse ES cells (331) and fibroblasts (160) deficient for the WT XLF protein are sensitive to ionizing radiation. To determine the effect of deletion of XLF in human cells, we used a drug, etoposide, a topoisomerase II inhibitor and a potent inducer of DNA DSB (196) The XLF $^{+/-}$ cells (242 and #72) were as sensitive as WT HCT116 cells (Fig. 6A). In contrast to the WT and XLF $^{+/-}$ cell lines, XLF $^{-/-}$ cell lines (61 and #320) were more than an order of magnitude more sensitive to etoposide (Fig. 6A). To extend these studies, the sensitivity of the cell lines to IR was determined. The D_{37} (the dose required to reduce survival to 37%) for parental and the XLF $^{+/-}$ line (242), was ~3.5 Gy, whereas D_{37} for the XLF $^{-/-}$ cell line (61) was ~0.5 Gy (Fig. 6B). Thus, XLF deficient cells have profound sensitivity to DNA damaging agents.

Stable expression of a full-length XLF protein (Fig. 8A) from a viral vector in XLF $^{-/-}$ cell line (61) restores the etoposide (Fig 6A) and IR (Fig. 6B) sensitivities back

to WT levels, demonstrating that XLF deficiency is specifically responsible for the increased etoposide and IR sensitivity of the XLF $^{-/-}$ cell lines.

To determine whether the etoposide and IR sensitivities of XLF deficient cell lines are associated with an intrinsic defect in DNA DSB repair, we measured the capacity of NHEJ efficiency of XLF deficient cells using an *in vivo* plasmid end joining assay that has been utilized previously (302), (259). This assay allows, in addition to the generation of defined DSBs, also the following of their repair in cells without other forms of DNA damage. In this rapid-readout, direct-reporting plasmid assay, end joining is measured by the restitution of GFP expression (Seluanov et al., 2004). Principle characteristics of the plasmid (pEGFP-Pem1-Ad2) used in the assay (Fig. 8A) is the interruption of the EGFP sequence by the Pem1 intron, within which restriction sites for HindIII is engineered upstream and downstream of the Ad2 exon (Fig. 8A). Digestion with HindIII at both sites generates a linear plasmid with cohesive 5'-overhangs. Because of the retention of the Ad2 exon, un-digestion or partial digestion at only one restriction site generates upon ligation a product unable to express GFP. Due to the 'buffering' capacity of the intron, end joining of transfected, linearized plasmid by the cellular repair apparatus re-constitutes GFP expression, even when extensive additions or deletions of nucleotides have occurred (259). As a result, a wide spectrum of end joining events can be detected.

When *HindIII* linearized plasmid is introduced into parental cell line HCT116, intracellular circularization allowing GFP expression can be detected and quantitated by flow cytometry (Fig. 8B & C). The parental cell line repaired this linearized construct at least an order of magnitude better than the XLF-null cells (Fig. 8 B &C). As expected, the XLF-null cells complemented with a wild-type cDNA had almost wild-type levels of NHEJ activity, but unexpectedly so did the L115A and L179A mutants (Fig. 8 B &C). Thus, the *in vitro* results (7) were not recapitulated in our *in vivo* systems in which to interrogate presumptive mutations.

To confirm these results we used a different, but complementary, assay. This assay uses a reporter plasmid that is biased towards detecting B-NHEJ events. pDVG94 is designed such that the relative efficiency of C-NHEJ versus B-NHEJ events can be assessed (177), (299). When pDVG94 is digested with *AfeI* and *EcoRV* it results in a blunt-ended linear substrate with 6-bp repeat at both ends (Fig. 9 A). C-NHEJ can rejoin these ends and yield a wide variety of junctions but B-NHEJ almost exclusively generates a single product in which 2 repeats have been reduced to 1, which simultaneously generates a novel *BstXI* restriction enzyme site (Fig. 9 A). Thus, linearized pDVG94 plasmid was transfected into XLF-null cells as well as cells expressing WT, L115A or L179A XLF cDNA and 48 hr later, repaired plasmids were recovered, and then used as substrates for PCR using a 5'-radiolabeled PCR primer (Fig. 9 A & B). The level of B-NHEJ was subsequently determined by quantitation of the *BstXI*- digested PCR products. For XLF-null cells ~97% of all repair products were mediated by B-NHEJ as shown by their susceptibility to *BstXI* digestion (Fig. 9 C), whereas the cleavage product was only produced about 2-3% of the time from the plasmids re-isolated from either the wild-type or null cell line complemented with a wild-type or mutant (L115A and L179A) cells suggesting that again these two mutants *in vivo* complemented the XLF deficiency.

So in summary, XLF deficiency results in etoposide sensitivity (Fig. 6A), IR sensitivity (Fig. 6B), severe C-NHEJ repair defects (Fig. 8 B, C) and a dramatic induction of B-NHEJ (Fig. 9 C). So we concluded that XLF is necessary for the efficient repair of DSBs (C-NHEJ) in human somatic cells.

Intracellular localization of mutant XLF proteins:

To expand these studies described above, we have also constructed 3 naturally occurring patient mutations: R57G, C123R and R178X (26). As expected, none of these mutants was capable of restoring NHEJ activity to the XLF-null cell line assayed by the *in vivo* plasmid end-joining assay (data not

shown). To try and explore this defect in more detail, we made fusion proteins with pCherry for each of these proteins as well as for wild-type and the L115A and L179A derivatives. These constructs were then transiently transfected into the XLF-null cell line. The L115A, L179A and R178X proteins were expressed at levels comparable to wild-type (Supp Fig. 9A). C123R and R57G were expressed less well, suggesting that the mutations result in a misfolded and/or unstable proteins. All of the proteins were expressed at sufficient levels, however, to determine their cellular localization. Unexpectedly, the wild-type protein showed pancellular staining and while significant amounts of the protein were nuclear the majority of the protein appeared to reside in the cytoplasm (Supp Fig. 9B) Similar staining patterns were seen for the L115A, L179A and R178X proteins (Supp Fig. 9B). The C123R and especially the R57G proteins, however, were virtually cytoplasmic (Supp Fig. 9B). A comparable result for R57G result using a c-myc epitope tag and a different cell line has also been reported (179), suggesting that this is a biologically relevant and reproducible result. Several tentative conclusions can be drawn from these preliminary results. First, the patient mutations C123R and R57G appear to result in unstable proteins that might mis-localize to the cytoplasm. Secondly, it appears as if the wild-type XLF protein is regulated by nuclear/cytoplasmic partitioning. If the latter conclusion is true, the mechanism is probably atypical as the R178X mutation, which removes a classical monopartite nuclear localization signal located at the extreme C-terminus of the protein, still localizes to the nucleus as well as wild-type protein (Supp Fig. 9B) Moreover, although XLF is an extremely leucine-rich protein (42 of 299 residues are leucine), there are no obvious leucine-rich nuclear export consensus sequences (87). Take together, this data imply, but by no means prove, that the C123R and R57G residues, which in 3-dimentional space reside near each other may define a nuclear localization, retention or export domain.

Absence of XLF leads to defect in V(D)J recombination in human cells:

To evaluate the role of XLF in V(D)J recombination in human cells, we used a transient V(D)J recombination assay (91), (90). WT HCT116, XLF$^{+/-}$, XLF $^{-/-}$ and XLF $^{-/-}$ cell lines expressing either full-length WT XLF or mutant cDNA were transfected with vectors that express full-length RAG1 and RAG2 proteins and a plasmid recombination substrate that is designed to measure the frequency of either signal joint (pGG49) or coding joint (pGG51) (Table 1). XLF-null cells were dramatically deficient for both SJ and CJ formation, whereas heterozygous mutants were capable of performing V(D)J recombination at wild-type levels. To confirm that the signal and coding joining defects observed in XLF$^{-/-}$ cells is due to deletion of XLF, we assayed XLF $^{-/-}$ cells expressing full-length XLF cDNA and found essentially WT levels of signal and coding joint formations, indicating that the observed defects were specifically associated with the deletion of XLF gene (Table 1). And once again, the L115A and L179A mutant cells complemented the XLF deficiency indicating that these mutations do not abrogate XLF function.

Genomic stability in XLF deficient cells:

To determine potential roles of XLF in the maintenance of genomic stability, we used a FISH assay that combines DAPI staining with a telomere-specific PNA probe (T-FISH) to assay metaphase chromosomes in WT and XLF-null cells. XLF deficient cells did not show any significant increased level of chromosomal abnormality (Supp Fig. 4) relative to WT cells. XLF-null cells were also cytogenetically analyzed by G-banding. There is no significant genetic instability in XLF null cells relative to WT HCT116 cells.

Discussion

XLF has recently been shown to be involved in C-NHEJ (4), (26), (331), (160), which is the main pathway for the repair of DNA double-strand breaks in human cells. Here, we have demonstrated that, inactivation of XLF in human somatic HCT116 cells results in severe proliferation defect (Fig. 5), hypersensitivity to DNA damaging agents (Fig. 6), defects in DSB repair (Fig. 7), and severe defect in extra-chromosomal V(D)J recombination (Table 1) assay. These phenotypic features found in this study, are consistent with the observation found in human patients carrying XLF mutations (26), (4) and XLF deficient mouse ES cells (331).

We found that loss of even one allele of XLF in human somatic cells results in growth retardation, and the loss of both XLF alleles result in a severe proliferation defects. This is identical to the phenotypes of human patients carrying XLF mutations (growth retardation) (26) or the mouse ES cell line heterozygous or null for XLF (331) but in contrast with the XLF deficient mouse embryonic fibroblast (MEFs) generated from the $XLF^{\Delta/\Delta}$ mouse (160). Thus in this regard, human patients, human somatic cells and mouse ES are different than the whole mouse. In $XLF^{\Delta/\Delta}$ mouse exon 4 and 5 of XLF locus has been targeted which hypothetically produce an in-frame truncated XLF protein which may explain the lack of proliferation defect in mouse model, but does not explain why the ES has defect in cell proliferation.

Fibroblasts of XLF patients or XLF knockdown in human cells showed increased sensitivity to IR and to DSB inducing agent bleocin, impaired NHEJ-dependent random chromosomal plasmid integration in vivo, and impaired end ligation of restriction enzyme-induced DSBs *in vivo* and *in vitro* in comparison to XLF proficient cells (4). Similarly targeted disruption of XLF in human somatic cells resulted severe IR and etoposide sensitivity and impaired *in vivo* plasmid end joining. These observations support a DSB repair defects in XLF-deficient human cell line and suggests a role of XLF for C-NHEJ. The residual DSB repair

activity of XLF deficient cells in *in vivo* plasmid end joining assay is dependent on B-NHEJ pathway (Fattah et al. 2009 manuscript in preparation).

Patients with mutations in the XLF gene showed growth retardation, microcephaly, and immunodeficiency (26). The immunological defects were due to T and B lymphocytopenia and hypogammaglobulinemia of serum IgG and IgA antibodies. These observations from human patients reflect a role of XLF in V(D)J recombination, particularly in accurate signal join formation, a minor role in the prevention of nucleotide loss at coding joins, and a potential role in class switch recombination. The $XLF^{\Delta/\Delta}$ ES cells were severely impaired for ability to form V(D)J coding and RS joins in transient assay and were IR sensitive (331). Like XLF-mutant human fibroblast (56), (26) and mouse ES cells (331), XLF –deficient human cells are highly defective in the ability to support coding and signal joint formation in transient RAG-initiated V(D)J recombination assay (Table 1). XLF deficient human cells are defective for both coding and signal similar to mouse cells deficient for core NHEJ components (Ku, XRRCC4, and LIG IV) and distinct from Artemis or DNA-PK_{cs} deficient ES cells, which makes nearly normal signal joints. But surprisingly, lymphocytes from XLF deficient mouse show no or little V(D)J recombination defect but are still sensitive for IR, suggesting a lymphocyte specific compensation mechanism for XLF function (160).

Over-expression of a WT XLF cDNA rescued the growth defect (Fig.5), IR and etoposide sensitivity (Fig 6) and V(D)J recombination (Table 1) phenotypes in XLF-deficient cells suggesting a role of XLF in those processes.

The mouse ES cells (331) and MEFs isolated from $XLF^{\Delta/\Delta}$ mice (160) showed genomic instability. But surprisingly, XLF-deficient HCT116 cells did not show significant elevation of genomic instability in comparison to wild-type cells. So further works needed to be done in human patients' cell line to address in role of XLF in maintaining genomic stability in human cells.

Though human XLF mutations are associated with microcephaly (26), and most recently, a balanced translocation that interrupts XLF gene, has been

identified in a fetal autopsy samples and suggested to be associated with polymicrogyria (PMG) (35), the $XLF^{\Delta/\Delta}$ mouse did not show any excessive neuronal cell death or a significant reduction of brain weight in embryonic or adult $XLF^{\Delta/\Delta}$ mice.

Site-directed mutagenesis revealed the distinct functional domains in XLF (7). Amino acid substitutions at L174, R178 and L179 in the evolutionary conserved hinge region abolish the stimulation of the LIGIV activity, while these mutations do not affect the association with XRCC4 or DNA. A mutation at L115 disrupts the interaction with XRCC4. Here, we introduced point mutations into XLF cDNA and tested the mutant proteins for their ability to complement XLF deficiency in XLF null cells. The mutation at positions L115 and L179 was able to complement XLF deficiency comparable to WT XLF cDNA in *in vivo* plasmid end joining assay as well as V(D)J recombination assay. This observation is in complete contrast with the observation by Andres et al. (7). It is possible that in vitro some necessary factor/s were missing which were important for XLF function.

In Miss-sense mutations R57G and C123R were found in XLF defective patient (26) and are mapped on the surface of the N-terminal globular head domain by the structure analysis. XLF protein harboring either of these miss-sense mutations is not retained in the nucleus and exported out into the cytoplasm, even though these mutant proteins have a typical nuclear localization signal at their C-terminal ends (Supp Fig. 3), and this is probably the basis for the NHEJ defects in these patient. Other mutations e.g. L178X (26), and a balanced translocation that interrupts XLF gene, has been identified in human patients (35). These XLF transcripts encode the N-terminal portion of XLF, but still cannot support its' function, and excluded from nucleus (Supp Fig.3) means the c-terminal residues are important for XLF's function. This data in agreement with

the *in vitro* observation that the C-terminal 75 residues are required for DNA binding and the activation of XRCC4.LigIV (7).

In conclusion, this is the first report of targeted XLF inactivation in a human somatic cell line. Our characterizations of XLF deficient cell line suggest that XLF is a member of C-NHEJ pathway. Using this cell line, the structure-function analysis of XLF and its actual function in the C-NHEJ is under investigation in our lab.

Acknowledgment

The authors are indebted to Steve Jackson (Cambridge University, UK), Dr. V. Gorbunova (University of Rochester, NY), Dr. G. Illakis (University of Duisburg-Essen Medical School, Germany) and Dr. D van Gent (Erasmus University, Netherlands) and members of their laboratory who were extremely generous with their reagents and advice. We would like to acknowledge the assistance of the Flow Cytometry Core Facility of the Masonic Cancer Center, a comprehensive cancer center designated by the National Cancer Institute, supported in part by P30 CA77598. These studies were supported in part by National Institutes of Health grants GM 069576 and HL079559 to EAH.

Figure 1. Scheme for functional inactivation of the human XLF locus. (A) Cartoon of partial XLF genomic locus in the HCT116 cell line. Exons are shown (not to scale) as numbered open rectangles. (B) The cartoon of the rAAV targeting vector. In the targeting vector open boxes are the left and the right inverted terminal repeats (ITR); black triangles, loxP sites; PGK, phosphoglycerate kinase eukaryotic promoter; Neo, neomycin-resistance gene; EM7, EM7 prokaryotic promoter; Zeo, zeomycin-resistance gene; gray rectangles, left and right homology arms to facilitate targeting by homologous recombination. (C) Cartoon of a first-round targeted allele. The targeting vector has replaced exon 4 on one chromosome. a and b are the external and Zeo is the internal probes that were used for Southern blot analysis. L-ITR and R-ITR are lost upon vector integration.

A. Partial XLF Genomic Locus

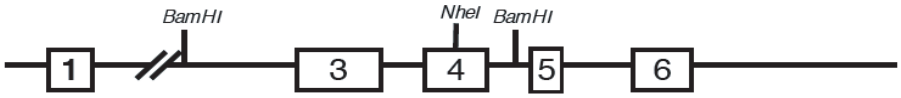

B. Targeting Vector

C. XLF Targeted Allele

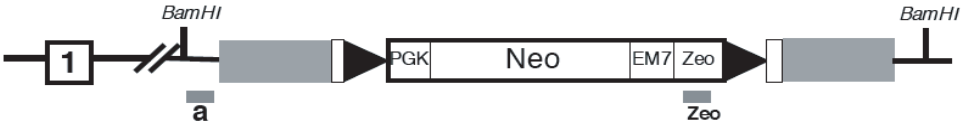

Figure 2. Identification of $XLF^{+/-}$ cell lines. (A) Primers used for the diagnostic PCR screening for $XLF^{+/-}$ clones. (B) Four diagnostic PCR were carried out: an experimental 5' PCR to confirm correct targeting events on the 5' side, using the primers XLF F1 and LarmR; an experimental 3' PCR to confirm correct targeting events from the 3' side, using the primers RarmF and XLF R1; a vector control PCR to confirm the presence of the targeting vector in the cell lines, using the primers RarmF and XLF 4R2; and a DNA quality PCR to confirm the quality of the genomic DNA preparation, using primers XLF 4F2 and XLF R1. All the gels are ethidium bromide-stained, with a 1000 bp marker ladder on the far left. Genomic DNA was isolated from two heterozygous clones (#27 and # 72), two randomly targeted clones (# 38 and # 47), and the WT HCT116 cell line.

A.

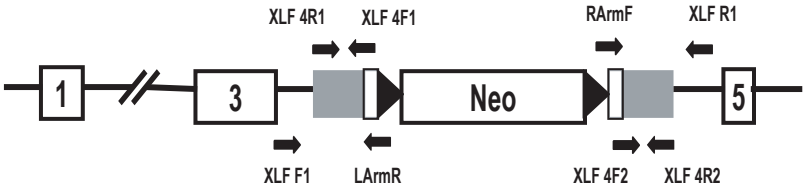
XLF 4R1
XLF 4F1
RArmF
XLF R1
1
3
Neo
5
XLF F1
LArmR
XLF 4F2
XLF 4R2

B.

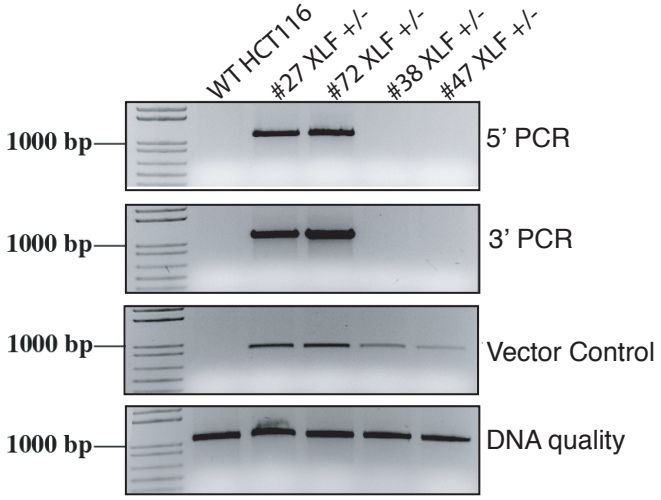
WT HCT116
#27 XLF +/-
#72 XLF +/-
#38 XLF +/-
#47 XLF +/-
1000 bp
5' PCR
1000 bp
3' PCR
1000 bp
Vector Control
1000 bp
DNA quality

Figure 3. Identification of XLF $^{-/-}$ cell line. (A) PCR strategy and primers used for the generation of XLF $^{-/-}$ cells. (B) Three diagnostic PCRs were carried out to confirm the loss of exon 4 sequences. The first primer pair is Ex4 F1 and XLF R2, the second primer pair is Ex4 F2 and XLF R2 and the third primer pair is Neo F2 and XLF R2. WT is the HCT116 cell line; #27 cre is a $XLF^{+/-}$ clone after cre treatment; #27 is a $XLF^{+/-}$ clone; #101 is the $XLF^{-/-}$ clone. All the agarose gel pictures are ethidium bromide-stained, with a 1-kb plus marker ladder on the far left.

A.

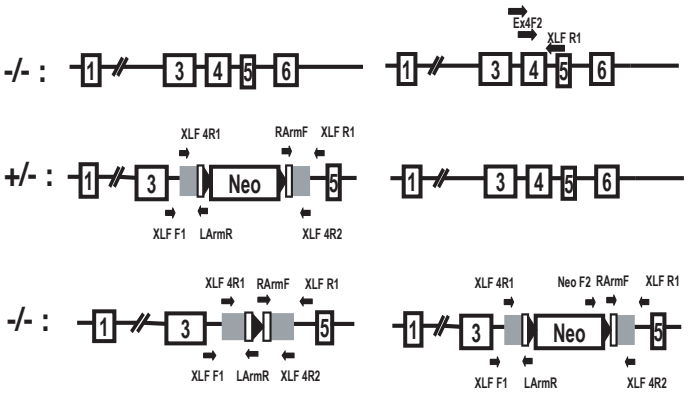
Allele 1
Allele 2
-/- :
+/- :
-/- :
Ex4F2
XLF R1
XLF 4R1
RArmF
XLF R1
Neo
XLF F1
LArmR
XLF 4R2
Neo F2

B.

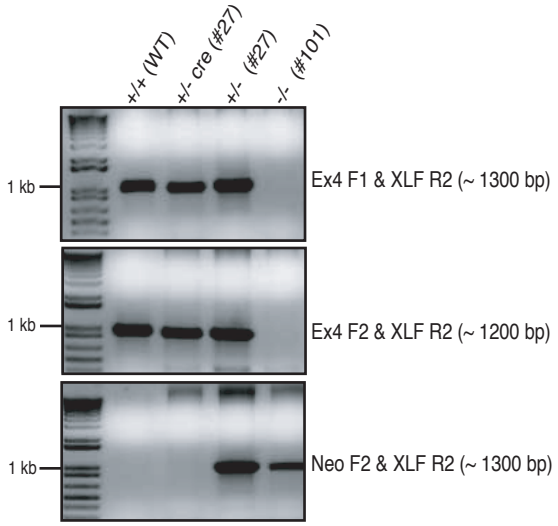
+/+ (WT)
+/- cre (#27)
+/- (#27)
-/- (#101)
1 kb
Ex4 F1 & XLF R2 (~ 1300 bp)
Ex4 F2 & XLF R2 (~ 1200 bp)
Neo F2 & XLF R2 (~ 1300 bp)

Figure 4. Documentation of loss of XLF protein. Whole- cell extracts were prepared from wild-type HCT116, clone # 27 (XLF $^{+/-}$), clone # 72 (XLF $^{+/-}$), clone # 101 (XLF $^{-/-}$), and clone # 320 (XLF $^{-/-}$) cells. The extracts were analyzed by immunoblot for XLF protein using a c-terminal XLF-antibody. One single blot was also sequentially probed with three more antibodies: XRCC4, LigIV and α-tubulin.

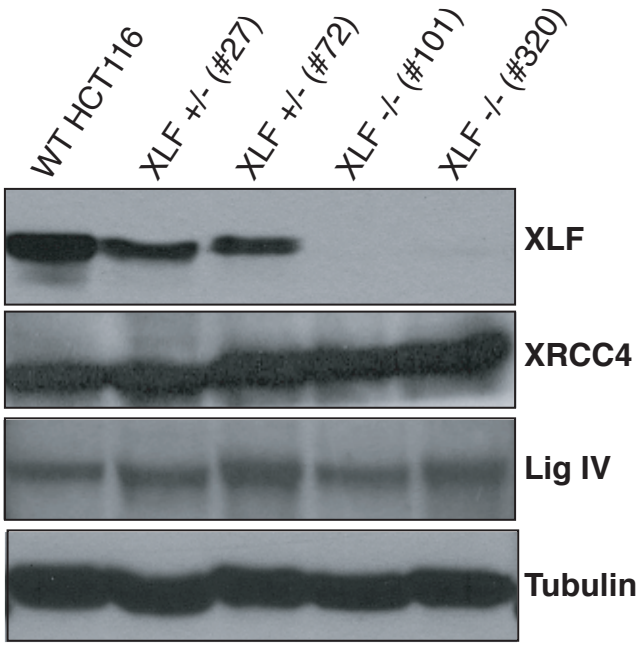
WT HCT116
XLF +/- (#27)
XLF +/- (#72)
XLF -/- (#101)
XLF -/- (#320)
XLF
XRCC4
Lig IV
Tubulin

Figure 5. Growth defects of human somatic cells with reduced and no XLF expression. Wild-type (WT), XLF $^{+/-}$ (#27 and #72), XLF $^{-/-}$ (#101 and #320), non-targeted and XLF $^{-/-}$ stably over-expressing WT XLF cDNA HCT116 cells were seeded on tissue culture plates (3 X 10^3), and the increase in cell number was determined by counting trypan blue-excluding cells at daily intervals. The averages (+/- standard deviations of three independent experiments, each done in duplicate, are shown.

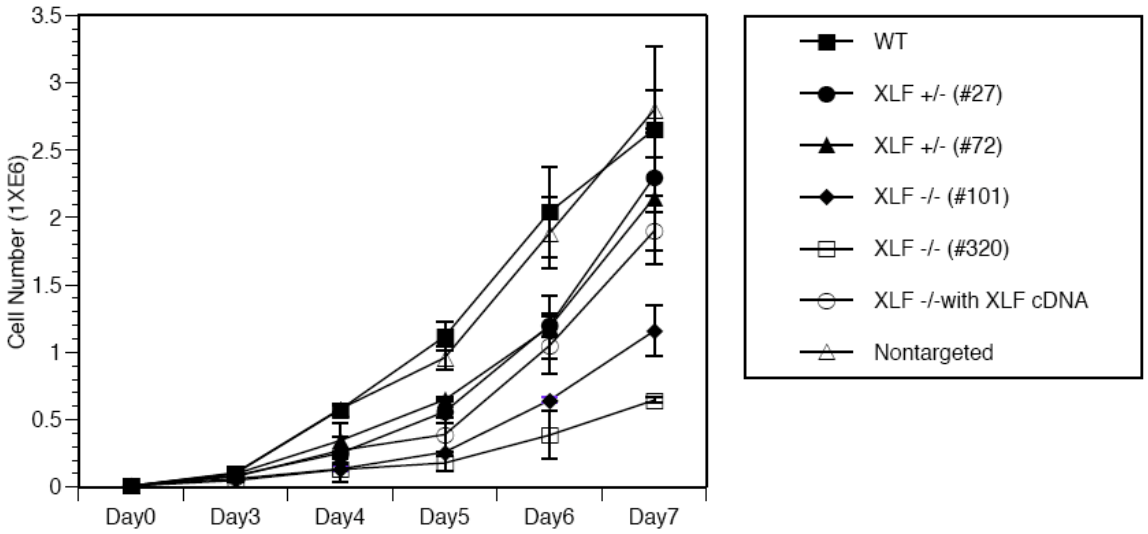
Cell Number (1XE6)
3.5
3
2.5
2
1.5
1
0.5
0
Day0
Day3
Day4
Day5
Day6
Day7
WT
XLF +/- (#27)
XLF +/- (#72)
XLF -/- (#101)
XLF -/- (#320)
XLF -/-with XLF cDNA
Nontargeted

Figure 6. XLF deficient cells are sensitive to DNA-damaging agents. (A) Etopodide sensitivity. 300 wild-type (WT), XLF $^{+/-}$ (#27 and #72), XLF $^{-/-}$ (#101 and #320), and XLF $^{-/-}$ stably over-expressing WT XLF cDNA HCT116 cells were seeded on tissue culture plates in duplicate and exposed to indicated levels of etoposide. Cells surviving to form colonies of at least 50 cells after 15 days were scored. (B) IR sensitivity. 300 wild-type (WT), XLF $^{+/-}$ (#27), XLF $^{-/-}$ (#101) and XLF $^{-/-}$ stably over-expressing WT XLF cDNA HCT116 cells were seeded on tissue culture plates in duplicate and X-irradiated at the increasing doses. Cells surviving to form colonies of at least 50 cells after 15 days were scored. Both profiles show the averages (+/- standard deviations) of at least two independent experiments.

A.

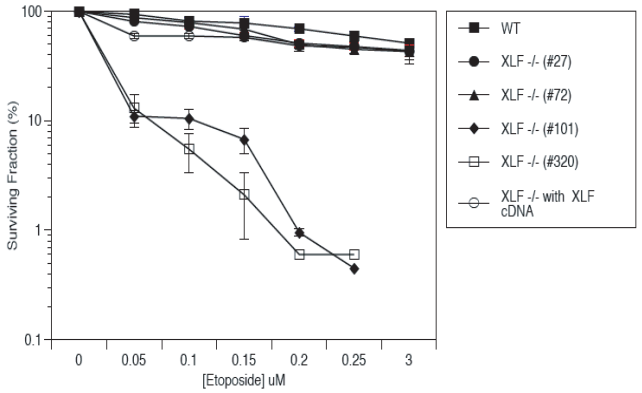
100
10
1
0.1
Surviving Fraction (%)
0
0.05
0.1
0.15
0.2
0.25
3
[Etoposide] uM
WT
XLF -/- (#27)
XLF -/- (#72)
XLF -/- (#101)
XLF -/- (#320)
XLF -/- with XLF cDNA

B.

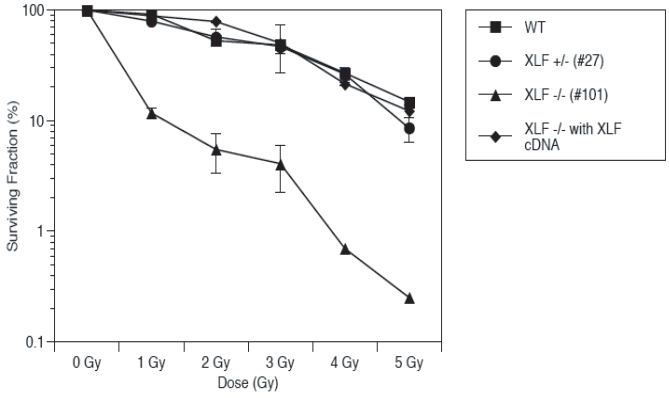
100
10
1
0.1
Surviving Fraction (%)
0 Gy
1 Gy
2 Gy
3 Gy
4 Gy
5 Gy
Dose (Gy)
WT
XLF +/- (#27)
XLF -/- (#101)
XLF -/- with XLF cDNA

Figure 7. Over-expression of XLF protein. (A) WT XLF cDNA was stably expressed in $XLF^{-/-}$ cells using a retroviral vector. Two stable clones are shown (Clone #1 and clone # 2). (B) Mutant XLF cDNAs , L115A and L179A , are stably expressed in $XLF^{-/-}$ cells using a retroviral vector.

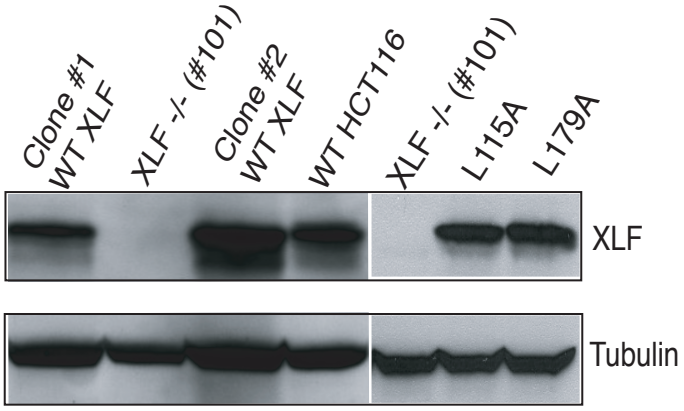
Clone #1 WT XLF
XLF -/- (#101)
Clone #2 WT XLF
WT HCT116
XLF -/- (#101)
L115A
L179A
XLF
Tubulin

Figure 8. Effect of NHEJ in XLF deficient Cells using an *in vivo* end-joining assay. (A) Reporter substrate for analysis of NHEJ. The reporter substrate consists of GFP with an artificially engineered intron, interrupted by an adenoviral exon, flanked by restriction site (HindIII) for induction of DSBs. (B) Efficiency of NHEJ in WT (HCT116), XLF $^{-/-}$, XLF $^{-/-}$ stably over-expressing WT XLF cDNA, mutant cDNA L115A and L179A. Cells were cotransfected with HindII digested reporter substrate and pCherry expression vector. The number of green (GFP+) and cherry + cells were determined by FACS analysis. (C) Quantitation of results shown in (B). Plotted is relative plasmid rejoining. The ratio of GFP+ to cherry+ was used as a measure of NHEJ efficiency. The profile shows the averages (+/- standard deviations) of at least two independent experiments.

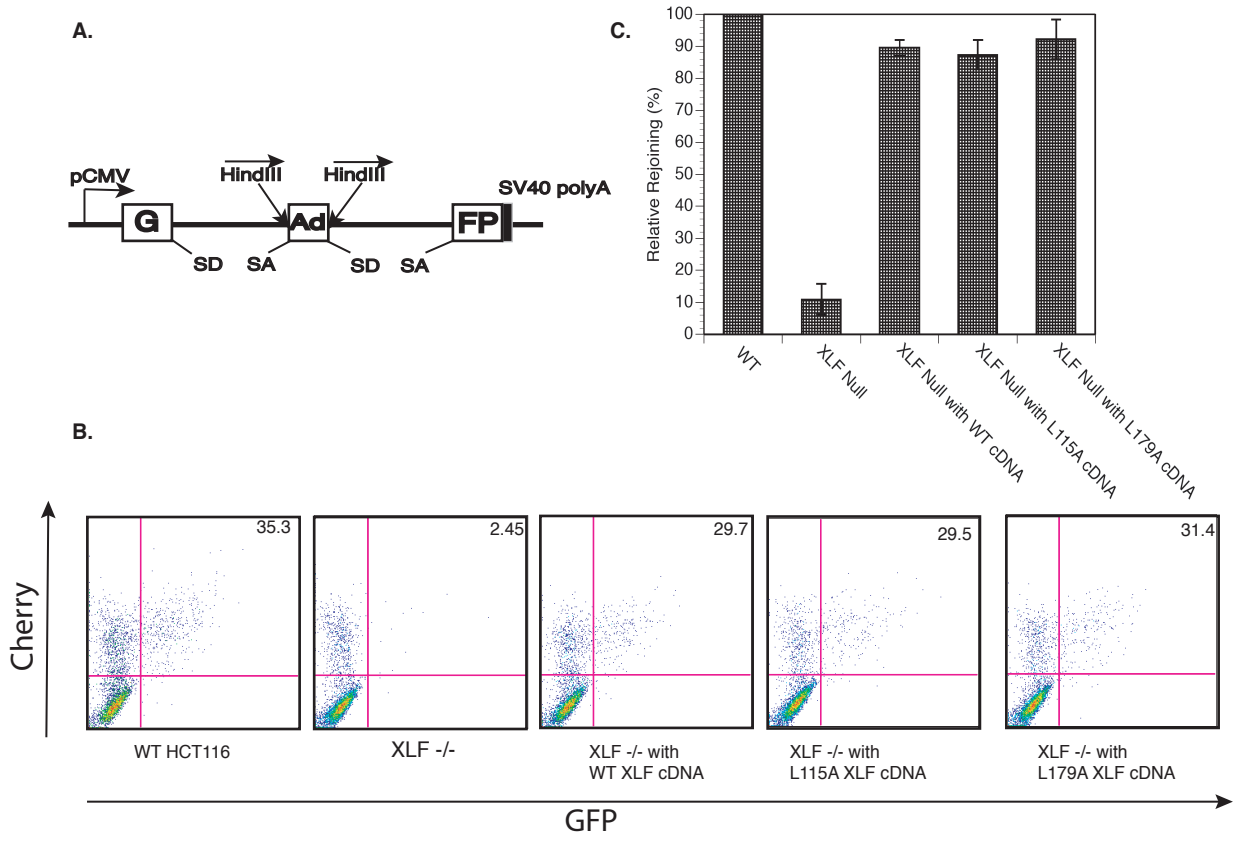
A.
pCMV
HindIII
HindIII
SV40 polyA
G
Ad
FP
SD
SA
SD
SA
C.
Relative Rejoining (%)
100
90
80
70
60
50
40
30
20
10
0
WT
XLF Null
XLF Null with WT cDNA
XLF Null with L115A cDNA
XLF Null with L179A cDNA
B.
Cherry
35.3
2.45
29.7
29.5
31.4
WT HCT116
XLF -/-
XLF -/- with WT XLF cDNA
XLF -/- with L115A XLF cDNA
XLF -/- with L179A XLF cDNA
GFP

Figure 9. Use of microhomology based repair in C-NHEJ mutant cell lines measured by Dik van Gent assay Reporter substrate biased for use by B-NHEJ. The reporter has been designed such that cleavage with *EcoRV* and *Afe1* results in a blunt-ended linear substrate with 6-bp direct repeats (open boxes) at both ends. C-NHEJ will result in the retention of some of both repeats (double boxes) whereas B-NHEJ should generate a single repeat (single box), which is the substrate for BstXI [modified after (Verkail *et al.*, 2002)]. (A) Cartoon showing the experimental scheme for analysis of the plasmids recovered from transfected cells. (B) The plasmids are subjected to PCR using one radioactively labeled (asterisk) primer. The PCR products are then subjected to *BstXI* restriction enzyme digestion. (C) Autoradiogram of one such Dik van Gent assay using the indicated cell lines. The size of the primary PCR products (180 bp) and the *BstXI* cleavage product (120 bp) are indicated as are calculated microhomology usage [represented in the graph right side of each autoradiogram) from 2 independent experiments] based upon quantitation of phosphoimager data.

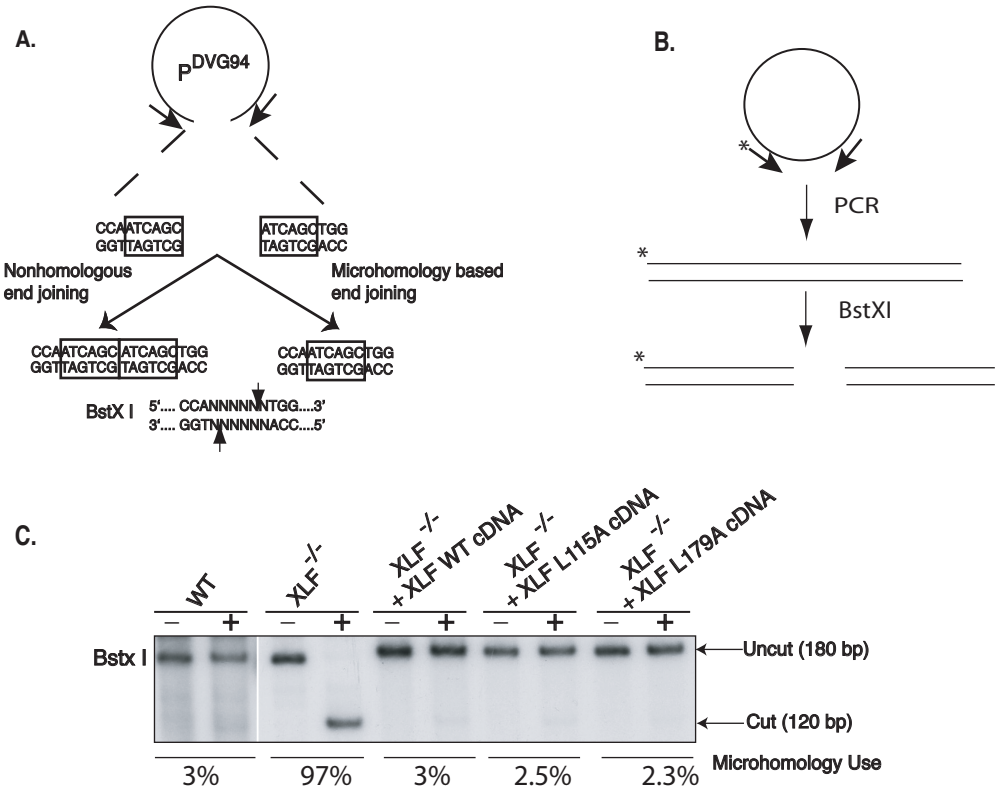
A.
P DVG94
CCAATCAGC
GGTTAGTCG
ATCAGCTGG
TAGTCGACC
Nonhomologous
end joining
Microhomology based
end joining
CCAATCAGC ATCAGCTGG
GGTTAGTCG TAGTCGACC
CCAATCAGCTGG
GGTTAGTCGACC
BstX I
5'.... CCANNNNNNTGG....3'
3'.... GGTNNNNNNACC....5'
B.
PCR
BstXI
C.
WT
XLF -/-
XLF -/- + XLF WT cDNA
XLF -/- + XLF L115A cDNA
XLF -/- + XLF L179A cDNA
– + – + – + – + – +
Bstx I
Uncut (180 bp)
Cut (120 bp)
3%
97%
3%
2.5%
2.3%
Microhomology Use

Supplemental Figure 1. Southern hybridization for identification of correct XLF targeting events. (A) A cartoon of the WT allele and XLF targeted allele showing the restriction enzyme sites and probe positions. Southern blot analysis of wild-type, XLF heterozygous (+/-) and XLF homozygous (-/-) cells. Genomic DNA samples were doubly digested with *HindIII* and *NheI* and hybridized with the either probe ‘a’ (B) or probe ‘zeo’ (C). Approximate molecular markers are shown on the right.

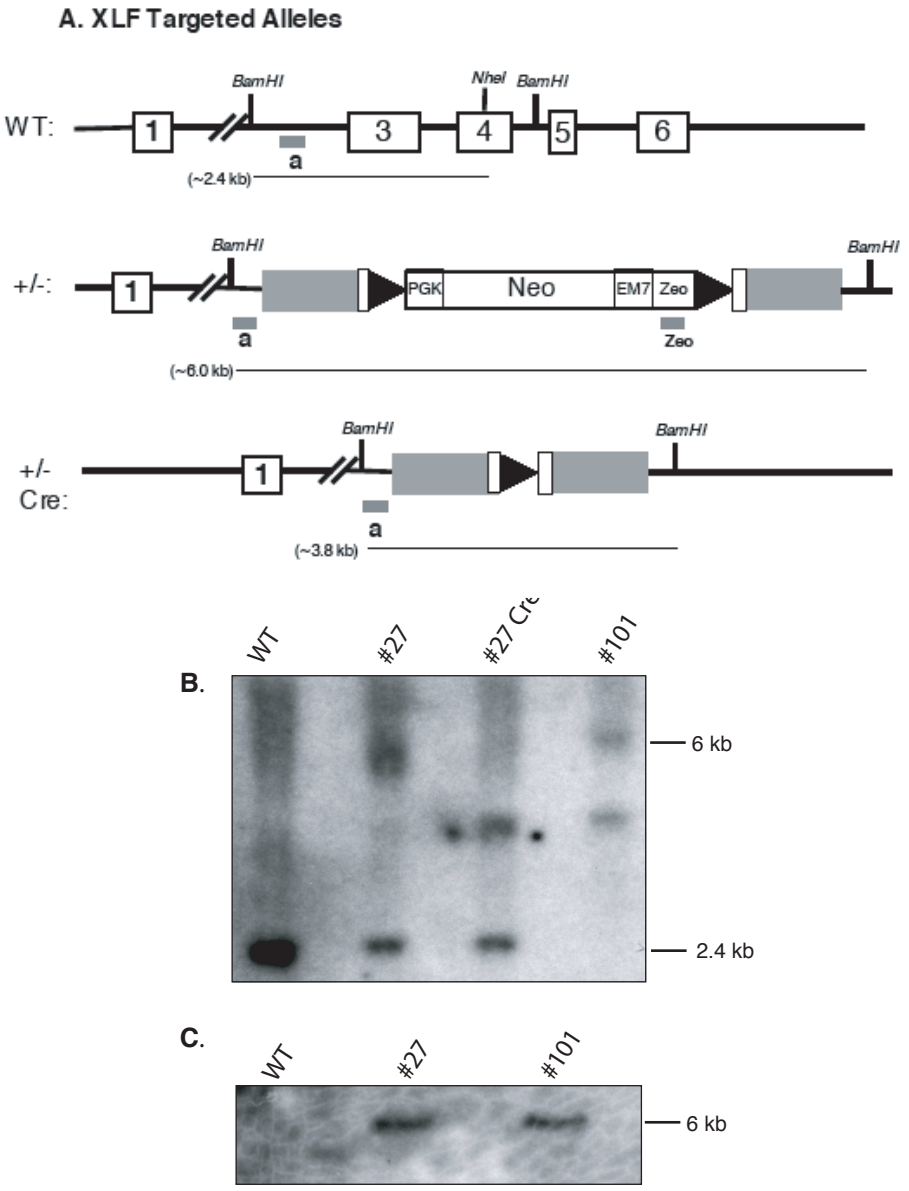
A. XLF Targeted Alleles
WT:
BamHI
NheI
BamHI
1
3
4
5
6
a
(~2.4 kb)
+/-:
BamHI
BamHI
1
PGK
Neo
EM7
Zeo
a
Zeo
(~6.0 kb)
+/-
Cre:
BamHI
BamHI
1
a
(~3.8 kb)
B.
WT
#27
#27 Cre
#101
6 kb
2.4 kb
C.
WT
#27
#101
6 kb

Supplemental Figure 2. RT-PCR analysis of XLF deficient cells. (A) A cartoon of XLF genomic locus showing the primers position used for the RT-PCR analysis. (B) RT-PCR reactions were carried out to demonstrate the lack of full length mRNA in XLF deficient cell line. Total mRNA from indicated cell lines were reverse transcribed using primer Cer 7/8 R1. This first strand cDNA was then used in three different PCR reactions with primers indicated on the right side of each panel. The PCR products were identified on an ethidium bromide-stained agarose gel. The predicted PCR fragments were indicated along with the primers used.

A.

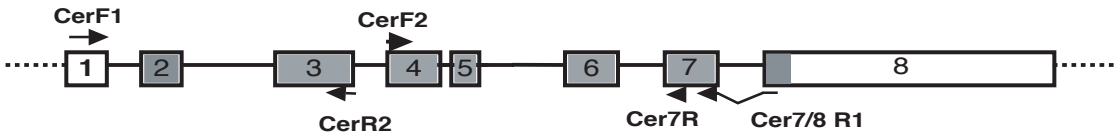
CerF1
CerF2
1
2
3
4
5
6
7
8
CerR2
Cer7R
Cer7/8 R1

B.

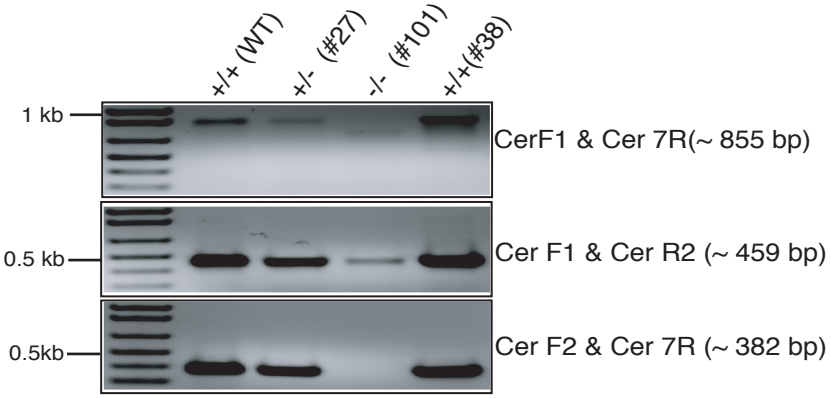
+/+ (WT)
+/- (#27)
-/- (#101)
+/+(#38)
1 kb
0.5 kb
0.5kb
CerF1 & Cer 7R(~ 855 bp)
Cer F1 & Cer R2 (~ 459 bp)
Cer F2 & Cer 7R (~ 382 bp)

Supplemental Figure 3. Intracellular localization of XLF. (A) WT or the indicated mutant XLFs were expressed in $XLF^{-/-}$ cells as pCherry fusion proteins. Whole cell extracts were probed with XLF or actin antibodies. * indicates a truncated protein.(B) The proteins were transiently expressed in $XLF^{-/-}$ cells and their localization was examined by flurescent microscopy.

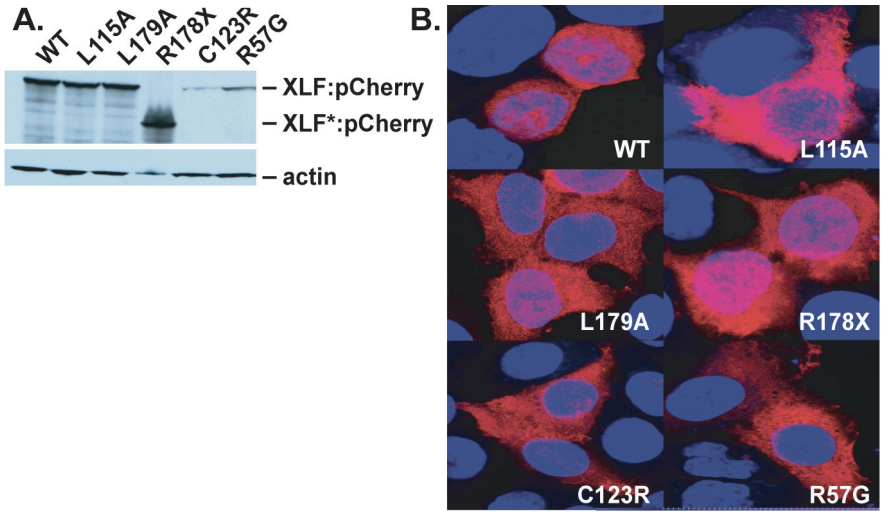
A.
WT
L115A
L179A
R178X
C123R
R57G
– XLF:pCherry
– XLF*:pCherry
– actin
B.
WT
L115A
L179A
R178X
C123R
R57G

Supplemental Figure 4: G-band Karyotype. The red arrows show instances of observed aberrant chromosomal abnormalities.

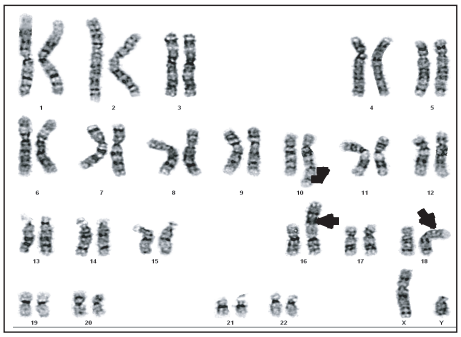

46,XY,dup(10)(q24.1q26.3),der(16)t(8;16)(q13;p13.3),
der(18)t(17;18)(q21;p11.2)

WT HCT116

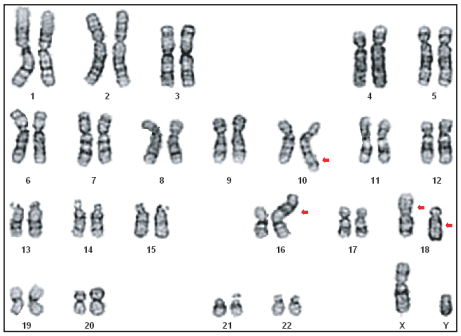

46,XY,dup(10)(q24.1q26.3),der(16)t(8;16)(q13;p13.3),
der(18)t(17;18)(q21;p11.2), add (18) (q21)

XLF +/- (#27)

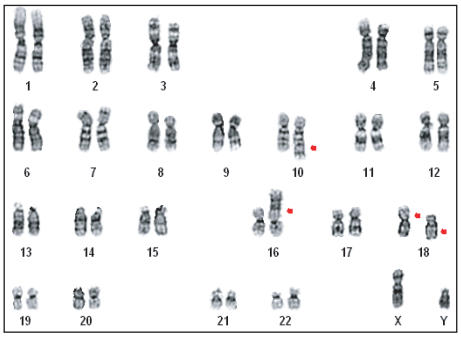

46,XY,dup(10)(q24.1q26.3),der(16)t(8;16)(q13;p13.3),
der(18)t(17;18) (q21;p11.2), add (18) (q22)

XLF -/- (#101)

Table 1. V(D)J Recombination

Cell Lines	Substrate			
	pGG49 (SJ Substrate)		pGG51 (CJ Substrate)	
	DAC/DA[a]	SJ Formation (%)	DAC/DA[a]	CJ Formation (%)
WT HCT116	107/129600	0.82%	257/120000	0.21%
	2625/72000	3.64%	32/6000	0.53%
	2014/1200000	0.16%	27/43200	0.06%
XLF +/-	96/77400	0.12%	160/65400	0.24%
	214/180000	0.11%	10/3600	0.27%
	942/324000	0.29%	64/20700	0.30%
XLF -/-	21/450000	0.0046%	0/10950	<0.009%
	21/420000	0.005%	0/70200	<0.001%
	53/468000	0.0011%	10/186000	0.005%
XLF $^{-/-}$ with WT cDNA	685/87300	0.78%	214/87300	0.24%
	1928/540000	0.35%	192/540000	0.035%
	106/23880	0.44%	31/27360	0.11%
XLF $^{-/-}$ with L115A cDNA	61/31440	0.19%	30/38700	0.077%
	3/21120	0.014%		
XLF $^{-/-}$ with L179A cDNA	23/39480	0.058%	280/64200	0.43%

Transient V(D)J recombination assays were performed in the presence of RAG-1 and RAG-2 expression vectors.

[a]DAC, numbers of ampicillin-chloramphenicol-resistant E. coli transformants after DpnI treatment; DA, numbers of ampicillin-resistant transforments after DpnI treatment.

Data generated by Junghun Kweon, Farjana Fattah and Natalie Lichter

CHAPTER IV

'Ku' regulates the pathway choice of non-homologous end joining in human somatic cells.

Introduction

One of the most harmful lesions to DNA is a double-strand break (DSB). Efficient repair of DSBs is critical for the maintenance of genomic integrity (295). DSBs in genomic DNA are generated endogenously during normal cellular processes like replication, V(D)J and class-switch recombination and are induced by a variety of genotoxic agents like ionizing radiation (30).

Cells have evolved two main mechanistically distinct pathways to repair DSBs: non homologous end joining (NHEJ), a process which directly joins the breaks without any sequence homology between the broken ends (30), and homologous recombination (HR) (296), which takes advantage of either homologous chromosome or sister chromatid to join the broken DNA end. NHEJ appears to consist of at least two sub-pathways: the main end-joining pathway described above (C-NHEJ) and one interchangeably referred to as microhomology mediated end joining (MMEJ), alternative NHEJ (Alt-NHEJ), or backup NHEJ (B-NHEJ) (hereafter B-NHEJ). It is believed that while C-NHEJ results in minimum DNA end processing (29), (106) B-NHEJ often results in a deletion with microhomology at the repair junction (106), (182), (52), (321), (108), (109), (302), (62). HR pathway can also be subdivided in homology-directed repair/ gene conversion (HDR/GC) and single stranded annealing (SSA) (317). HDR/GC uses homologous sequence for gene conversion and SSA involves homologous single strands to invade the DSB, resulting in deletion between repeats.

There are seven major proteins involved in C-NHEJ: Ku70, Ku86, the catalytic subunit of the DNA dependent protein kinase (DNA-PK_{cs}), Artemis, XRCC4, XLF and DNA ligase IV. Ku70 and Ku86 form a heterodimer and bind to broken DNA ends (166), (167) and recruits DNA-PK_{cs}, a Ser/Thr kinase belonging to the PI3 family of kinases. DNA-PK_{cs} phosphorylates the nuclease Artemis which cleans up the broken ends by cleaving the DNA structures

containing single to double-strand transition. At the final step the ligation is catalyzed by DNA LIGIV that forms a complex with XLF and XRCC4.

In order to get insights into NHEJ mechanisms, both *in vitro* and *in vivo* approaches have been carried out. In 1996 the Jackson laboratory (24) described the existence of a backup nonhomologous end-joining pathway using extrachromosomal DSB repair studies in budding yeast deficient for yKu70. They reported the repair junctions isolated from *yku*70Δ cells have nucleotide deletions and microhomologies. Several *in vitro* assays have brought substantial evidence for a backup DNA-PK independent end-joining pathway (47 [Feldmann, 2000 #145), (301), (334), (224), (302). Moreover, it has been recently shown that classical NHEJ is dispensable for the repair of DSBs involving microhomology directed repair (16), (106), (268), (321), (52).

There are evidences of B-NHEJ pathway in NHEJ-deficient cells from mammals (133), (79), (334), (16), (106), (285), (314), (108), Arabidopsis (117) budding yeast (182), (327), fission yeast (187), (62) and *Xenopus* egg extracts (97). These studies provide evidence that B-NHEJ is clearly a distinct pathway from classical NHEJ.

Studies from a number of different groups tried to find factors involved in alternative NHEJ. Several laboratories have described the DNA-PK independent B-NHEJ pathway in mammalian cells that rely on poly (ADP-ribose) polymerase-1 (PARP-1)/ XRCC1/DNA ligase III complex and polynucleotide kinase PNK as well as Fen-1 (10), (97), (301), (165), (302). These studies found that microhomology regions are often located away from the ends at naturally occurring DSBs, implying both extensive exonuclease degradation and 3'-flap removal for the annealing at microhomologous regions. The B-NHEJ pathway is distinct from classical NHEJ because it does not rely on Ku and LIGIV proteins for completion. Ku-independent B-NHEJ mechanism in mammalian cells has been shown to be also independent of XRCC4 (108).

Yeast strains deficient for NHEJ proteins, like LIGIV or any subunit of MRX complex joins linearized plasmid or broken chromosomes using B-NHEJ (332), (307), (197), (251). Both budding and fission yeast Ku70-Ku80 inhibits B-NHEJ and increases the extent of microhomology required for repair (332), (152). Mre11's nucleolytic activity is essential for B-NHEJ in *S. cerevisiae* (152). CtIP, human homolog of Sae2 can promote B-NHEJ-like repair (15).

B-NHEJ results in a deletion of one of the two microhomologous sequence and the sequence between them, and thus, is always mutagenic. B-NHEJ has been implicated in generation of large deletions and other genomic rearrangements in mammalian cells. Microhomology is often found at the recombination junctions of radiation-induced genomic rearrangements (213) implying that radiation-induced DSBs can be repaired by B-NHEJ. Microhomologies are frequently detected at breakpoints for chromosomal deletions and translocations in human cancer cells (18), (34), (83), (264), (128), (313), (313) (178) (143), (122), (144). Therefore, B-NHEJ is considered to be a cause for accumulation of genetic alteration during carcinogenesis. However, the mechanisms and the physiological significance of B-NHEJ have been largely unknown.

From the above described evidences, we hypothesized that human cells can use backup pathways to repair their DNA if the most preferred pathway is impaired. In this study, we examined the ability of NHEJ deficient human cell lines to join DNA ends using an *in vivo* plasmid end joining assay that has been employed previously to study end joining in mammalian cells (259), (302). Our results indicate that the inactivation of any core NHEJ component except 'Ku' results in severe defects in DSBs repair. Most importantly, we also found that reduced level of Ku in LIGIV knockout cells facilitates the induction of B-NHEJ pathway suggesting Ku being the determinant of NHEJ pathway choice. Using another plasmid substrate biased towards detecting microhomology-mediated NHEJ pathway (299), we found that, all the mutant lines deficient for C-NHEJ

factors use microhomologies based B-NHEJ pathway. Moreover, nucleotide sequence analysis of repaired junctions from all the mutant lines revealed a striking predominance of microhomologies, also suggesting the existence of a B-NHEJ-pathway. Surprisingly, deficiency of any of the core NHEJ factors does not affect the accuracy of end-joining of cohesive ends. Our results also showed that Ku86 is required to protect DNA ends from degradation. Over-expression of XLF and DNA-PK_{cs} in the deficient cell lines caused a significant reduction in the proportion of junctions with microhomologies as well as perfect joining of cohesive ends. These results suggest that, the C-NHEJ proteins play a critical role in directing end joining and in absence of them a B-NHEJ process operate which uses microhomology predominantly.

Methods and Materials:

Cell Culture: The human wild-type HCT116 cell line and its derivatives were cultured in McCoy's 5A medium containing 10% FBS, 100 U/ml penicillin, and 100 U/ml streptomycin in a humidified incubator with 5% CO2 at 37°C. Cell lines derived from correct gene targeting were grown under G418 (1 mg/ml) selection. Cell lines carrying exogenous cDNA (either XLF or DNA-PK_{cs}) were grown in 2 ug/ml of Puromycin.

Gene-targeting: $Ku70^{+/-}$/$LIGIV^{-/-}$ cells were generated using the rAAV targeting technology described elsewhere (78), (Oh S *et al.*, unpublished).

Ku86 Cre treatment method: To generate Ku86-null cells the $Ku86^{flox/-}$ ($Ku86^{F/-}$) cells were plated onto 6-well plate at a density of 5 X 10^4 cells per well and allowed to attach for 18 hr. Adenoviral infection was carried out by adding 2 ml of fresh media containing 5 X 10^8 virus particles (Ad-empty or Ad-Cre) to each well. After 4 days (96 hr) of incubation the cells were re-plated into 6-well plates and allowed to incubate for another 24 hr before the cells were transfected with linearized NHEJ substrate and flow cytometry was carried out after an additional incubation for 24 hr.

Knockdown of Ku70: For the RNAi experiments, pre-designed, double-stranded siRNAs (SMARTPool) targeting human Ku70 were purchased from Dharmacon.

End-Joining Assay, Transfection and FACS Analysis: The *in vivo* end-joining reporter plasmid pEGFP-Pem1-Ad2 has been described previously (259). The plasmid was digested with *HindIII* or *I-Sce*I (NEB) for 8 to 12h to generate different types of DNA ends. Supercoiled pEGFP-Pem1 plasmid was used to optimize the transfection and analysis conditions. The pCherry plasmid (Clontech) was co-transfected with either linearized pEGFP-Pem1-Ad2 or with

supercoiled pEGFP-Pem1 as a control of transfection efficiency. Cells were split a day before the transfection and were 60 to 70% confluent during transfection. All the plasmids were transfected using Lipofectamine 2000 (Invitrogen) according to manufacture's instructions. Green (EGFP) and red (Cherry) fluorescence were measured by flow cytometry 24h later (302). For FACS analysis the cells were harvested, washed in 1X PBS and fixed using 2% paraformaldehyde. FACS analysis was done on FACSCalibur instrument (BD Biosciences). For HCT116 cell line a red-versus-green standard curve was derived with varying amounts of cherry and green (pEGFP-Pem1) plasmids to avoid measurements near the plateau region. The values of repaired events is a ratio of cells that are double positive for red and green fluorescence over total cells that are only positive for red fluorescence. This ratio normalizes the repair events to the transfection controls. In the summary chart, the value from the mutants is a percent repair of wild type cells.

Plasmid Rescue: The repaired NHEJ reporter substrates pEGFP-Pem1-Ad2 were rescued from human cells using a modified Qiagen miniprep protocol and transformed into *E. Coli* (TOP10), and colonies carrying the repaired plasmids were selected on LB plates containing 30 μg/ml of kanamycin. To access the accuracy of rejoining, the plasmid DNA from individual colonies was digested using the restriction enzyme *Hind*III prior to sequencing. The fidelity of NHEJ events was examined by sequencing using primers upstream and downstream of Ad2 exon-sequence. Those events that had not restored the original restriction site are analyzed by sequencing. The primer sequences will be available upon request. For *I-Sce*I digested substrate all the repair products were directly sequenced, as incompatible *I-Sce*I sites should not restore the original restriction sites.

Dik van Gent Assay: The Dik van Gent assay was performed as described

previously (299). In brief, 2.5 µg of *EcoR*V (NEB) and *Afe*I (NEB) digested plasmid pDVG94 were transfected into cells at 60% confluency, in 6 well plates, using Lipofectamine 2000 (Invitrogen) according to manufacture's instruction. The transfection efficiency of wild type HCT116 and other mutant lines were determined using the plasmid pEGFP-Pem1 described above. 48h after transfection, plasmid DNA was recovered using modified Qiagen miniprep protocol. Repaired pDVG94 plasmid was PCR amplified using the primer DAR5 (γ-32P)-ATP labeled) and FM30 (299). The PCR product was digested with *BstX*I (NEB). Restriction fragments were separated along with undigested PCR product in a 6% polyacrylamide gel in TBE buffer. The gel was dried and exposed to film. The bands representing the undigested PCR product (180 bp) or cut (120 bp) and uncut (180 bp) PCR product after *BstX*I digestion were quantified using ImageQuant software and compared.

Results:

Cell lines and Strategy

To elucidate the roles of C-NHEJ factors, we made use of a recently developed extrachromosomal reporter assay system that has been successfully used in mammalian cells before (259), (302). This assay allows, in addition to the generation of defined DSBs, also follow up of their repair in cells without other forms of DNA damage. In this rapid-readout, direct-reporting plasmid assay, end joining is measured by the restitution of GFP expression (259). The reporter consists of the GFP (green fluorescent protein) gene engineered such that it is interrupted by a 2.4kb intron derived from rat Pem1 gene (Fig. 1A). An exon derived from adenovirus is located in the middle of the intron and it is flanked by either *HindIII* or inverted *I-SceI* restriction enzymes. In the unmodified configuration, GFP is not expressed because the adenoviral exon is efficiently incorporated into the GFP mRNA. Digestion of the plasmid either with *HindIII* or *I-SceI*, or using both enzymes, generates a linear plasmid with compatible 5'-overhanging cohesive ends and incompatible ends respectively. Because of the retention of the Ad2 exon, un-digestion or partial digestion at only one restriction site generates upon ligation a product unable to express GFP. Due to the 'buffering' capacity of the intron, end joining of transfected, linearized plasmid by the cellular repair apparatus re-constitutes GFP expression, even when extensive additions or deletions of nucleotides have occurred (259). As a result, a wide spectrum of end joining events can be detected and quantitated by FACS (fluorescently activated cell sorting). As a transfection control, cells are also always co-transfected with pCherry expression plasmid and the data are expressed as the percentage of cherry-positive cells that are also green-positive. This system has many advantages. First, because the Pem1 intron is 2.4kb long, this construct can tolerate large deletions and still yield a productive repair product. Secondly, the *HindIII* sites are arranged in such that cohesive 4-bp overlapping ends are generated (Fig. 1B). In addition, the *I-SceI* sites are

arranged in an inverted orientation (Fig. 1A), which demands that some sort of processing must occur before the ends can be rejoined. Thus, the impact of loss-of-function NHEJ gene mutations on these aspects of DSB repair can be individually assessed. Lastly, pEGFP-Pem1-Ad2 contains a bacterial origin of replication and an antibiotic resistance gene such that the plasmids can be recovered from the human cells and rescued in *E. coli*. Consequently, the structure of the repair junctions, which provides enormous mechanistic insight into the type of repair that was utilized, can be identified by DNA sequencing.

In this study, we used a series of human cell lines deficient for the major components of C-NHEJ (Table 1) namely, Ku70, Ku86, DNA-PK_{cs}, XLF and DNA LIGIV in HCT116 background. The wild type HCT116 is a human adenocarcinoma somatic tissue culture cell line, is diploid and has a stable karyotype which makes this cell line a popular choice for somatic cell gene-targeting. This study, to our knowledge, is the first study, where the roles of core NHEJ factors have been investigated using a series of human genetic knockout cell lines in an isogenic background.

C-NHEJ deficient cells are not significantly haploinsufficient for the frequency of plasmid DNA end joining *in vivo:*

When *HindIII* or *I-SceI* linearized plasmid is introduced into parental cell line HCT116, intracellular circularization allowing GFP expression is detected and quantitated by flow cytometry (Fig. 2). The parental cell line repaired (*HindIII* – 48.5% and *I-Sce-I* - 62%) this linearized construct very similarly to Ku70 (*HindIII* – 45.3% and *I-Sce-I* – 52.3%) or Ku86 (*HindIII* – 49.8% and *I-Sce-I* – 51.7%) heterozygous cells but DNA-PK_{cs} heterozygous cells were partially impaired (*HindIII* – 31.9% and *I-Sce-I* – 36.3%). On the other hand, XLF heterozygous cells have even more difficulty repairing *I-SceI* induced incompatible ends (38.3%) compared to *HindIII* cleaved 5'-cohesive ends (45.8%) observed in other *in vitro* studies (Tsai *et al.*, 2007). Lastly, it is

remarkable that even deletion of one allele of DNA LIGIV results in significant reduction in repair efficiency of both cohesive and incompatible ends (*HindIII* – 26.3% and *I-Sce-I* – 30.3%). Importantly, a partial defect in LIGIV affects the efficiency of end-joining more strongly than the defect in Ku-heterodimer.

Taken together, these data show that, *in vivo*, there is an alternative pathway, which retains ~50% of the efficiency of total NHEJ regardless of the structure of the ends.

Absence of DNA-PK$_{cs}$, XLF and LIGIV but not Ku86 reduce DNA repair efficiency:

It has been shown previously that cells deficient in any of the three components (Ku70, Ku86 and DNA-PK$_{cs}$) of DNA-dependent protein kinase, DNA-PK, are partially deficient in joining of DSBs (Lieber, 1997 #76), (155), (127). To test whether DNA-PK deficient human cells are also impaired in DSB repair, we used a Ku86 conditional null cell line as well as a DNA-PK$_{cs}$-null and XLF- null and LIGIV cell lines for *in vivo* plasmid end-joining assay.

The parental cell line repaired (*HindIII* – 51.2% and *I-Sce-I* – 64.4%) this linearized construct very similarly to Ku86 conditional null cell line (Supp Fig. 1) (*HindIII* – 57.7% and *I-Sce-I* – 66.1%) (Fig. 5A) but DNA-PK$_{cs}$ –null cells were highly impaired (*HindIII* – 2.9 % and *I-Sce-I* – 5.1%) (Fig.3).

Next we examined the DSB repair efficiency in XLF-null and LIGIV-null cells as they are involved in the ligation step of C-NHEJ pathway. Deletion of both XLF (*HindIII* – 5.3% and *I-Sce-I* – 6.2%) and LIGIV (*HindIII* – 2.4% and *I-Sce-I* – 0.64%) severely impaired the DSB repair efficiency (Fig. 3) suggesting that C-NHEJ pathway is the major pathway of repair in human cell. While XLF null cells were extremely compromised for repair, they were reproducibly more active than the LIGIV-null cells, which were barely above background activity. This is consistent with XLF playing an important, but not essential, role in DNA DSB ligation. Of note, the data indicate that a small fraction of DSBs was still

rejoined in the absence of a functional LIGIV complex though the *I-SceI* induced incompatible ends are barely repaired in LIGIV-null cells. Most strikingly, we found that absence of Ku did not lead to a reduction in DSB repair, which markedly contrasts with more than ~20 fold reduced rejoining ability of LIGIV null cells. The DSB repair defect of DNA-PK_{cs} and XLF null cells were rescued by the over-expression of DNA-PK_{cs} (Fig. 4 & Sup Fig. 2) and XLF cDNA suggesting the phenotypes were due to the deficiency of these proteins. Figure 6. is representing the repair efficiency of 4 independent experiments in all the cell line we analyzed. In conclusion, deletion of DNA-PK_{cs}, XLF and LIGIV, but not Ku86, reduced DNA repair efficiency in human somatic cells.

B - NHEJ is negatively regulated by Ku in human cells:

It has been previously described that in chicken DT40 cells, the ionizing radiation sensitivity of LIGIV deficient cells can be rescued by deletion of Ku (2). Moreover, mouse cell lines deficient for Ku86 repair DSBs with similar frequency to wild-type cells (255). On the other hand, LIGIV deficiency results in embryonic lethality that can be rescued by the deletion of Ku86 (134). So it is possible that in human cells, the repair defects of LIGIV null cells can be rescued by the absence of Ku. To test the hypothesis, whether 'Ku' is directing the pathway choice, we generated a double knockout cell line, which is, Ku70 $^{+/-}$ and LIGIV$^{-/-}$, using previously described rAAV-based gene targeting technology (Oh et al., Unpublished; (Fattah, 2008 #982) (Data not shown). When we used this cell line for DSB repair assay, it essentially behaved like LIGIV null cells because it could not repair DSBs (Fig.5B). This cell line has ~50% level of Ku70 compare to wild-type HCT116 cells. It has been shown a number of times previously that reducing the level of any subunit of Ku destabilize the other subunit (161),(77). Next we used, siRNA against Ku70 to reduce the level of 'Ku' protein further in Ku70$^{+/-}$ /LIGIV$^{-/-}$ double knockout cells which should also result in reduction of Ku86 level. This siRNA treated cell line has very low level (~5% of wild-type) of

'Ku' protein. Then we used this siRNA treated Ku70$^{+/-}$ /LIGIV$^{-/-}$ double knockout cells for *in vivo* plasmid end-joining assay. As we expected, the reduction of 'Ku' level in Ku70$^{+/-}$ /LIGIV$^{-/-}$ double knockout cells (*HindIII* – 7.5% and *I-Sce-I* – 10.9%) partially rescued the repair phenotype of Ku70$^{+/-}$ /LIGIV$^{-/-}$ double knockout cells (*HindIII* – 1.6% and *I-Sce-I* – 1.5%) (Fig 5B) suggesting in presence of Ku the B-NHEJ machinery cannot gain excess of broken DNA ends. So elimination of Ku helps for the induction of B-NHEJ pathway. Though the level of repair in Ku70$^{+/-}$ /LIGIV$^{-/-}$ double knockout cells is not as dramatic as the Ku86 conditional null because probably siRNA is not as effective as genetic knockout.

'Ku' protects DNA ends from degradation:

The absence of a defect on rejoining efficiency in Ku86- conditional null cells does not preclude the possibility of an alteration in the fidelity of repair. Thus we proceeded to perform DNA sequencing on individual colonies rescued in *E. coli* cells. We analyzed the sequences at the novel junctions. The NHEJ reporter cassette contains the bacterial origin of replication and the kanamycin resistance gene (Fig 1), which enables rescue of the reporter plasmid in *E. coli*. We detected a significant increase in deletion size in Ku86 null cells compared to wild-type cells (Table 2). In wild-type cells the median deletion size was 595bp where as in Ku86 null cells it was 1158bp for *HindIII* cleaved junctions. This same trend was also observed in *I-SceI* cleaved junctions as in Ku86 null cells the median deletion size was 1197bp in comparison to 321bp in wild type cells. In addition, Ku86 hetrozygous and null cells used significantly more often microhomologies of >6-bp than the wild-type cells (Table 2), suggesting the loss of Ku86 changes the mechanism of rejoining.

In DNA-PK$_{cs}$-null (Table 3), XLF-null (Table 4) and LIGIV-null (Table 5) cell lines we observed a spectrum of repair products similar, although not identical, to the repair phenotype of Ku86 null cells. But surprisingly, deletion of DNA-PK$_{cs}$ (Table 3), XLF (Table 4) and LIGIV (Table 5) resulted in less

degradation of DNA ends compared to wild-type cells. In DNA-PK_{cs}-null, XLF-null and LIGIV-null cell lines the Ku heterodimer is still present and may protect the DNA ends, though cannot carry out C-NHEJ due to the absence of other essential component to finish the whole end joining process. In all the null cell lines we have seen a significant number of microhomology use and in some cases the length of microhomology is >6 bp. In XLF-null cell line *I-SceI* cleaved breaks were rejoined using a preferential microhomology sequence that resulted in 13-bp signature deletion. We repeatedly have seen this hotspot of microhomology from a number of different independent experiments in XLF-null cells.

Due to low recovery of recombinants obtained from LIGIV null cells repairing *I-SceI* cleaved joints in the above experiment, several additional transfections were carried out to increase the number of recombinants available for analysis. We were unable to obtain significant number of transformants for analysis suggesting that LIGIV deficiency severely impair the joining of non-complementary DNA ends.

Absence of C-NHEJ factors enhances error free rejoining of cohesive DNA ends:

Previous studies with extrachromosomal substrates in mammalian cells suggested that Ku86 is involved in the precise ligation of complementary DNA ends (108). As outlined above in Fig.1, cohesive ends are created when the plasmid substrate is digested with *HindIII*. Error free ligation creates one *HindIII* site that can be easily detected by digesting the recovered plasmids with *HindIII,* which linearizes the plasmid backbone. Examples of such single cleavage events are shown in figure 7B. In a typical analytical gel *HindIII* digestion from wild-type or Ku86 heterozygous cells produces an average of 2-3 perfect joining events, whereas in Ku86 null cells the majority of recovered plasmid can be cleaved by *HindIII,* (Only 23% junctions showed high-fidelity perfect end joining in wild-type

cells whereas in Ku86 null cells 77% junctions were perfect joining) suggesting an induction of repair mechanism producing error free joining of 5'- cohesive ends in absence of Ku86. Similar results were obtained from all the null cells that we used for our study: DNA-PK_{cs}, XLF and LIGIV (Fig 7C). Later we sequenced most of these perfect end join producing plasmids to further confirm the restriction digestion pattern. More importantly, when DNA-PK_{cs} null and XLF null cells were complemented by over-expressing the DNA-PK_{cs} and XLF cDNA respectively, the perfect end joining spectrum of these null cells were shifted towards wild-type cells, suggesting that indeed the deficiency of DNA-PK_{cs} and XLF were responsible for this phenotype (Fig 7C).

A robust induction of microhomology-mediated B-NHEJ in core NHEJ deficient cells:

Previous studies (133), (299), (108) showed that Ku86 and DNA-PK_{cs} defective rodent cell lines showed a marked preference for microhomology-directed end-joining of DSBs. We analyzed end-joining in Ku86, DNA-PK_{cs}, XLF and LIGIV-deficient human cells using Dik van gent assay (299) (Fig. 8). This assay uses a reporter plasmid that is biased towards detecting B-NHEJ events. pDVG94 is designed such that the relative efficiency of C-NHEJ versus B-NHEJ events can be assessed (177), (299). When pDVG94 is digested with *AfeI* and *EcoRV* it results in a blunt-ended linear substrate with 6-bp repeat at both ends (Fig. 8A). C-NHEJ can rejoin these ends and yield a wide variety of junctions but B-NHEJ almost exclusively generates a single product in which 2 repeats have been reduced to 1, which simultaneously generates a novel *BstXI* restriction enzyme site (Fig. 8A). Human cell line conditionally null for Ku86 gene showed an average of >40% microhomology use compared to <5% in the parental cell line HCT116 (Fig. 8C). When we analyzed DNA-PK_{cs} deficient cells we found that >80% cells were using microgomology (Fig. 8D). Most importantly, microhomology use was significantly reduced (<40%) in the DNA-PK_{cs} deficient

cell lines over-expressing a wild-type DNA-PK_{cs} cDNA, showing that the phenotype was indeed caused by the deficiency of DNA-PK_{cs}. The microhomolgy use was more pronounced in DNA-PK_{cs} deficient cells compared to Ku86 deficient cells because it is often difficult to achieve 100% Cre-infection in conditional-null cell line.

XRCC4, XLF and LIGIV work in a complex to catalyze the ligation reaction of end-joining. In addition to the mutants in DNA-PK components, mutation of the XRCC4 gene has also been shown to result in preferential use of microhomologies in the end-joining process (133), (299), (108) in rodent cells. So next we wanted to investigate the deficiency of XLF and LIGIV on microhomology use. As expected, both XLF (Fig 8E) and LIGIV (Fig. 8F) – defective cell lines showed a significant increase in (>95%) microhomology use compared to wild-type cells. And once again, in the XLF cDNA complemented cell line microhomology use was reduced to wild-type level, confirming that XLF was the inhibitory factor for this pathway. In conclusion, all the human mutant cell lines deficient for core NHEJ factors showed a significant increase of microhomology use in our end-joining assay.

Discussion:

Although NHEJ represents the major DSB repair mechanism in mammalian cells, little is known about its efficiency. Two factors, the frequency and fidelity of rejoining, are important parameters in the efficiency of repair. The frequency, representing the capacity of cells to rejoin the DSB, is likely to correlate with survival. The fidelity represents the ability to rejoin the breaks accurately and may influence other end points such as genomic stability and the onset of oncogenesis.

In this study, using a series of human genetic knockout cell lines for major genes involved in classical NHEJ, we showed that the absence of DNA-PK_{cs}, XLF or LIGIV, but not 'Ku', result in decreased frequency of end joining in an *in vivo* plasmid end joining assay. Although extrachromosomal DSBs, which are probably more accessible than the DSBs encountered in a chromosomal context, may result in higher repair efficiency, data from budding yeast suggests that extrachromosomal assays mirror chromosomal breaks in several respects (135).

The remarkably different phenotype of Ku knockout cells, in comparison to knockouts of the other NHEJ factors with regard to the repair of DSBs mirrors the embryonic lethality of LIGIV knockout mice as opposed to the viability of the Ku86 and LIGIV double knockout (134). Our results are in agreement with the previous studies done in mouse (15), hamster (108) or human (265) cell lines deficient for components of C-NHEJ pathway.

We also showed that deficiency of the catalytic subunit of DNA-PK, DNA-PK_{cs}, results in significant repair defect confirming that C-NHEJ is the major DSB repair pathway in human cell. Previously Perrault et al., (224) used a DNA-PK_{cs} defective (M059J) whole cell extracts for *in vitro* plasmid end joining assay using restriction enzyme linearized plasmid. They showed that MO59J cell line supports active end joining. When they treated HeLa cells with a PI3K inhibitor, Wortmannin, which should inhibit DNA-PK_{cs} kinase activity, the overall DNA end joining is inhibited, suggesting that kinase inactive DNA-PK binding to DNA ends

inhibits classical NHEJ and also prevents the operation of backup pathway. In their assay they found that HeLa cells as well as M059J cells joining is mostly error-free (90%). Similar to their observation we found that in DNA-PK_{cs} deficient cells there is residual activity of end joining which rely on mainly microhomology sequences for end-joining and the rest of the joints which did not use microhomolgy, surprisingly are error-free.

The residual activity with decreased fidelity is also observed in the LIGIV and XLF - null cell lines, demonstrating the existence of an LIGIV-independent end-joining process, a feature consistent with the observation seen in XRCC4 deficient rodent (108) and murine (255) cell lines. This rejoining activity appears to be more proficient in rejoining cohesive-ends relative to noncomplementary ends, similar to observation in human cells null for LIGIV (265). In budding yeast deletion of DNL4 (LIG4 homolog) and its accessory factor NEJ1 (XLF homolog) reduces MMEJ repair approximately by half but does not completely eliminate it (182) suggesting DNL4's role in the ligation step of MMEJ. Yeast doesn't have LIGIII. So probably yeast uses LIGIV as one of its liagse for MMEJ. This observation is in complete contrast with ours as in LIG4 null or XLF null lines we see a dramatic activation of microhomology repair. So in human cell LIG4 complex negatively regulates B-NHEJ pathway. Although microhomologies have been previously reported to help NHEJ-mediated repair of DSBs (243), (280), (280) the MMEJ pathway is distinct from NHEJ because it does not rely on Ku and LIGIV NHEJ proteins for completion.

Similar to our findings, in contrast to XRCC4-null MEFs, Ku86 knock-out MEFs were almost as competent in rejoining *I-SceI*-induced DSB as wild-type cells (255). Analysis of repair products in Ku86 deficient cells showed that Ku-independent end-joining is mechanistically distinct from repair in wild-type cells, suggesting a switch to another pathway (107), (255). In human cells B-NHEJ of linear plasmid substrate is still functioning in both XLF- and LIGIV- deficient cells, suggesting that another ligase is responsible for coupling the DNA ends in this

pathway. One possible alternative is the PARP1/XRCC1/LIGIII dependent end-joining in absence of Ku (302), (11). It has been already shown that human DNA LIGI and LIGIII contribute to microhomology end joining (165).

We found that Ku controls the uses of backup pathways. The Ku heterodimer is probably involved in a very early step of DSB repair, most likely in the initial recognition of the DNA ends. Ku is a strong inhibitor of extrachromosomal B-NHEJ. These data support a protective role for the Ku heterodimer, which by binding to DNA ends, presumably reduce access to exonucleases (92), thereby limiting the B-NHEJ process. Together our work with the work in budding yeast showing that the B-NHEJ repair of DSBs is facilitated by deletion of Ku (24), and our study supports a role for Ku in repressing B-NHEJ repair of DSBs.

Taken together our data indicate that microhomology-directed end-joining does not require either the early or the late-acting components of the C-NHEJ pathway, suggesting that it constitutes a completely separate DSB repair pathway. We propose that the whole repair complex has to be assembled before the joining pathway is irreversibly determined.

Previous studies with extrachromosomal substrates suggested that Ku86 and LIGIV are involved in the precise ligation of complementary DNA ends (79), (265), (136). Using a linearized plasmid DNA with microhomologous sequences of 10 bp at both ends, Katsura *et al.* recently has shown that in CHO cells Ku86-deficiency caused approximately 75% reduction of the MMEJ activity. This observation is in contrast with the result we obtained using the similar MMEJ biased plasmid substrate in Ku86 null cells as absence of Ku increased the B-NHEJ repair compared to wild-type cells. The reason for the discrepancy between our data and the data from CHO cells is not clear. However, we have to consider that all the MMEJ processes against chromosomal DSBs are not necessarily reproduced on the present plasmid DNA substrates. The 6-bp perfect homology that would only very rarely be encountered in vivo was set as a

microhomologous sequence in this assay. In addition, deletions at DNA ends frequently occurred before joining, as commonly observed in DNA end joining assay in which linear DNAs were introduced into cells as repair substrates (133), (164). These facts might have made MMEJ more representative in the assay than in physiological DSB repair due to the extreme ease of finding microhomology at DNA ends in the repair.

In the present study, we focused on the usage of microhomology in the DNA end joining to investigate the mechanism of MMEJ, a representative mutagenic DSB repair.

However, it has been shown that NHEJ also results in mutagenic repair associated with deletions and insertions at DNA ends (169), (136). The mechanism for the occurrence of such mutagenic NHEJ has not been fully understood. Sequence analysis of the inaccurately rejoined junctions has also provided insights into the events taking place at DNA ends. In the present study, the majority of NHEJ products from wild-type cells had deletions at DNA ends, supporting the occurrence of mutagenic NHEJ in vivo. Another observation is that, the wild type cells has deletion larger because the used primers often failed to produce the sequencing data and we had to analyze a large number of rescued plasmids to obtain significant number of sequencing data. No consistent change in deletion size was seen in LIGIV or XLF deficient lines.

Microhomology was observed frequently in the inaccurately rejoined junctions, demonstrating that DNA LIGIV-independent rejoining can exploit direct repeat sequences to aid rejoining. Interestingly, deletions of DNA ends occurred more predominately in a substrate with compatible ends than in substrate with incompatible ends. This result was in contrast with a recent proposal that incompatibility of DNA ends is a cause for the occurrence of NHEJ with deletions at DNA ends (169). In the present study, repaired products were analyzed by sequencing primers located within the 2.4 kb region of Pem1 intron sequence, thus, only the repair products that retain the sequence within the primer

sequences were investigated. Therefore, repaired products with huge deletions of DNA that extended over the location of primers were not included in the analysis even if such products were produced in the cells. Thus, DNA end joining associated with deletions might have been under-represented in the present study. This study suggested that the structure of substrates, including intervening sequence between microhomologous sequences and compatibility of DNA ends, affects the joining. Thus, more comprehensive analyses of DNA end joining using a set of DNA substrate with different structures will lead to a further elucidation of the mechanism of mutagenic DSB repair.

It has been known for years that Ku-deficient mice are viable and is not defective for V(D)J recombination. On the other hand, XRCC4 or LIGIV deficient mice are inviable. These phenotypes suggest that, there may be an XRCC4/LIGIV-dependent pathway that works independent of Ku. But the results we presented here suggest that, the previous interpretation is probably not correct. The evidences we showed here in human cells suggest that Ku may play an XRCC4/LIGIV-independent role in regulating NHEJ, probably by preventing the B-NHEJ machinery from gaining access to the DSB ends when Ku-heterodimer is associated with the ends. In our study we found that Ku-deficiency results in end degradation. In budding yeast and in rodent cells lines Ku-deficiency results in similar phenotypes suggesting that Ku protects the DNA ends from degradation. Moreover, B-NHEJ requires resection of DNA ends for the search of microhomology. So it is evident that, in absence of Ku the B-NHEJ gains access the DNA ends. Lastly, our findings can help to explain why LIGIV deficiency can be rescued by Ku-deletion in mice (134) and may be intriguing to imagine that absence of Ku probably activate B-NHEJ pathway for the maintenance of genomic integrity.

Acknowledgment

The authors are indebted to Dr. V. Gorbunova (University of Rochester, NY), Dr. G. Illakis (University of Duisburg-Essen Medical School, Germany) and Dr. D van Gent (Erasmus University, Netherlands) and members of their laboratory who were extremely generous with their reagents and advice. We would like to acknowledge the assistance of the Flow Cytometry Core Facility of the Masonic Cancer Center, a comprehensive cancer center designated by the National Cancer Institute, supported in part by P30 CA77598. These studies were supported in part by National Institutes of Health grants GM 069576 and HL079559 to EAH.

Figure 1. Reporter substrate for analysis of NHEJ. A cartoon of the reporter construct (pEGFP-Pem1-Ad2). (A) The construct is essentially a GFP cassette whose expression is driven by CMV promoter and terminated by the SV40 polyA sequence. “G” is separated from “FP” by a 2.4 kb intron containing an exon (Ad) from adenovirus that is flanked by HindIII and I-SceI restriction sites. Splice donor (SD) and splice acceptor (SA) sites are shown. (B) Restriction sites used to introduce DSBs. Digestion with HindIII generate compatible cohesive ends. Because I-SceI has a nonpalindromic 18-bp recognition site, clevage of the two inverted I-SceI sites generates incompatible ends. (C) Due to the presence of Ad-exon into the middle of the Pem1 intron, the Ad exon is efficiently spliced into the middle of the GFP ORF, inactivating the GFP activity and thus making the starting substrate GFP negative. On the both side of the Ad-2 exon has HindIII/I-Sce-I restriction sites. Cleavage with either of these endonucleases removes the killer exon and upon successful intracellular plasmid circularization GFP expression is restored and can be quantitated by flow cytometery.

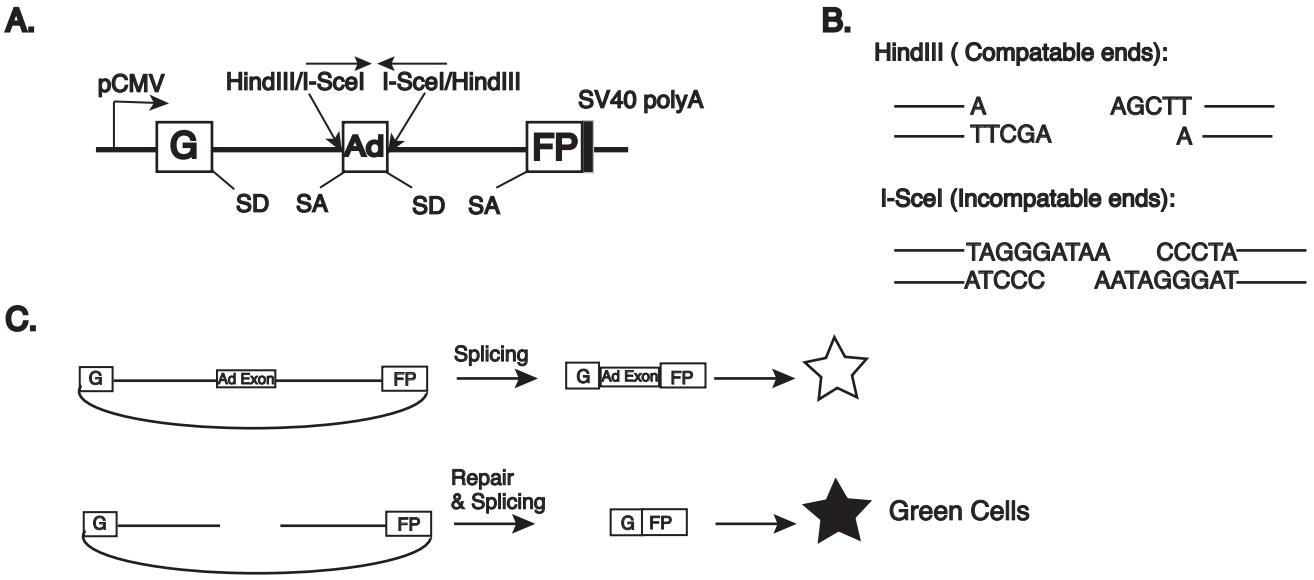
A.
pCMV
HindIII/I-SceI
I-SceI/HindIII
SV40 polyA
G
Ad
FP
SD
SA
SD
SA
B.
HindIII (Compatable ends):
A
AGCTT
TTCGA
A
I-SceI (Incompatable ends):
TAGGGATAA
CCCTA
ATCCC
AATAGGGAT
C.
G
Ad Exon
FP
Splicing
G
Ad Exon
FP
Repair
& Splicing
G
FP
G
FP
Green Cells

Figure 2. Efficiency of NHEJ in WT HCT116 and C-NHEJ mutant (heterozygous) cell lines. Indicated cell line was transfected with HindIII or I-SceI linearized pEGFP-Pem1-Ad2 together with supercoiled pCherry (to monitor transfection efficiency). The number in the top right corner corresponds to the percentage of cells that turned green after 24 hr to the percentage of cells productively transfected.

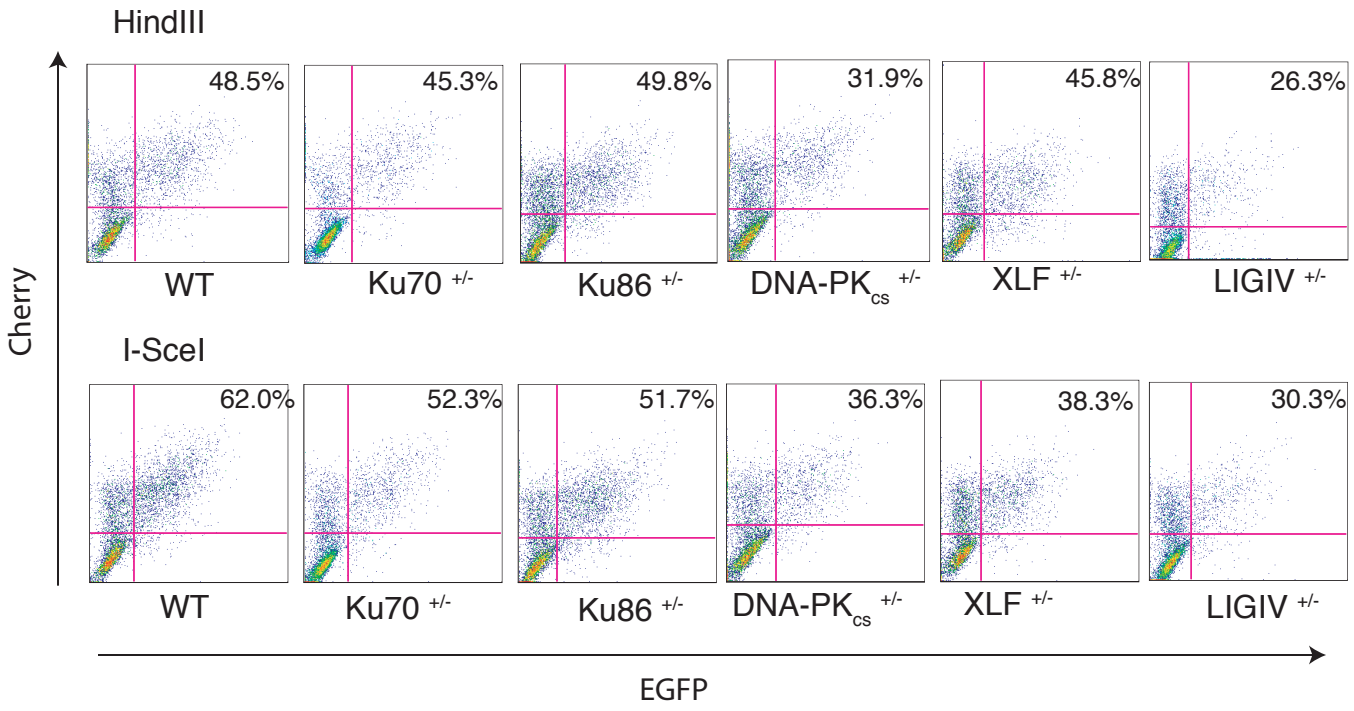

Data generated by Farjana Fattah and Eu Han Lee

Figure 3. Efficiency of NHEJ in WT HCT116 and C-NHEJ mutant (homozygous) cell lines. Indicated cell line was transfected with HindIII or I-SceI linearized pEGFP-Pem1-Ad2 together with supercoiled pCherry (to monitor transfection efficiency). The number in the top right corner corresponds to the percentage of cells that turned green after 24 hr to the percentage of cells productively transfected.

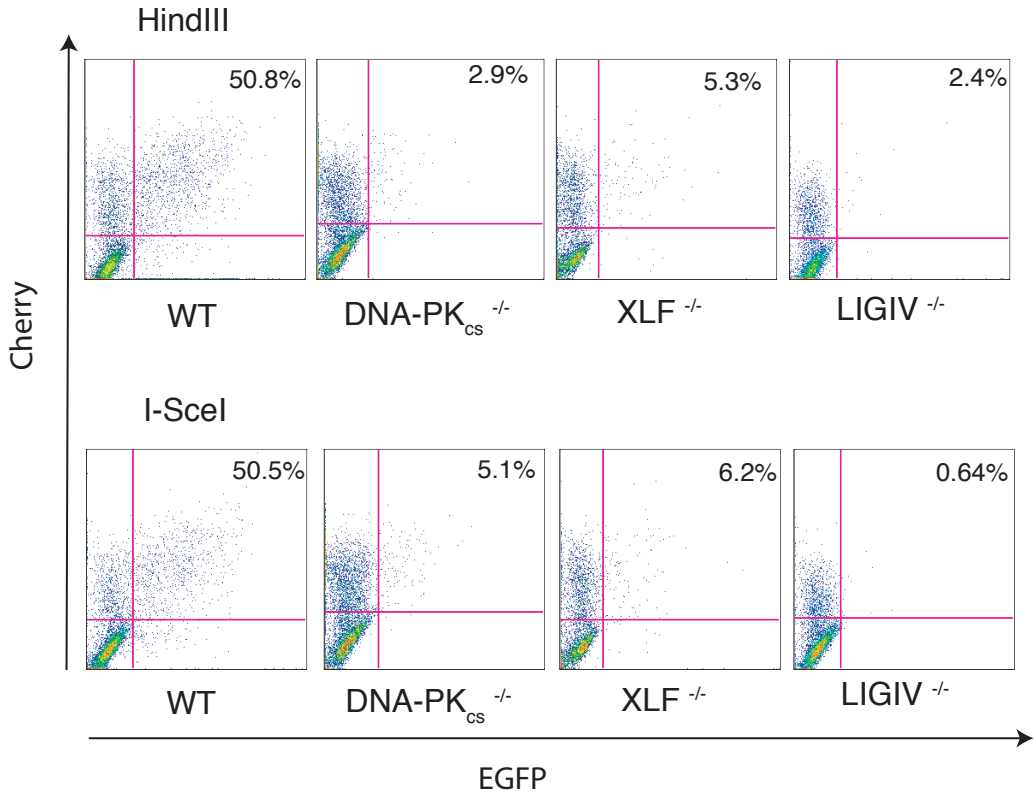

Data generated by Farjana Fattah and Eu Han Lee

Figure 4. Efficiency of NHEJ in WT HCT116 and C-NHEJ mutant complemented cell lines. Indicated cell line was transfected with HindIII or I-SceI linearized pEGFP-Pem1-Ad2 together with supercoiled pCherry (to monitor transfection efficiency). The number in the top right corner corresponds to the percentage of cells that turned green after 24 hr to the percentage of cells productively transfected.

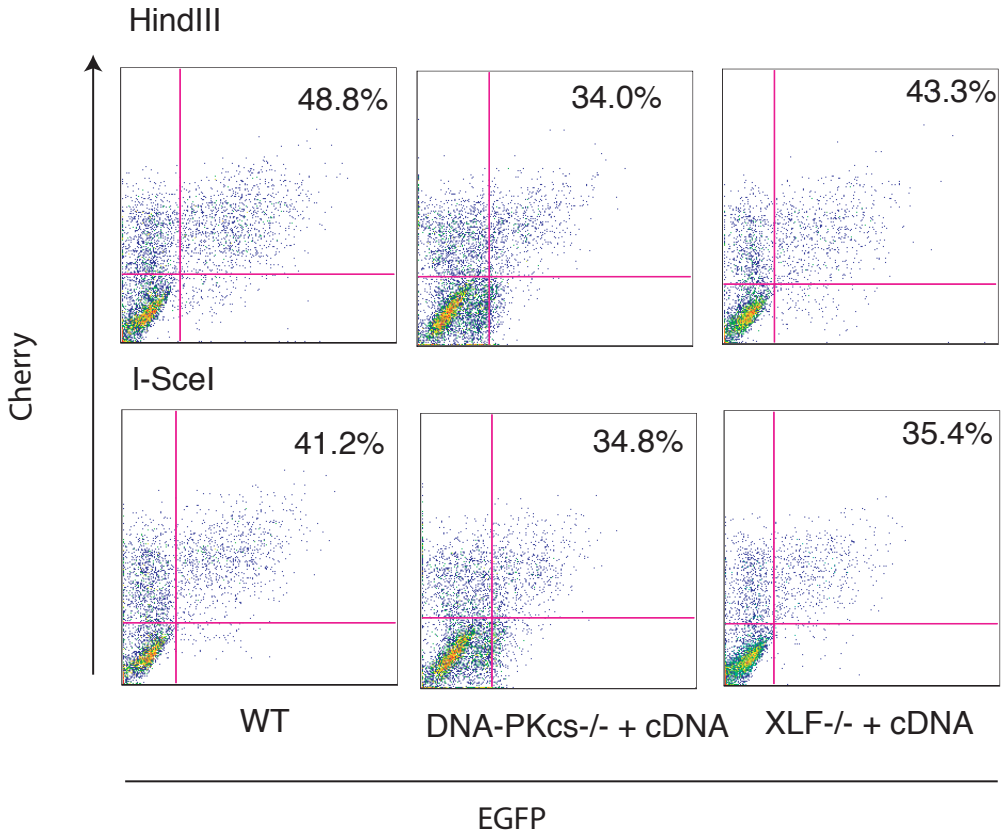

Data generated by Farjana Fattah and Eu Han Lee

Figure 5. Efficiency of NHEJ in WT HCT116, Ku86 and C-NHEJ mutant siRNA treated cell lines. Plotted is the $GFP^{+}/Cherry^{+}$ ratio for the indicated cell lines. Indicated cell line was transfected with HindIII or I-SceI linearized pEGFP-Pem1-Ad2 together with supercoiled pCherry (to monitor transfection efficiency). The number in the top right corner corresponds to the percentage of cells that turned green after 24 hr to the percentage of cells productively transfected. Plasmids were transfected 48 hr after treatment with siRNA and flow cytometry was carried out after an additional incubation for 24 hr. (A) Ku86 conditional cell line upon Cre-treatment. (B) Ku70 siRNA treatment in $LIGIV^{-/-}/Ku70^{+/-}$ cells.

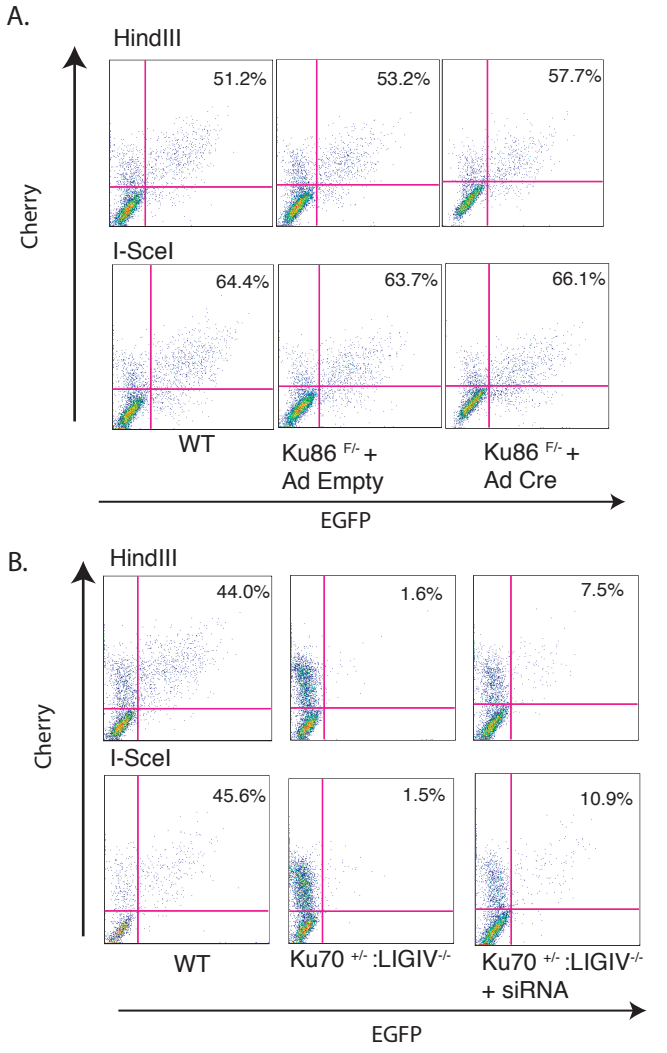

Data generated by Farjana Fattah and Eu Han Lee

Figure 6. Quantitation of four experiments similar to showed in FACS data 2 and 3. Plotted is relative plasmid rejoining in WT HCT116 and C-NHEJ mutant cell lines as calculated by dividing GFP^+/$Cherry^+$ ratios of samples. Results obtained with cells transfected with HindIII as well as I-Sce-I linearized plasmid are shown. The WT HCT116 plasmid rejoining efficiency is set to 100%.

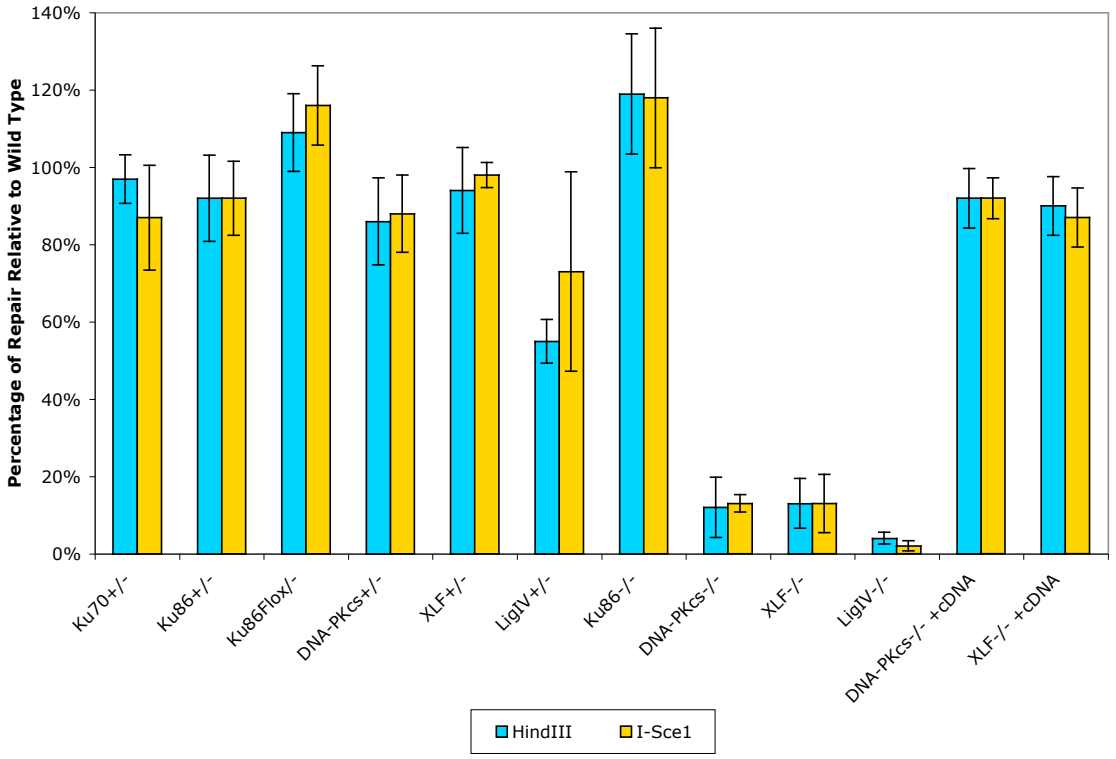
Percentage of Repair Relative to Wild Type
140%
120%
100%
80%
60%
40%
20%
0%
Ku70+/-
Ku86+/-
Ku86Flox/-
DNA-PKcs+/-
XLF+/-
LigIV+/-
Ku86-/-
DNA-PKcs-/-
XLF-/-
LigIV-/-
DNA-PKcs-/- +cDNA
XLF-/- +cDNA
HindIII
I-Sce1

Figure 7. Analysis of plasmid repair products demonstrating backup DSB repair pathways operates in C-NHEJ mutant backgrounds. (A) Restriction enzyme map of the pEGFP-Pem1-Ad2 indicating the location of the HindIII cleavage sites that flank the Ad2 exon. (B) Individual transformants arising after the WT HCT116, Ku86 $^{+/-}$ and Ku86$^{-/-}$ cell lines had been transfected by HindIII-linearized pEFGP-Pem1-Ad2 were isolated and the repaired pEGFP-Pem1-Ad2 plasmid molecules that they contained were rescued into E. coli, then were amplified and purified. After cleavage of 19 representative plasmid preparations (1-19) with HindIII, the digestion products were separated by electrophoresis on a 1% agarose gel and then were visualized by ethidium bromide staining and UV irradiation. (C) The percentage of perfect joining in all the cell line analyzed.

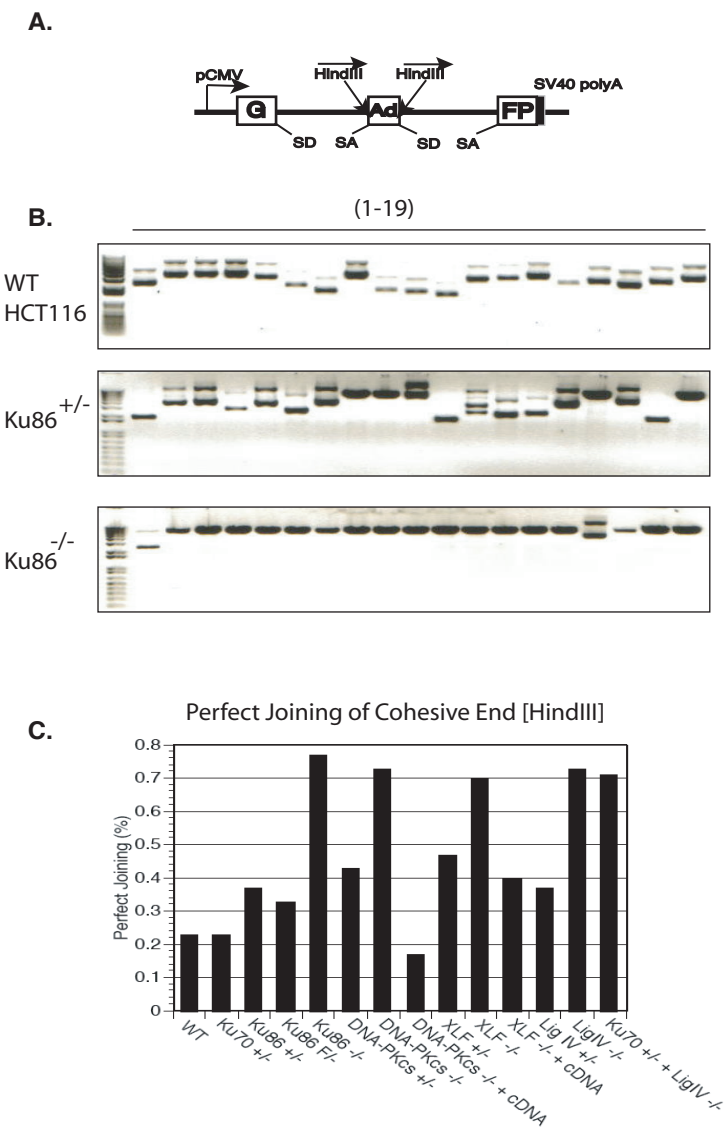

Data generated by Farjana Fattah and Natalie Waisensel

Figure 8. Use of microhomology based repair in C-NHEJ mutant cell lines measured by Dik van Gent assay Reporter substrate biased for use by B-NHEJ. The reporter has been designed such that cleavage with *EcoRV* and *Afe1* results in a blunt-ended linear substrate with 6-bp direct repeats (open boxes) at both ends. C-NHEJ will result in the retention of some of both repeats (double boxes) whereas B-NHEJ should generate a single repeat (single box), which is the substrate for BstXI [modified after (Verkail *et al.*, 2002)]. Cartoon showing the experimental scheme for analysis of the plasmids recovered from transfected cells. The plasmids are subjected to PCR using one radioactively labeled (asterisk) primer. The PCR products are then subjected to *BstXI* restriction enzyme digestion. (C), (D), (E) and (F) Autoradiogram of one such Dik van Gent assay using the indicated cell lines. The size of the primary PCR products (180 bp) and the *BstXI* cleavage product (120 bp) are indicated as are calculated microhomology usage [represented in the graph right side of each autoradiogram) from 2 independent experiments] based upon quantitation of phosphoimager data.

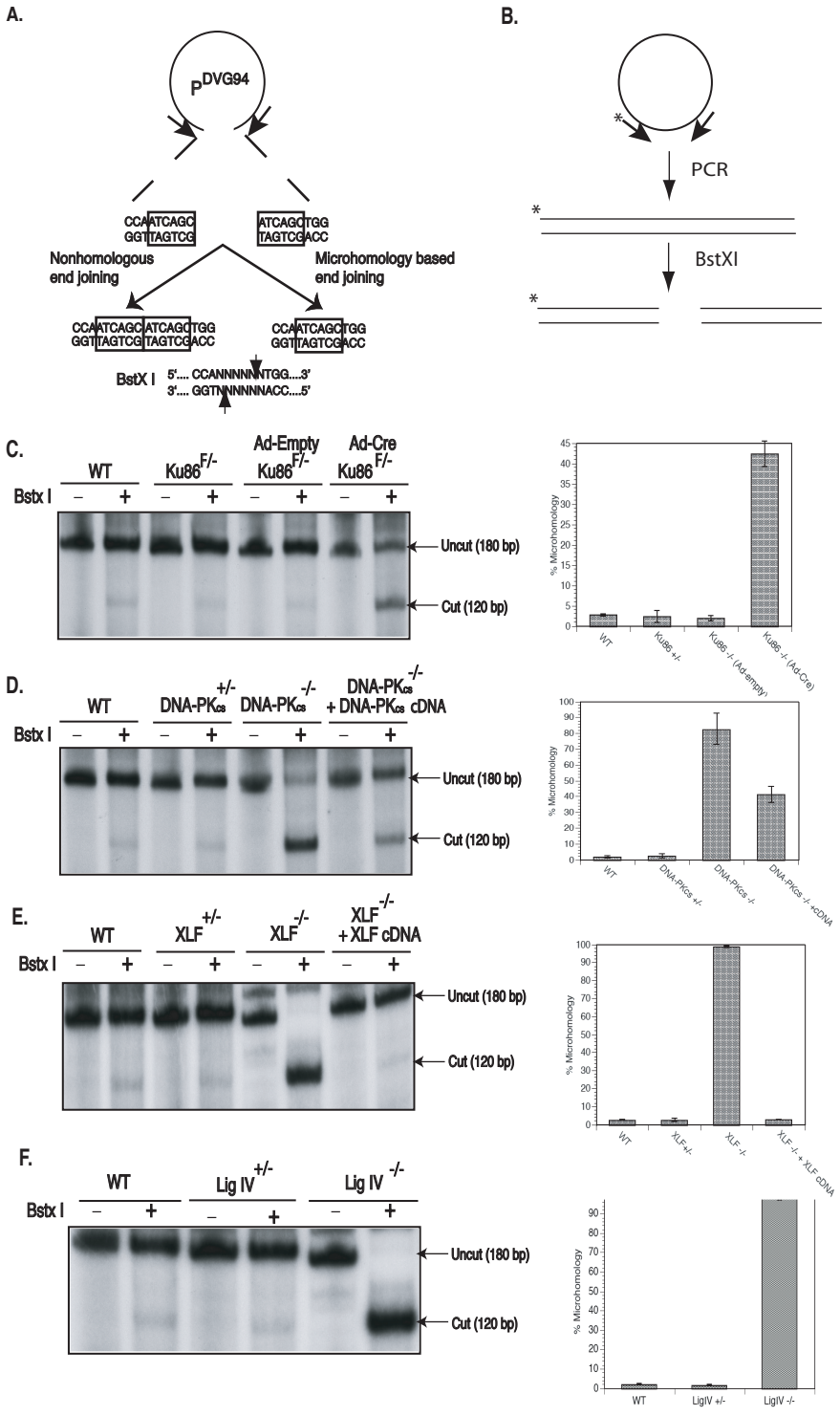
A.
P DVG94
CCAATCAGC
GGTTAGTCG
ATCAGCTGG
TAGTCGACC
Nonhomologous end joining
Microhomology based end joining
CCAATCAGCATCAGCTGG
GGTTAGTCGTAGTCGACC
CCAATCAGCTGG
GGTTAGTCGACC
BstX I 5'.... CCANNNNNTGG....3'
3'.... GGTNNNNNACC....5'
B.
PCR
BstXI
C.
WT
Ku86 F/-
Ad-Empty Ku86 F/-
Ad-Cre Ku86 F/-
Bstx I – + – + – + – +
Uncut (180 bp)
Cut (120 bp)
% Microhomology
WT
Ku86 +/-
Ku86 -/- (Ad-empty)
Ku86 -/- (Ad-Cre)
D.
WT
DNA-PKcs +/-
DNA-PKcs -/-
DNA-PKcs -/- + DNA-PKcs cDNA
Bstx I – + – + – + – +
Uncut (180 bp)
Cut (120 bp)
% Microhomology
WT
DNA-PKcs +/-
DNA-PKcs -/-
DNA-PKcs -/- +cDNA
E.
WT
XLF +/-
XLF -/-
XLF -/- + XLF cDNA
Bstx I – + – + – + – +
Uncut (180 bp)
Cut (120 bp)
% Microhomology
WT
XLF +/-
XLF -/-
XLF -/- + XLF cDNA
F.
WT
Lig IV +/-
Lig IV -/-
Bstx I – + – + – +
Uncut (180 bp)
Cut (120 bp)
% Microhomology
WT
LigIV +/-
LigIV -/-

Supplimental Figure 1. Ku protein level in Ku86 conditional cell line. $Ku86^{F/-}$ cell line was exposed to either Ad-empty or Ad-Cre and 96, 120 or 144 hr later whole cell extracts were prepared and analyzed by Western analysis using antibodies directed against Ku86 and tubulin.

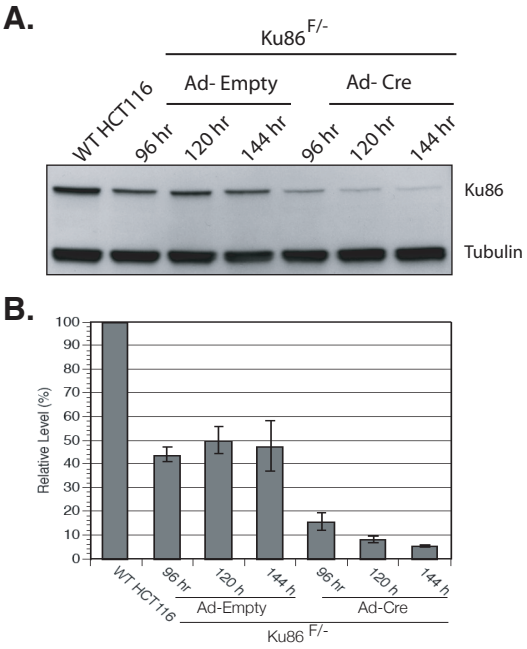
A.
Ku86 F/-
Ad- Empty
Ad- Cre
WT HCT116
96 hr
120 hr
144 hr
96 hr
120 hr
144 hr
Ku86
Tubulin
B.
Relative Level (%)
100
90
80
70
60
50
40
30
20
10
0
WT HCT116
96 hr
120 h
144 h
96 hr
120 h
144 h
Ad-Empty
Ad-Cre
Ku86 F/-

Supplimental Figure 2. Over-expression of DNA-PK_{cs} protein. (A) WT DNA-PK_{cs} cDNA was stably expressed in DNA-$PK_{cs}^{-/-}$.

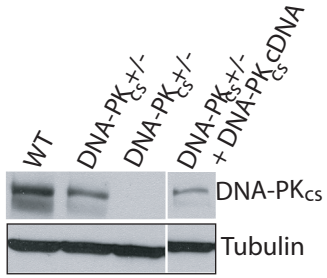
WT
DNA-PKcs+/-
DNA-PKcs+/-
DNA-PKcs+/-
+ DNA-PKcs cDNA
DNA-PKcs
Tubulin

Table 1. Cell Lines.

Cell Line	References
WT HCT116	Brattain *et al.*, 1981
$Ku70^{+/-}$	Fattah *et al.*, 2008
$Ku86^{F/-}$	Wang *et al.*, Unpublished
$Ku86^{-/-}$	Wang *et al.*, Unpublished
$DNA\text{-}PK_{cs}^{+/-}$	Ruis *et al.*, 2008
$DNA\text{-}PK_{cs}^{-/-}$	Ruis *et al.*, 2008
$DNA\text{-}PK_{cs}^{-/-}$ + cDNA	This Study
$XLF^{+/-}$	Fattah *et al.*, Unpublished
$XLF^{-/-}$	Fattah *et al.*, Unpublished
$XLF^{-/-}$ + cDNA	Fattah *et al.*, Unpublished
$LigIV^{+/-}$	Oh *et al.*, Unpublished
$LigIV^{-/-}$	Oh *et al.*, Unpublished
$LigIV^{-/-}$ + $Ku70^{+/-}$	This Study

Table Explanation

Hind III Tables:

Samples shown in the table do not include those that perfectly joined their ends after HindIII digestion, hence the variation in column height across cell lines. The percentage of perfect joins within the thirty samples is shown in the last row. The nucleotide deletions upstream (left column) and downstream (right column) are shown for each sample. Total nucleotide deletion data are skewed to the right so both the mean and median of total nucleotide deletions are summarized below the individual sample data. Letters in the middle column describe microhomology sequences. Numbers in the middle column represent the number of nucleotide insertions, and all other samples bluntly ligated the double-stranded DNA break. The percentage of both microhomology and insertions are also summarized.

ISce-1 Tables:

Thirty samples are collected from three or more independent transfections, and the nucleotide deletions upstream (left column) and downstream (right column) for each sample are given. Total nucleotide deletion data are skewed to the right so both the mean and the median of the total nucleotide deletions are summarized below the individual sample data. Letters in the middle column describe microhomology sequences. Numbers in the middle column represent the number of nucleotide insertions, and all other samples bluntly ligated the double-stranded DNA break induced by ISce-1 digestion. The percentage of both microhomology and insertions are also summarized.

Table 2

HindIII Data

WT			Ku70$^{+/-}$			Ku86 $^{+/-}$			Ku86$^{Flox/-}$			Ku86 $^{-/-}$		
del		**del**	**del**		**del**	**del**		**del**	**del**		**del**	**del**		**del**
0	4 bp	0	0	4 bp	0				0	5 bp	0			
0	5 bp	5	28	...	12				0	3 bp	5			
6	...	0	14	**AgCAT**	34				9	**TG**	25			
2	...	4	55	63 bp	12				53	**GG**	79			
3	...	18	89	...	13	**del**		**del**	109	...	61			
43	...	97	27	73 bp	76	2	...	55	109	...	61			
60	...	94	98	8 bp	13	2	...	55	94	**TGGc**	130			
126	...	228	89	**GGGGG**	79	3	...	55	95	**TGG**	130			
352	23 bp	17	1	**AAG**	186	34	...	68	61	...	164			
53	2 bp	379	9	...	185	47	**AGGGgAAAGAg**	226	94	1 bp	133			
253	**AGG**	304	167	...	287	163	...	140	120	**T**	133			
256	...	339	177	...	300	197	**A**	111	147	**CTG**	114			
368	**TT**	246	924	47 bp	134	172	...	207	133	...	156			
337	3 bp	293	875	**C**	237	349	...	66	267	**CA**	119			
746	...	296	248	**CC**	1072	149	**C**	431	248	**GCaACC**	427			
352	18 bp	720	674	...	708	290	**GGATtGtGC**	317	347	11 bp	345	**del**		**del**
369	5 bp	887	1455	...	274	453	**G**	302	668	...	304	62	...	4
823	...	443	629	**CC**	1202	668	...	304	361	...	676	234	75 bp	335
51	**GGG**	698	1878	...	4	1002	...	127	4	**T**	2033	214	...	828
699	...	838	2368	...	223	881	77 bp	358	410	...	1667	830	**GT**	328
1884	**TG**	4	2354	**G**	217	1472	...	164	410	...	1667	1441	35 bp	36
352	93 bp	2355	2354	**G**	217	1569	...	95	334	**A**	1800	0	...	1754
337	...	2428	353	68 bp	2355	2354	**G**	217	2504	...	175	244	...	1815
AVERAGE:	325		465	646		341	545		183	286		452	432		729
Total Deletion Average:		820			984			723			739			1161
Total Deletion Median:		*595*			*477*			*498*			*267*			*1158*
Percent Microhomology:		*13%*			*27%*			*20%*			*33%*			*3%*
Percent Insertions:		*27%*			*20%*			*3%*			*13%*			*7%*
Percent Perfect Joins:		**23%**			**23%**			**40%**			**23%**			**77%**

ISce-1 Data

WT			Ku70 $^{+/-}$			Ku86 $^{+/-}$			Ku86$^{Flox/-}$			Ku86 -/-		
del		**del**	**del**		**del**	**del**		**del**	**del**		**del**	**del**		**del**
2	...	0	2	3 bp	0	0	1 bp	0	0	...	0	4	...	0
2	...	0	3	4 bp	0	1	1 bp	0	3	...	1	4	3 bp	0
3	...	0	4	...	0	8	12 bp	5	4	4 bp	0	9	**AAGCTT**	5
4	...	0	4	4 bp	0	9	**AAGCTT**	5	4	5 bp	0	18	**CC**	0
9	**aAAGCTT**	4	7	7 bp	0	11	...	6	8	8 bp	0	4	...	26
9	**AAGCTT**	5	16	...	9	26	...	6	17	...	0	44	2 bp	15
9	155 bp	8	26	1 bp	0	27	33 bp	6	23	5 bp	0	139	...	0
16	...	8	67	...	1	27	15 bp	8	7	40 bp	33	67	**GG**	85
16	6 bp	10	8	**T**	67	54	1 bp	12	34	...	15	187	3 bp	0
22	**TGT**	10	86	19 bp	2	1	1 bp	85	28	**T**	23	192	...	0
41	**AA**	15	110	...	126	22	103 bp	85	56	...	7	208	**G**	103
18	**C**	79	26	2 bp	289	204	**AC**	18	66	...	13	413	...	2
58	97 bp	59	221	...	181	211	**AC**	18	1	3 bp	87	23	2 bp	470
259	**CC**	1	139	6 bp	470	161	6 bp	85	124	**TG**	136	294	...	546
168	**T**	145	599	...	85	163	...	195	273	257 bp	1	253	**T**	729
69	...	260	366	16 bp	375	55	**CTT**	344	190	...	207	706	...	505
168	**AT**	175	209	**AG**	589	816	**GCTTGTC**	7	286	4 bp	223	693	1 bp	583
119	**GG**	315	240	1 bp	613	366	18 bp	483	286	**A**	226	693	1 bp	583
388	35 bp	413	649	...	316	865	57 bp	24	289	**A**	223	1673	**C**	173
165	**C**	693	87	3 bp	903	172	...	787	271	**CT**	298	1773	...	328
59	**GGA**	844	92	117 bp	1017	351	...	755	271	**CCT**	298	2107	**G**	27
681	**T**	275	769	...	353	769	...	353	243	**C**	331	1889	**CAAG**	336
977	...	236	270	7 bp	1094	769	7 bp	361	228	...	834	994	**TGAAcCCA**	1355
525	**TCA**	788	1705	**A**	210	276	**G**	908	769	...	353	748	...	1687
617	...	931	1713	...	225	794	**GG**	405	399	**TCCA**	1492	2501	...	0
2179	...	491	626	**T**	1534	30	**AC**	1247	227	6 bp	1822	199	63 bp	2361
2613	...	117	67	**G**	2455	712	**C**	1142	196	...	2089	1436	**TGCTGCTGC**	1137
1201	**T**	1773	548	**tTTT**	2374	1636	**A**	239	2343	...	0	1457	**TGCTGCTGC**	1137
145	271 bp	4313	673	...	2315	195	**GG**	1872	61	141 bp	2297	2624	2 bp	0
218	318 bp	4277	511	**G**	2738	100	130 bp	2302	54	**C**	2393	1283	...	1846
AVERAGE:	359		542	328		611	294		392	225		447	755		468
Total Deletion Average:		900			939			686			672			1223
Total Deletion Median:		*321*			*713*			*379*			*336*			*1097*
Percent Microhomology:		*47%*			*23%*			*37%*			30%			*37%*
Percent Insertions:		*20%*			*43%*			*43%*			33%			*27%*

Table 3*

HindIII Data

WT del		WT del	DNA-PKcs +/- del		DNA-PKcs +/- del	DNA-PKcs -/- del		DNA-PKcs -/- del	Ku70+/- PKcs-/- del		Ku70+/- PKcs-/- del
0	4 bp	0									
0	5 bp	5									
6	...	0									
2	...	4									
3	...	18	0	20 bp	0						
43	...	97	1	...	0				0	4 bp	0
60	...	94	23	...	12				11	4 bp	0
126	...	228	42	**CT**	112				3	**CA**	9
352	23 bp	17	56	...	100				4	2 bp	12
53	2 bp	379	56	...	100				19	...	9
253	**AGG**	304	52	**GA**	116				92	**CCC**	40
256	...	339	177	**CT**	154				80	...	62
368	**TT**	246	268	**AGCAC**	187				73	**GAGTGACC**	69
337	3 bp	293	173	5 bp	464	del		del	73	**GAGTGGACC**	69
746	...	296	668	...	304	55	...	15	179	**GGCC**	79
352	18 bp	720	668	...	304	41	**CCTT**	81	47	**AGGGgAAAGAg**	226
369	5 bp	887	352	21 bp	823	105	**GCCTTG**	80	189	**CA**	119
823	...	443	1030	**G**	302	148	...	41	311	**CCC**	39
51	**GGG**	698	81	**A**	1735	47	**AGGGaAAAGAG**	226	268	**AGCAC**	187
699	...	838	90	7 bp	1735	142	**CCTGGAAAG**	267	341	**CACCCCCA**	1108
1884	**TG**	4	757	2 bp	1088	144	**CCTGGAA**	267	2186	116 bp	94
352	93 bp	2355	764	4 bp	1085	676	**AC**	999			
337	...	2428									
AVERAGE: 325		465	292		479	170		247	242		133
Total Deletion Average:	820			771			417			375	
Total Deletion Median:	*595*			*546*			*231*			*142*	
Percent Microhomology:	*13%*			20%			*20%*			*33%*	
Percent Insertions:	*27%*			20%			*0%*			*13%*	
Percent Perfect Joins:	**23%**			**43%**			**73%**			**47%**	

ISce-1 Data

WT del		WT del	DNA-PKcs +/- del		DNA-PKcs +/- del	DNA-PKcs -/- del		DNA-PKcs -/- del	Ku70+/- PKcs-/- del		Ku70+/- PKcs-/- del
2	...	0	2	...	0	4	...	2	2	...	0
2	...	0	2	...	0	6	...	1	2	...	0
3	...	0	4	...	0	5	...	5	2	...	0
4	...	0	2	...	5	7	162 bp	3	4	...	1
9	**aAAGCTT**	4	9	**AAGCTT**	5	6	**AG**	6	3	**A**	4
9	**AAGCTT**	5	15	...	0	9	**aAAGCTT**	4	5	...	3
9	155 bp	8	17	...	0	9	**AAGCTT**	5	7	**TA**	3
16	...	8	11	...	7	9	**AAGCTT**	5	4	...	6
16	6 bp	10	21	...	0	17	...	0	5	...	6
22	**TGT**	10	19	**C**	15	17	**CA**	13	17	...	0
41	**AA**	15	21	...	13	23	...	21	17	...	0
18	**C**	79	32	...	2	39	**AGA**	16	9	4 bp	14
58	97 bp	59	21	**TT**	35	10	1 bp	67	8	8 bp	18
259	**CC**	1	57	**CC**	46	60	...	47	22	...	16
168	**T**	145	163	**C**	0	26	**CATGG**	82	24	...	19
69	...	260	148	**CTG**	71	64	4 bp	49	19	**C**	28
168	**AT**	175	193	...	139	55	**T**	67	15	**GTTTCtAAG**	33
119	**GG**	315	4	...	330	114	**TGGtTTC**	31	48	**C**	19
388	35 bp	413	397	**A**	159	87	**GAGTGACC**	75	74	...	19
165	**C**	693	425	...	318	123	...	67	87	**gGGAGTGACC**	74
59	**GGA**	844	371	**T**	400	60	**G**	223	180	...	57
681	**T**	275	191	...	570	61	**AGGGgAAAGAc**	232	161	**G**	77
977	...	236	879	**C**	273	159	1 bp	208	158	**CCTGGaA**	134
525	**TCA**	788	879	...	274	206	**GCAcAGGGc**	208	288	**GT**	55
617	...	931	1229	**GCTTG**	7	249	**T**	167	6	4 bp	481
2179	...	491	1177	**GA**	324	331	...	275	388	**T**	305
2613	...	117	823	32 bp	835	11	**C**	602	195	...	614
1201	**T**	1773	754	...	1123	835	...	1093	641	**CTTCCCAC**	597
145	271 bp	4313	657	...	2361	2038	...	209	148	13 bp	1289
218	318 bp	4277	47	...	4431	135	92 bp	2361	2614	...	208
AVERAGE: 359		542	286		391	159		205	172		136
Total Deletion Average:	900			677			364			308	
Total Deletion Median:	*321*			*191*			*111*			*45*	
Percent Microhomology:	*47%*			*37%*			*50%*			*37%*	
Percent Insertions:	*20%*			*3%*			*17%*			*13%*	

** See Table 1 Discription*

Table 4*

HindIII Data

WT del		WT del	XLF+/- del		XLF+/- del	XLF-/- del		XLF-/- del	XLF-/- + XLF pBabe del		XLF-/- + XLF pBabe del
0	4 bp	0	110	CTTG	53	0	7 bp	0	3	CA	9
0	5 bp	5	138	GAA	56	0	29 bp	9	4	1 bp	11
6	...	0	174	...	98	0	A	10	15	ACA	8
2	...	4	3	CCA	405	0	29 bp	10	4	TGTTTCC	84
3	...	18	253	AGG	304	4	11 bp	7	356	...	41
43	...	97	309	...	626	8	TT	6	450	GA	11
60	...	94	352	16 bp	885	823	...	443	223	TT	240
126	...	228	255	TGA	1041	341	CCA	1099	182	G	348
352	23 bp	17	488	...	958	2354	G	217	515	...	305
53	2 bp	379	688	TTCAaGT	941				751	...	2438
253	AGG	304	828	32 bp	835				23	A	972
256	...	339	1910	8 bp	181				509	CTCAga	520
368	TT	246	2242	C	2				1151	C	129
337	3 bp	293	701	AACC	1580				1455	49 bp	36
746	...	296	719	4 bp	1745				1701	1 bp	79
352	18 bp	720	639	...	1883				725	C	1801
369	5 bp	887	274	...	2293				817	T	2164
823	...	443							737	...	2432
51	GGG	698							1701	1 bp	79
699	...	838							725	C	1801
1884	TG	4							817	T	2164
352	93 bp	2355							737	...	2432
337	...	2428							751	...	2438
AVERAGE: 325		465	593		817	392		200	535		646
Total Deletion Average:		820			1410			592			1181
Total Deletion Median:		*595*			*1446*			*11*			*908*
Percent Microhomology:		*13%*			*27%*			*13%*			*37%*
Percent Insertions:		*27%*			*13%*			*13%*			*10%*
Percent Perfect Joins:		**23%**			**43%**			**70%**			**40%**

ISce-1 Data

WT del		WT del	XLF +/- del		XLF +/- del	XLF -/- del		XLF -/- del	XLF -/- + XLF pBabe del		XLF -/- + XLF pBabe del
2	...	0	2	...	0	0	2 bp	0	0	...	0
2	...	0	4	...	0	1	1 bp	0	2	...	0
3	...	0	4	...	0	4	4 bp	0	2	...	0
4	...	0	4	G	11	9	AAGCTT	5	2	...	0
9	aAAGCTT	4	17	A	6	9	AAGCTT	5	2	...	0
9	AAGCTT	5	36	...	0	9	AAGCTT	5	2	3 bp	0
9	155 bp	8	17	T	89	9	AAGCTT	5	4	4 bp	0
16	...	8	106	C	0	9	AAGCTT	5	14	1 bp	0
16	6 bp	10	119	11 bp	0	9	AAGCTT	5	18	4 bp	0
22	TGT	10	301	...	191	9	AAGCTT	5	4	...	26
41	AA	15	434	...	131	9	AAGCTT	5	29	A	4
18	C	79	366	16 bp	304	9	AAGCTT	5	31	...	4
58	97 bp	59	554	...	152	9	AAGCTT	5	55	CCTT	87
259	CC	1	100	CTGA	702	17	...	24	105	CCT	143
168	T	145	632	...	209	62	3 bp	85	248	C	0
69	...	260	90	6 bp	903	154	AG	6	193	2 bp	85
168	AT	175	353	C	691	87	GAGTGACC	75	192	6 bp	90
119	GG	315	521	A	662	187	3 bp	0	3	A	279
388	35 bp	413	1232	ATAGgC	387	366	16 bp	27	193	7 bp	90
165	C	693	87	C	1552	267	...	350	352	...	68
59	GGA	844	702	TTCaTGT	947	2	6 bp	619	194	AGGC	310
681	T	275	607	GG	1242	259	143 bp	502	356	...	209
977	...	236	838	3 bp	1093	708	...	311	118	10 bp	538
525	TCA	788	1608	...	391	101	TGGtCCTgCTG	1212	548	T	149
617	...	931	542	gAATA	1628	1193	361 bp	213	757	3 bp	250
2179	...	491	2037	...	208	543	...	958	349	...	932
2613	...	117	1040	3 bp	208	1705	A	210	868	...	415
1201	T	1773	193	...	2131	1280	AA	935	353	C	1324
145	271 bp	4313	208	...	2119	2292	...	214	2025	GG	187
218	318 bp	4277	787	...	1894	192	GAGGCCc	2447	127	C	2300
AVERAGE: 359		542	451		595	364		316	238		250
Total Deletion Average:		900			1080			680			488
Total Deletion Median:		*321*			*917*			*175*			*263*
Percent Microhomology:		*47%*			*40%*			*40%*			*33%*
Percent Insertions:		*20%*			*17%*			*30%*			*30%*

** See Table 1 Discription*

Table 4*

HindIII Data

WT del		WT del	Lig IV$^{+/-}$ del		Lig IV$^{+/-}$ del	LigIV$^{-/-}$ del		LigIV$^{-/-}$ del	Ku70$^{+/-}$ LigIV$^{-/-}$ del		Ku70$^{+/-}$ LigIV$^{-/-}$ del
0	4 bp	0							3	...	0
0	5 bp	5							4	TGTTTCC	84
6	...	0							80	...	62
2	...	4	42	T	6	4	TGTTTCC	84	38	AGGGAAAAGAG	226
3	...	18	31	T	54	83	1 bp	79	0	...	320
43	...	97	39	GA	62	70	184 bp	118	274	...	49
60	...	94	87	TTCTG	63	132	...	79	269	TGAGCA	145
126	...	228	46	gcatAgGGaGAAAGAGg	202	167	TTTCCC	86	336	CCCc	454
352	23 bp	17	213	A	57	192	GCAcAGGGc	202	29	TGCATTCT	1466
53	2 bp	379	47	AGGGgAAAGAg	226	192	...	11	1100	CTA	728
253	AGG	304	48	AGGGgAAAGA	226						
256	...	339	50	AGGGGAAA	226						
368	TT	246	47	AAGAg	231						
337	3 bp	293	140	aggGgAAAGAg	226						
746	...	296	147	...	237						
352	18 bp	720	457	...	3						
369	5 bp	887	258	C	247						
823	...	443	137	...	525						
51	GGG	698	342	...	355						
699	...	838	551	AT	158						
1884	TG	4	1030	G	302						
352	93 bp	2355	333	...	1373						
337	...	2428									
AVERAGE: 325		465	213		252	120		94	213		353
Total Deletion Average:	820			464			243			567	
Total Deletion Median:	*595*			*278*			*211*			*326*	
Percent Microhomology:	*13%*			*47%*			*10%*			*20%*	
Percent Insertions:	*27%*			*0%*			*7%*			*0%*	
Percent Perfect Joins:	23%			37%			77%			67%	

ISce-1 Data

WT del		WT del	Lig IV$^{+/-}$ del		Lig IV$^{+/-}$ del	LigIV$^{-/-}$ del		LigIV$^{-/-}$ del	Ku70$^{+/-}$ LigIV$^{-/-}$ del		Ku70$^{+/-}$ LigIV$^{-/-}$ del
2	...	0	0	...	0				3	...	0
2	...	0	0	...	0				9	AAGCTT	5
3	...	0	1	1 bp	0				17	...	0
4	...	0	1	1 bp	0	2	...	0	18	CC	1
9	aAAGCTT	4	2	...	0	9	AAGCTT	5	0	19 bp	43
9	AAGCTT	5	4	...	0	22	TGT	10	99	CCTTgTgaC	87
9	155 bp	8	4	G	7	15	GTTTCcAAG	33	104	...	85
16	...	8	4	G	11	48	...	74	105	CCCT	95
16	6 bp	10	3	...	14	87	GAGTGACC	75	6	TAG	285
22	TGT	10	82	AC	18	241	14 bp	57	61	AGGGaAAAGAc	232
41	AA	15	5	GG	103	356	...	211	304	...	332
18	C	79	88	...	54	304	...	332	739	CcCtAAAGC	0
58	97 bp	59	4	...	154	108	TCAgGGC	1726	682	...	310
259	CC	1	136	G	33	618	AAGaACT	1791	879	C	273
168	T	145	192	...	65				879	26 bp	300
69	...	260	191	1 bp	67						
168	AT	175	60	G	223						
119	GG	315	104	3 bp	243						
388	35 bp	413	293	...	129						
165	C	693	366	18 bp	90						
59	GGA	844	213	...	409						
681	T	275	325	...	339						
977	...	236	228	CC	749						
525	TCA	788	1010	...	19						
617	...	931	890	...	178						
2179	...	491	17	CCA	1105						
2613	...	117	351	CC	922						
1201	T	1773	792	...	967						
145	271 bp	4313	1277	...	792						
218	318 bp	4277	2320	TtTAT	384						
AVERAGE: 359		542	299		236	229		416	273		147
Total Deletion Average:	900			533			646			421	
Total Deletion Median:	*321*			*258*			*230*			*246*	
Percent Microhomology:	*47%*			*33%*			*50%*			*56%*	
Percent Insertions:	*20%*			*17%*			*0%*			*13%*	

** See Table 1 Discription*

CHAPTER V
CONCLUSIONS AND FUTURE DIRECTIONS

Conclusion:

From our lab, we (78) have been able to inactivate one allele of the Ku70 gene in human somatic cell line, HCT116. A second round of targeting to inactivate the second allele demonstrated that Ku70 is an essential protein in human cells since a clone null for Ku70 was never obtained. In contrast, I was able to repeatedly obtain clones in which the inactivated allele was once again targeted (re-targeting events) (77). This data provides a compelling argument that correct targeting of the second allele results in unviable null cells. A similar conclusion was reached earlier for the Ku86 gene (161). Also, our observations are consistent with the fact that no mutation of the Ku70 gene in any human patients has ever been reported. This essential nature of Ku for humans and human cells stands in stark contrast to that observed for mice and murine cells.

During the course of inactivating the second allele of Ku70 locus I found that, reduced level of Ku70 proteins leads to higher frequency of rAAV mediated gene targeting in human somatic cells. I used siRNA and shRNA mediated knockdown strategy to reduce the Ku70 protein level in wild-type cells and phenocopied the genetic observation that, reduced level of Ku indeed increases the frequency of gene targeting. This finding will advance the somatic cell gene-targeting field as well as the gene therapy approaches using homologous recombination. In collaboration with Eu Han Lee, I am testing whether the DNA-PK_{cs} also has role in gene-targeting. In this project, in addition to genetic knock-out and siRNA treated cells, we are using novel DNA-PK_{cs} inhibitor to test the absence of DNA-PK_{cs} on gene-targeting. Successful use of DNA-PK_{cs} inhibitor for enhancing gene targeting frequency will allow us to apply the technique to a variety of cell lines and will extend its application even in gene targeting in embryonic stem cell.

The newly described XLF gene has been suggested to be a core factor of C-NHEJ pathway (26), (4). To elucidate the role of XLF in human I generated XLF deficient human somatic cells using rAAV technology. Primary

characterization demonstrated that, XLF deficiency leads to significant growth defect, severe DSB repair defects and V(D)J recombination defect suggesting XLF is indeed a core C-NHEJ factor. Using an *in vivo* plasmid end-joining assay and a novel microhomology assay we demonstrated, how XLF contributes to the cellular end-joining pathways. I initiated works which in future should reveal the exact function of XLF in the process of NHEJ. By using site-directed mutagenesis I introduced point mutation in XLF cDNA to investigate the structure-function of this new protein. I also investigated how mutaions in XLF affects its intracellular localization.

It has been shown in other organisms that deficiency of C-NHEJ factors activate the B-NHEJ pathway (133), (79), (334), (16), (106), (Wu, 2008 #9), (108). Using a series of human knockout cell lines, I investigated, how the deletion of Ku, DNA-PK_{cs}, XLF and LIGIV affect the spectrum of end-joing in human somatic cells. I used a well-characterized *in vivo* plasmid end joining assay and an assay which estimate the microhomology use *in vivo*, to show that the B-NHEJ pathway operates in absence of C-NHEJ. Absence of C-NHEJ factors, DNA-PK_{cs}, XLF and LIGIV, except Ku leads to severe repair defects. In fact, our experiments showed that Ku is the master regulator of NHEJ pathway choice. We sequenced the repaired junctions of the rescued plasmids from cells and found that B-NHEJ pathway used microhomology predominantly for repair. And we also found that Ku is important for protecting the DNA ends from degradation.

In conclusion, my work elucidated important unknown functions of C-NHEJ factors in human somatic cells.

Future Directions

Generation of viable Ku70–null cells by expressing "floxed" exons:

It will be impressive if we can generate Ku70 null cell line using a conditional knockout approach. The Ku70 heterozygous cell line can be obtained using a conditional targeting vector which contains sequences for the exons that are being inactivated. This method has already been used with success in our lab previously (Wang *et al.*, unpublished data). The exons in the targeting vector will be flanked by loxP sequences. After the first round of targeting the selection cassette will be removed by Cre mediated recombination. This will make the first allele wild-type for Ku70 since the deleted exon sequences is now present in the arm of the targeting vector. A second round of targeting can now be carried out with a conventional vector to inactivate the second allele. Finally the first allele can be inactivated by another round of Cre recombination, which will take out the exon sequences from the targeting vector. This cell line will be null for Ku70.

What is the impact of loss-of-function mutation of DNA-PK_{cs} gene on rAAV-mediated gene targeting?

Recently our lab has described, the construction-using rAAV-mediated gene targeting-of human HCT116 cell lines that are wild-type, heterozygous or null for DNA-PK_{cs} expression (78). I used these 3 cell lines and subsequently infected either with either with a rAAV knockout vector for Ku70 or CCR5. Each of the vectors carried the NEO gene and thus productively infected cells became G418-resistant. All of the G418- resistant colonies (generally 100 t0 200) were then individually characterized for either random integration or correct integration using PCR (77). In wild-type cells the frequency of correct gene targeting for Ku70 was 0.7% and CCR5 1.2%. In DNA-$PK_{cs}^{+/-}$ cells, the frequency of targeting increased to 5.5% and 6.5% respectively. In DNA-$PK_{cs}^{-/-}$ cells, the frequency of

targeting increased even more, to 6.8% and 9.2%, respectively (data not shown). This observation can be extended using siRNA against DNA-PK_{cs} in wild-type HCT116 cells.

As described above (77) I have been able to demonstrate that genetic ablation of DNA-PK subunits results in enhanced rAAV-mediated gene targeting. Unfortunately, we have also demonstrated that long-term deficiency in either Ku or DNA-PK_{cs}, leads to severe telomere disfunction (207), (245). Thus from a practical point of view-and certainly from a clinical applicability point-of-view – the inhibition of DNA-PK is of debatable significance. Instead, what one would like to have available is a small molecule inhibitor of DNA-PK that an investigator could transiently add to their cell line of choice to create a "window-of-opportunity" to do enhanced rAAV-mediated gene targeting, and then remove the inhibitor so that there weren't any long-term detrimental effects to the cell line caused by the suppression of DNA-PK. In collaboration with Eu Han Lee, I transiently inhibit DNA-PK activity with the DNA-PK_{cs}- specific inhibitor, NU7441 (150) in wild-type HCT116 cells and infected with rAAV:CCR5 virus. The G418-resistant cells that resulted from this treatment showed 10.5% correct targeting in CCR5 locus. To extend this observation, wild-type HCT116 cells can be treated with NU7441 and other loci (e.g. Ku70, XLF) can be targeted to test the effect of DNA-PK_{cs} inhibition in gene-targeting in general. Moreover, So far I have able to show the effect of DNA-$PK_{cs}^{+/-}$ inhibition in HCT116 cells. This approach would be more practical if we can use this technique for gene-targeting by inhibiting DNA-PK_{cs} in other primary cells (e.g. RPE cells) or embryonic stem cells.

What is the role of XLF in NHEJ process?

C-NHEJ pathway is involved in V(D)J recombination, CSR and SHM in mammalian cells. I have shown, using XLF-null cells that, deficiency of XLF severely impair V(D)J recombination of an extrachromosomal substrate. To extend this observation, XLF deficient cell lines and the lines over-expressing the

wild-type or mutated XLF cDNA, can be used to investigate the role of XLF in CSR and SMH.

What is the impact on CSR?

CSR is an interesting model of DNA DSB repair because recent reports have demonstrated that B-NHEJ may play a significant role in the repair of CSR broken ends (in contrast to the repair of IR-induced ends, where the impact of B-NHEJ is negligible at best) (269), (321). Analysis of CSR in fibroblast is

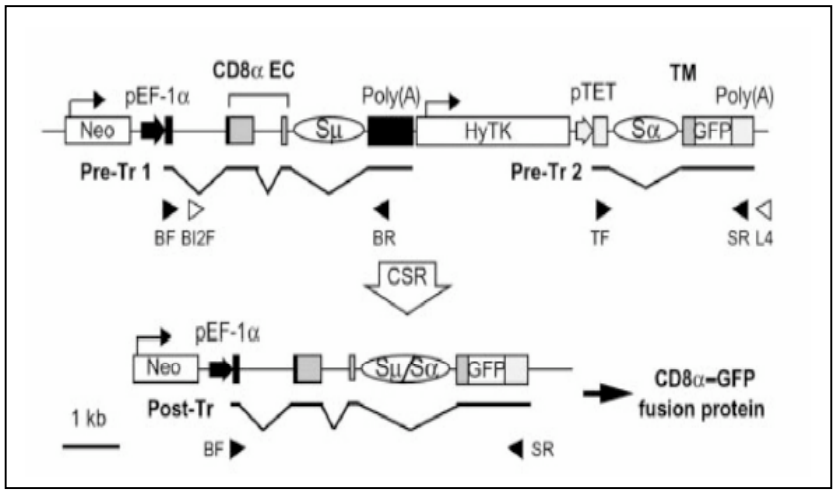

Figure 1. The structure of SCI(μ,α) and the substrate following CSR. See text for details. This figure is excerpted from Okazaki et al., 2002, Nature, 416:340.

conceptually identical to the assay we have used for V(D)J recombination. Our laboratory has obtained plasmid SCI (μ,α) from the laboratory of Dr. Honjo (Fig. 1). This plasmid could be linearized and transfected into the XLF-null cells as well as the cells lines expressing the wild-type or mutant XLF cDNA. Stable clones can be selected with hygromycin (Hy Tk gene) resistance and single integrants identified by Southern blotting. Cells can then be transiently transfected with EF1α- AID expression vector (also a gift from Dr. Honjo). AID catalyzes a CSR reaction between the Sμ and Sα regions of the vector and results in a product which expresses CD8α:GFP fusion protein, whose

expression can be quantified by FACS (Fig. 1).To date, virtually all of the studies on the impact of C-NHEJ gene mutations on CSR have been carried out in the mouse, so the XLF study should be particularly interesting and informative.

Generation of XLF deficient Ramos cell line/ What is the impact of XLF deficiency on SHM?

SHM occurs constitutively in the Ramos cell line. Using rAAV-mediated gene-targeting technology XLF gene can be deleted in Ramos cell line. XLF deficient Ramos cell line can be used to test whether XLF has any role in SHM. SHM altered the surface IgM positive phenotype of Ramos cells to negative due to the SHM_mediated introduction of inactivating point mutations in the variable portion of IgM locus (248).. This assay can be reverse by using a surface IgM negative subclone of Ramos cell and analyze the frequency of appearance of IgM positive cells that occur sue to SHM. Doing this assay in this reverse fashion is logistically superior because only about 1% of the cells undergo SHM. Since the screening is done by fluctuation analysis of FACS profiles using fluorescent antibodies directed against surface IgM, it is much easier to score the 1% positive cells against a null background than it is to quantitate the loss of 1% pf the cells from a 100% positive background (115).

Intracellular localization of XLF:

One of the interesting results from my study is that wild-type XLF appears to be predominately cytoplasmic and some of the XLF misssense mutations (from XLF patient mutations) expressed in the XLF-null cell line appear to be exclusively cytoplasmic. These data indicate that XLF may be a nucleo-cytoplasmic shuttiling protein and that its activity could be coordinately regulated by this process. So site-directed mutagenesis can be used with *in vivo* epitope-tagged (pCherry) expression system to define either nuclear localization or nuclear export signals in XLF. In addition, many of the factors that regulate

nuclear:cytoplasmic shuttling have been identified (e.g. CRM1; (Fried, 2003 #993) and chemical inhibitors to these factors can be used to complement our reverse genetic approaches.

B-NHEJ project:

The B-NHEJ pathway is poorly understood and all the B-NHEJ genes remain to be identified. Nonetheless, most investigators would probably agree that the three most compelling candidates to date are PARP-1, XRCC1 and LIGIII (11), (215), (302). PARP-1, XRCC1 and LIGIII physically interact and exist as a complex within cells (31), (32). PARP-1 is a highly abundant nuclear protein that binds rapidly to DNA DSBs and catalyzes the transfer of ADP-ribose from its substrate NAD^+ to a variety of DNA repair factors, but mainly to itself (312). PARP-1 has a well-documented role in single-stranded DNA repair (312), whereas its potential role in DSB repair has only recently been appreciated (310). Murine knockouts of PARP-1 are viable (303) although they show defects in chromosome stability, especially when crossed into p53-deficient backgrounds (50), (281). LigIII encodes two isoforms that differ at their C-termini, but LigIIIα, which is constitutively bound to XRCC1, appears to be biologically more important isoform. Murine knockouts of LigIII are not viable (230). XRCC1 does not contain any obvious enzymatic motif, but appears to serve as a scaffold into which other proteins bind (31). In addition, it acts as a stability factor for LigIII, as loss of XRCC1 expression is accompanied by reduced LigIII levels (175). Murine knockouts of XRCC1 are not viable (278).

What is the role of PARP-1 in B-NHEJ?

A recent study from Illakis laboratory (302) has shown that inhibition of PARP-1 activity in Ku- deficient hamster cell line and Lig IV-deficient murine cell line decreases the DNA repair and suggested a role for PARP in B-NHEJ. I showed that in human cell deficiency of C-NHEJ genes results repair defect though the residual repair activity probably achieved using the B-NHEJ pathway.

C-NHEJ defective cell line can be treated with PARP-1 inhibitor 3'-aminobenzamide (3'-AB) or 1.5'- dihydroxyisoquinoline (DIQ) and the repair activity can me monitored using the EGFP based *in vivo* plasmid end joining assay.

Generation of B-NHEJ defective cell lines:

Using rAAV-mediated gene-targeting strategy human somatic cell lines that are wither reduced or deficient for PARP-1, LIGIII, XRCC1 can be generated. Based on the mouse model, it is predictable that PARP-1 null human somatic cells might be viable whereas LIGIII and XRCC1 would be less likely to be alive. In this event, it is possible to make conditional knockouts. If these cell lines can be generated then these will serve as valuable tools for dissecting the B-NHEJ pathway mechanism.

Bibliography:

1. Abraham, R. T. 2001. Cell cycle checkpoint signaling through the ATM and ATR kinases. Genes Dev. 15:2177-2196.
2. Adachi, N., T. Ishino, Y. Ishii, S. Takeda, and H. Koyama. 2001. DNA ligase IV-deficient cells are more resistant to ionizing radiation in the absence of Ku70: Implications for DNA double-strand break repair. Proc. Natl. Acad. Sci. U S A 98:12109-12113.
3. Agapova, L. S., J. L. Volodina, P. M. Chumakov, and B. P. Kopnin. 2004. Activation of Ras-Ral pathway attenuates p53-independent DNA damage G2 checkpoint. J Biol Chem 279:36382-9.
4. Ahnesorg, P., P. Smith, and S. P. Jackson. 2006. XLF interacts with the XRCC4-DNA ligase IV complex to promote DNA nonhomologous end-joining. Cell 124:301-313.
5. Allen, C., A. Kurimasa, M. A. Brenneman, D. J. Chen, and J. A. Nickoloff. 2002. DNA-dependent protein kinase suppresses double-strand break-induced and spontaneous homologous recombination. Proc Natl Acad Sci U S A 99:3758-63.
6. Andreeva, A. V., and M. A. Kutuzov. 1999. Non-classical protein Ser/Thr phosphatases: what are they for? Biochemistry (Mosc) 64:228-87.
7. Andres, S. N., M. Modesti, C. J. Tsai, G. Chu, and M. S. Junop. 2007. Crystal structure of human XLF: a twist in nonhomologous DNA end-joining. Mol Cell 28:1093-101.
8. Arosio, D., S. Cui, C. Ortega, M. Chovanec, S. Di Marco, G. Baldini, A. Falaschi, and A. Vindigni. 2002. Studies on the mode of Ku interaction with DNA. J. Biol. Chem. 277:9741-9748.
9. Atchison, R. W., B. C. Casto, and W. M. Hammon. 1965. Adenovirus-Associated Defective Virus Particles. Science 149:754-6.
10. Audebert, M., B. Salles, and P. Calsou. 2008. Effect of double-strand break DNA sequence on the PARP-1 NHEJ pathway. Biochem Biophys Res Commun 369:982-8.
11. Audebert, M., B. Salles, and P. Calsou. 2004. Involvement of poly(ADP-ribose) polymerase-1 and XRCC1/DNA ligase III in an alternative route for DNA double-strand breaks rejoining. J Biol Chem 279:55117-26.
12. Bakkenist, C. J., and M. B. Kastan. 2003. DNA damage activates ATM through intermolecular autophosphorylation and dimer dissociation. Nature 421:499-506.
13. Barnes, D. E., G. Stamp, I. Rosewell, A. Denzel, and T. Lindahl. 1998. Targeted disruption of the gene encoding DNA ligase IV leads to lethality in embryonic mice. Curr. Biol. 8:1395-1398.

14. Bassing, C. H., W. Swat, and F. W. Alt. 2002. The mechanism and regulation of chromosomal V(D)J recombination. Cell 109:S45-S55.
15. Bennardo, N., A. Cheng, N. Huang, and J. M. Stark. 2008. Alternative-NHEJ is a mechanistically distinct pathway of mammalian chromosome break repair. PLoS Genet 4:e1000110.
16. Bentley, J., C. P. Diggle, P. Harnden, M. A. Knowles, and A. E. Kiltie. 2004. DNA double strand break repair in human bladder cancer is error prone and involves microhomology-associated end-joining. Nucleic Acids Res 32:5249-59.
17. Benzie, I. F. 2000. Evolution of antioxidant defence mechanisms. Eur J Nutr 39:53-61.
18. Betti, C. J., M. J. Villalobos, M. O. Diaz, and A. T. Vaughan. 2001. Apoptotic triggers initiate translocations within the MLL gene involving the nonhomologous end joining repair system. Cancer Res 61:4550-5.
19. Bliss, T. M., and D. P. Lane. 1997. Ku selectively transfers between DNA molecules with homologous ends. J. Biol. Chem. 272:5765-5773.
20. Block, W. D., Y. Yu, D. Merkle, J. L. Gifford, Q. Ding, K. Meek, and S. P. Lees-Miller. 2004. Autophosphorylation-dependent remodeling of the DNA-dependent protein kinase catalytic subunit regulates ligation of DNA ends. Nucleic Acids Res 32:4351-7.
21. Bochar, D. A., L. Wang, H. Beniya, A. Kinev, Y. Xue, W. S. Lane, W. Wang, F. Kashanchi, and R. Shiekhattar. 2000. BRCA1 is associated with a human SWI/SNF-related complex: linking chromatin remodeling to breast cancer. Cell 102:257-65.
22. Boskovic, J., A. Rivera-Calzada, J. D. Maman, P. Chacon, K. R. Willison, L. H. Pearl, and O. Llorca. 2003. Visualization of DNA-induced conformational changes in the DNA repair kinase DNA-PKcs. Embo J 22:5875-82.
23. Boulton, S. J., and S. P. Jackson. 1998. Components of the Ku-dependent non-homologous end-joining pathway are involved in telomeric length maintenance and telomeric silencing. EMBO J. 17:1819-1828.
24. Boulton, S. J., and S. P. Jackson. 1996. Saccharomyces cerevisiae Ku70 potentiates illegitimate DNA double-strand break repair and serves as a barrier to error-prone DNA repair pathways. Embo J 15:5093-103.
25. Branzei, D., and M. Foiani. 2008. Regulation of DNA repair throughout the cell cycle. Nat Rev Mol Cell Biol 9:297-308.
26. Buck, D., L. Malivert, R. de Chasseval, A. Barraud, M. C. Fondaneche, O. Sanal, A. Plebani, J. L. Stephan, M. Hufnagel, F. le Deist, A. Fischer, A. Durandy, J. P. de Villartay, and P. Revy. 2006. Cernunnos,

a novel nonhomologous end-joining factor, is mutated in human immunodeficiency with microcephaly. Cell 124:287-299.
27. Buller, R. M., J. E. Janik, E. D. Sebring, and J. A. Rose. 1981. Herpes simplex virus types 1 and 2 completely help adenovirus-associated virus replication. J Virol 40:241-7.
28. Burgers, P. M., E. V. Koonin, E. Bruford, L. Blanco, K. C. Burtis, M. F. Christman, W. C. Copeland, E. C. Friedberg, F. Hanaoka, D. C. Hinkle, C. W. Lawrence, M. Nakanishi, H. Ohmori, L. Prakash, S. Prakash, C. A. Reynaud, A. Sugino, T. Todo, Z. Wang, J. C. Weill, and R. Woodgate. 2001. Eukaryotic DNA polymerases: proposal for a revised nomenclature. J Biol Chem 276:43487-90.
29. Burma, S., B. P. Chen, and D. J. Chen. 2006. Role of non-homologous end joining (NHEJ) in maintaining genomic integrity. DNA Repair (Amst) 5:1042-8.
30. Cahill, D., B. Connor, and J. P. Carney. 2006. Mechanisms of eukaryotic DNA double strand break repair. Front Biosci. 11:1958-1976.
31. Caldecott, K. W. 2003. XRCC1 and DNA strand break repair. DNA Repair (Amst) 2:955-69.
32. Caldecott, K. W., S. Aoufouchi, P. Johnson, and S. Shall. 1996. XRCC1 polypeptide interacts with DNA polymerase beta and possibly poly (ADP-ribose) polymerase, and DNA ligase III is a novel molecular 'nick-sensor' in vitro. Nucleic Acids Res 24:4387-94.
33. Callebaut, I., L. Malivert, A. Fischer, J. P. Mornon, P. Revy, and J. P. de Villartay. 2006. Cernunnos interacts with the XRCC4 x DNA-ligase IV complex and is homologous to the yeast nonhomologous end-joining factor Nej1. J Biol Chem 281:13857-60.
34. Canning, S., and T. P. Dryja. 1989. Short, direct repeats at the breakpoints of deletions of the retinoblastoma gene. Proc Natl Acad Sci U S A 86:5044-8.
35. Cantagrel, V., A. M. Lossi, S. Lisgo, C. Missirian, A. Borges, N. Philip, C. Fernandez, C. Cardoso, D. Figarella-Branger, A. Moncla, S. Lindsay, W. B. Dobyns, and L. Villard. 2007. Truncation of NHEJ1 in a patient with polymicrogyria. Hum Mutat 28:356-64.
36. Carney, J. P., R. S. Maser, H. Olivares, E. M. Davis, M. Le Beau, J. R. Yates, 3rd, L. Hays, W. F. Morgan, and J. H. Petrini. 1998. The hMre11/hRad50 protein complex and Nijmegen breakage syndrome: linkage of double-strand break repair to the cellular DNA damage response. Cell 93:477-86.
37. Cary, R. B., S. R. Peterson, J. Wang, D. G. Bear, E. M. Bradbury, and D. J. Chen. 1997. DNA looping by Ku and the DNA-dependent protein kinase. Proc Natl Acad Sci U S A 94:4267-72.
38. Casellas, R., A. Nussenzweig, R. Wuerffel, R. Pelanda, A. Reichlin, H. Suh, X. F. Qin, E. Besmer, A. Kenter, K. Rajewsky, and M. C.

Nussenzweig. 1998. Ku80 is required for immunoglobulin isotype switching. EMBO J. 17:2404-2411.
39. Chamberlain, J. R., U. Schwarze, P. R. Wang, R. K. Hirata, K. D. Hankenson, J. M. Pace, R. A. Underwood, K. M. Song, M. Sussman, P. H. Byers, and D. W. Russell. 2004. Gene targeting in stem cells from individuals with osteogenesis imperfecta. Science 303:1198-201.
40. Chan, D. W., B. P. Chen, S. Prithivirajsingh, A. Kurimasa, M. D. Story, J. Qin, and D. J. Chen. 2002. Autophosphorylation of the DNA-dependent protein kinase catalytic subunit is required for rejoining of DNA double-strand breaks. Genes Dev 16:2333-8.
41. Chen, C., and R. D. Kolodner. 1999. Gross chromosomal rearrangements in *Saccharomyces cerevisiae* replication and recombination defective mutants. Nat. Genet. 23:81-85.
42. Chen, C. F., P. L. Chen, Q. Zhong, Z. D. Sharp, and W. H. Lee. 1999. Expression of BRC repeats in breast cancer cells disrupts the BRCA2-Rad51 complex and leads to radiation hypersensitivity and loss of G(2)/M checkpoint control. J Biol Chem 274:32931-5.
43. Chen, J., D. P. Silver, D. Walpita, S. B. Cantor, A. F. Gazdar, G. Tomlinson, F. J. Couch, B. L. Weber, T. Ashley, D. M. Livingston, and R. Scully. 1998. Stable interaction between the products of the BRCA1 and BRCA2 tumor suppressor genes in mitotic and meiotic cells. Mol Cell 2:317-28.
44. Chen, J. J., D. Silver, S. Cantor, D. M. Livingston, and R. Scully. 1999. BRCA1, BRCA2, and Rad51 operate in a common DNA damage response pathway. Cancer Res 59:1752s-1756s.
45. Chen, L., K. Trujillo, W. Ramos, P. Sung, and A. E. Tomkinson. 2001. Promotion of Dnl4-catalyzed DNA end-joining by the Rad50/Mre11/Xrs2 and Hdf1/Hdf2 complexes. Mol Cell 8:1105-15.
46. Chen, L., K. Trujillo, P. Sung, and A. E. Tomkinson. 2000. Interactions of the DNA ligase IV-XRCC4 complex with DNA ends and the DNA-dependent protein kinase. J Biol Chem 275:26196-205.
47. Cheong, N., A. R. Perrault, H. Wang, P. Wachsberger, P. Mammen, I. Jackson, and G. Iliakis. 1999. DNA-PK-independent rejoining of DNA double-strand breaks in human cell extracts *in vitro*. Int. J. Radiat. Biol. 75:67-81.
48. Cohen, H. Y., C. Miller, K. J. Bitterman, N. R. Wall, B. Hekking, B. Kessler, K. T. Howitz, M. Gorospe, R. de Cabo, and D. A. Sinclair. 2004. Calorie restriction promotes mammalian cell survival by inducing the SIRT1 deacetylase. Science 305:390-2.
49. Collis, S. J., T. L. DeWeese, P. A. Jeggo, and A. R. Parker. 2005. The life and death of DNA-PK. Oncogene 24:949-61.
50. Conde, C., M. Mark, F. J. Oliver, A. Huber, G. de Murcia, and J. Menissier-de Murcia. 2001. Loss of poly(ADP-ribose) polymerase-1

causes increased tumour latency in p53-deficient mice. Embo J 20:3535-43.
51. Connor, F., D. Bertwistle, P. J. Mee, G. M. Ross, S. Swift, E. Grigorieva, V. L. Tybulewicz, and A. Ashworth. 1997. Tumorigenesis and a DNA repair defect in mice with a truncating Brca2 mutation. Nat Genet 17:423-30.
52. Corneo, B., R. L. Wendland, L. Deriano, X. Cui, I. A. Klein, S. Y. Wong, S. Arnal, A. J. Holub, G. R. Weller, B. A. Pancake, S. Shah, V. L. Brandt, K. Meek, and D. B. Roth. 2007. Rag mutations reveal robust alternative end joining. Nature 449:483-6.
53. Cromie, G. A., J. C. Connelly, and D. R. Leach. 2001. Recombination at double-strand breaks and DNA ends: conserved mechanisms from phage to humans. Mol. Cell 8:1163-1174.
54. d'Adda di Fagagna, F., G. R. Weller, A. J. Doherty, and S. P. Jackson. 2003. The Gam protein of bacteriophage Mu is an orthologue of eukaryotic Ku. EMBO Rep. 4:47-52.
55. D'Amours, D., and S. P. Jackson. 2001. The yeast Xrs2 complex functions in S phase checkpoint regulation. Genes Dev 15:2238-49.
56. Dai, Y., B. Kysela, L. A. Hanakahi, K. Manolis, E. Riballo, M. Stumm, T. O. Harville, S. C. West, M. A. Oettinger, and P. A. Jeggo. 2003. Nonhomologous end joining and V(D)J recombination require an additional factor. Proc. Natl. Acad. Sci. U S A 100:2462-2467.
57. Daley, J. M., R. L. Laan, A. Suresh, and T. E. Wilson. 2005. DNA joint dependence of pol X family polymerase action in nonhomologous end joining. J Biol Chem 280:29030-7.
58. Davies, A. A., J. Y. Masson, M. J. McIlwraith, A. Z. Stasiak, A. Stasiak, A. R. Venkitaraman, and S. C. West. 2001. Role of BRCA2 in control of the RAD51 recombination and DNA repair protein. Mol Cell 7:273-82.
59. de Jager, M., J. van Noort, D. C. van Gent, C. Dekker, R. Kanaar, and C. Wyman. 2001. Human Rad50/Mre11 is a flexible complex that can tether DNA ends. Mol Cell 8:1129-35.
60. Deans, B., C. S. Griffin, M. Maconochie, and J. Thacker. 2000. Xrcc2 is required for genetic stability, embryonic neurogenesis and viability in mice. Embo J 19:6675-85.
61. DeChiara, T. M. 2001. Gene targeting in ES cells. Methods Mol. Biol. 158:19-45.
62. Decottignies, A. 2007. Microhomology-mediated end joining in fission yeast is repressed by pku70 and relies on genes involved in homologous recombination. Genetics 176:1403-15.
63. DeFazio, L. G., R. M. Stansel, J. D. Griffith, and G. Chu. 2002. Synapsis of DNA ends by DNA-dependent protein kinase. EMBO J. 21:3192-3200.

64. Di Virgilio, M., and J. Gautier. 2005. Repair of double-strand breaks by nonhomologous end joining in the absence of Mre11. J Cell Biol 171:765-71.
65. Digweed, M., and K. Sperling. 2004. Nijmegen breakage syndrome: clinical manifestation of defective response to DNA double-strand breaks. DNA Repair (Amst) 3:1207-17.
66. Douglas, P., G. B. Moorhead, R. Ye, and S. P. Lees-Miller. 2001. Protein phosphatases regulate DNA-dependent protein kinase activity. J Biol Chem 276:18992-8.
67. Douglas, P., G. P. Sapkota, N. Morrice, Y. Yu, A. A. Goodarzi, D. Merkle, K. Meek, D. R. Alessi, and S. P. Lees-Miller. 2002. Identification of in vitro and in vivo phosphorylation sites in the catalytic subunit of the DNA-dependent protein kinase. Biochem J 368:243-51.
68. Downs, J. A., and S. P. Jackson. 2004. A means to a DNA end: the many roles of Ku. Nat Rev Mol Cell Biol 5:367-78.
69. Dresser, M. E. 2000. Meiotic chromosome behavior in Saccharomyces cerevisiae and (mostly) mammals. Mutat Res 451:107-27.
70. Dudasova, Z., A. Dudas, and M. Chovanec. 2004. Non-homologous end-joining factors of Saccharomyces cerevisiae. FEMS Microbiol Rev 28:581-601.
71. Dudley, D. D., J. Chaudhuri, C. H. Bassing, and F. W. Alt. 2005. Mechanism and control of V(D)J recombination versus class switch recombination: similarities and differences. Adv Immunol 86:43-112.
72. Dunham, M. A., A. A. Neumann, C. L. Fasching, and R. R. Reddel. 2000. Telomere maintenance by recombination in human cells. Nat. Genet. 26:447-450.
73. Dynan, W. S., and S. Yoo. 1998. Interaction of Ku protein and DNA-dependent protein kinase catalytic subunit with nucleic acids. Nucleic Acids Res 26:1551-9.
74. Essers, J., R. W. Hendriks, S. M. A. Swagemakers, C. Troelstra, J. de Wit, D. Bootsma, J. H. J. Hoeijmakers, and R. Kanaar. 1997. Disruption of mouse *RAD54* reduces ionizing radiation resistance and homologous recombination. Cell 89:195-204.
75. Essers, J., H. van Steeg, J. de Wit, S. M. Swagemakers, M. Vermeij, J. H. Hoeijmakers, and R. Kanaar. 2000. Homologous and non-homologous recombination differentially affect DNA damage repair in mice. Embo J 19:1703-10.
76. Falck, J., J. Coates, and S. P. Jackson. 2005. Conserved modes of recruitment of ATM, ATR and DNA-PKcs to sites of DNA damage. Nature 434:605-11.
77. Fattah, F. J., N. F. Lichter, K. R. Fattah, S. Oh, and E. A. Hendrickson. 2008. Ku70, an essential gene, modulates the frequency of rAAV-

mediated gene targeting in human somatic cells. Proc Natl Acad Sci U S A 105:8703-8.
78. Fattah, K. R., B. L. Ruis, and E. A. Hendrickson. 2008. Mutations to Ku reveal differences in human somatic cell lines. DNA Repair (Amst) 7:762-74.
79. Feldmann, E., V. Schmiemann, W. Goedecke, S. Reichenberger, and P. Pfeiffer. 2000. DNA double-strand break repair in cell-free extracts from Ku80-deficient cells: implications for Ku serving as an alignment factor in non-homologous DNA end joining. Nucl. Acids Res. 28:2585-2596.
80. Fernandez-Capetillo, O., A. Lee, M. Nussenzweig, and A. Nussenzweig. 2004. H2AX: the histone guardian of the genome. DNA Repair (Amst) 3:959-67.
81. Ferrari, F. K., X. Xiao, D. McCarty, and R. J. Samulski. 1997. New developments in the generation of Ad-free, high-titer rAAV gene therapy vectors. Nat Med 3:1295-7.
82. Fishman-Lobell, J., and J. E. Haber. 1992. Removal of nonhomologous DNA ends in double-strand break recombination: the role of the yeast ultraviolet repair gene RAD1. Science 258:480-4.
83. Florl, A. R., and W. A. Schulz. 2003. Peculiar structure and location of 9p21 homozygous deletion breakpoints in human cancer cells. Genes Chromosomes Cancer 37:141-8.
84. Frank, K. M., J. M. Sekiguchi, K. J. Seidl, W. Swat, G. A. Rathbun, H. L. Cheng, L. Davidson, L. Kangaloo, and F. W. Alt. 1998. Late embryonic lethality and impaired V(D)J recombination in mice lacking DNA ligase IV. Nature 396:173-177.
85. Frank-Vaillant, M., and S. Marcand. 2001. NHEJ regulation by mating type is exercised through a novel protein, Lif2p, essential to the ligase IV pathway. Genes Dev. 15:3005-3012.
86. Frank-Vaillant, M., and S. Marcand. 2002. Transient stability of DNA ends allows nonhomologous end joining to precede homologous recombination. Mol Cell 10:1189-99.
87. Fried, H., and U. Kutay. 2003. Nucleocytoplasmic transport: taking an inventory. Cell Mol Life Sci 60:1659-88.
88. Gao, Y., J. Chaudhuri, C. Zhu, L. Davidson, D. T. Weaver, and F. W. Alt. 1998. A targeted DNA-PK_{cs}-null mutation reveals DNA-PK-independent functions for Ku in V(D)J recombination. Immunity 9:367-376.
89. Gatei, M., D. Young, K. M. Cerosaletti, A. Desai-Mehta, K. Spring, S. Kozlov, M. F. Lavin, R. A. Gatti, P. Concannon, and K. Khanna. 2000. ATM-dependent phosphorylation of nibrin in response to radiation exposure. Nat Genet 25:115-9.

90. Gauss, G. H., I. Domain, C. L. Hsieh, and M. R. Lieber. 1998. V(D)J recombination activity in human hematopoietic cells: correlation with developmental stage and genome stability. Eur J Immunol 28:351-8.
91. Gauss, G. H., and M. R. Lieber. 1992. The basis for the mechanistic bias for deletional over inversional V(D)J recombination. Genes Dev 6:1553-61.
92. Getts, R. C., and T. D. Stamato. 1994. Absence of a Ku-like DNA end binding activity in the xrs double-strand DNA repair-deficient mutant. J Biol Chem 269:15981-4.
93. Girard, P. M., E. Riballo, A. C. Begg, A. Waugh, and P. A. Jeggo. 2002. Nbs1 promotes ATM dependent phosphorylation events including those required for G1/S arrest. Oncogene 21:4191-9.
94. Goedecke, W., M. Eijpe, H. H. Offenberg, M. van Aalderen, and C. Heyting. 1999. Mre11 and Ku70 interact in somatic cells, but are differentially expressed in early meiosis. Nat. Genet. 23:194-198.
95. Goodarzi, A. A., Y. Yu, E. Riballo, P. Douglas, S. A. Walker, R. Ye, C. Harer, C. Marchetti, N. Morrice, P. A. Jeggo, and S. P. Lees-Miller. 2006. DNA-PK autophosphorylation facilitates Artemis endonuclease activity. Embo J 25:3880-9.
96. Goodman, M. F., M. D. Scharff, and F. E. Romesberg. 2007. AID-initiated purposeful mutations in immunoglobulin genes. Adv Immunol 94:127-55.
97. Gottlich, B., S. Reichenberger, E. Feldmann, and P. Pfeiffer. 1998. Rejoining of DNA double-strand breaks in vitro by single-strand annealing. Eur J Biochem 258:387-95.
98. Gottlieb, T. M., and S. P. Jackson. 1993. The DNA-dependent protein kinase: requirement for DNA ends and association with Ku antigen. Cell 72:131-142.
99. Grawunder, U., M. Wilm, X. Wu, P. Kulesza, T. E. Wilson, M. Mann, and M. R. Lieber. 1997. Activity of DNA ligase IV stimulated by complex formation with XRCC4 protein in mammalian cells. Nature 388:492-495.
100. Grawunder, U., D. Zimmer, S. Fugmann, K. Schwarz, and M. R. Lieber. 1998. DNA ligase IV is essential for V(D)J recombination and DNA double-strand break repair in human precursor lymphocytes. Mol. Cell 2:477-484.
101. Grawunder, U., D. Zimmer, P. Kulesza, and M. R. Lieber. 1998. Requirement for an interaction of XRCC4 with DNA ligase IV for wild-type V(D)J recombination and DNA double-strand break repair in vivo. J Biol Chem 273:24708-14.
102. Grenon, M., C. Gilbert, and N. F. Lowndes. 2001. Checkpoint activation in response to double-strand breaks requires the Mre11/Rad50/Xrs2 complex. Nat Cell Biol 3:844-7.

103. Griffin, C. S., P. J. Simpson, C. R. Wilson, and J. Thacker. 2000. Mammalian recombination-repair genes XRCC2 and XRCC3 promote correct chromosome segregation. Nat Cell Biol 2:757-61.
104. Gu, J., H. Lu, A. G. Tsai, K. Schwarz, and M. R. Lieber. 2007. Single-stranded DNA ligation and XLF-stimulated incompatible DNA end ligation by the XRCC4-DNA ligase IV complex: influence of terminal DNA sequence. Nucleic Acids Res 35:5755-62.
105. Gu, Y., S. Jin, Y. Gao, D. T. Weaver, and F. W. Alt. 1997. Ku70-deficient embryonic stem cells have increased ionizing radiosensitivity, defective DNA end-binding activity, and inability to support V(D)J recombination. Proc. Natl. Acad. Sci. USA 94:8076-8081.
106. Guirouilh-Barbat, J., S. Huck, P. Bertrand, L. Pirzio, C. Desmaze, L. Sabatier, and B. S. Lopez. 2004. Impact of the KU80 pathway on NHEJ-induced genome rearrangements in mammalian cells. Mol Cell 14:611-23.
107. Guirouilh-Barbat, J., S. Huck, and B. S. Lopez. 2008. S-phase progression stimulates both the mutagenic KU-independent pathway and mutagenic processing of KU-dependent intermediates, for nonhomologous end joining. Oncogene 27:1726-36.
108. Guirouilh-Barbat, J., E. Rass, I. Plo, P. Bertrand, and B. S. Lopez. 2007. Defects in XRCC4 and KU80 differentially affect the joining of distal nonhomologous ends. Proc Natl Acad Sci U S A 104:20902-7.
109. Haber, J. E. 2008. Alternative endings. Proc Natl Acad Sci U S A 105:405-6.
110. Haber, J. E. 2000. Partners and pathwaysrepairing a double-strand break. Trends Genet 16:259-64.
111. Hacein-Bey-Abina, S., A. Garrigue, G. P. Wang, J. Soulier, A. Lim, E. Morillon, E. Clappier, L. Caccavelli, E. Delabesse, K. Beldjord, V. Asnafi, E. MacIntyre, L. Dal Cortivo, I. Radford, N. Brousse, F. Sigaux, D. Moshous, J. Hauer, A. Borkhardt, B. H. Belohradsky, U. Wintergerst, M. C. Velez, L. Leiva, R. Sorensen, N. Wulffraat, S. Blanche, F. D. Bushman, A. Fischer, and M. Cavazzana-Calvo. 2008. Insertional oncogenesis in 4 patients after retrovirus-mediated gene therapy of SCID-X1. J Clin Invest 118:3132-42.
112. Hakem, R. 2008. DNA-damage repair; the good, the bad, and the ugly. Embo J 27:589-605.
113. Hammarsten, O., and G. Chu. 1998. DNA-dependent protein kinase: DNA binding and activation in the absence of Ku. Proc. Natl. Acad. Sci. USA 95:525-530.
114. Han, Z., C. Johnston, W. H. Reeves, T. Carter, J. H. Wyche, and E. A. Hendrickson. 1996. Characterization of a Ku86 variant protein that results in altered DNA binding and diminished DNA-dependent protein kinase activity. J. Biol. Chem. 271:14098-14104.

115. Harris, R. S., D. S. Croom-Carter, A. B. Rickinson, and M. S. Neuberger. 2001. Epstein-Barr virus and the somatic hypermutation of immunoglobulin genes in Burkitt's lymphoma cells. J Virol 75:10488-92.
116. Hartley, K. O., D. Gell, G. C. M. Smith, H. Zhang, N. Divecha, M. A. Connelly, A. Admon, S. P. Lees-Miller, C. W. Anderson, and S. P. Jackson. 1995. DNA-dependent protein kinase catalytic subunit: a relative of phosphotidylinositol 3-kinase and the ataxia telangiectasia gene product. Cell 82:849-856.
117. Heacock, M., E. Spangler, K. Riha, J. Puizina, and D. E. Shippen. 2004. Molecular analysis of telomere fusions in Arabidopsis: multiple pathways for chromosome end-joining. Embo J 23:2304-13.
118. Helleday, T., J. Lo, D. C. van Gent, and B. P. Engelward. 2007. DNA double-strand break repair: from mechanistic understanding to cancer treatment. DNA Repair (Amst) 6:923-35.
119. Hendrickson, E. A. 2007. Gene targeting in human somatic cells., p. in press. *In* M. Conn (ed.), Sourcebook of models for biomedical research. The Humana Press Inc., Totowa, NJ.
120. Hendrickson, E. A., J. L. Huffman, and J. A. Tainer. . 2006. Structural aspects of Ku and the DNAdependent
protein kinase complex., p. 629-684 *In* Y. W. K. W. Seide, and P. Doetsch (ed.), DNA
Damage Recognition. Taylor and Francis Group, , New York.
121. Hentges, P., P. Ahnesorg, R. S. Pitcher, C. K. Bruce, B. Kysela, A. J. Green, J. Bianchi, T. E. Wilson, S. P. Jackson, and A. J. Doherty. 2006. Evolutionary and functional conservation of the DNA non-homologous end-joining protein, XLF/Cernunnos. J Biol Chem 281:37517-26.
122. Henthorn, P. S., O. Smithies, and D. L. Mager. 1990. Molecular analysis of deletions in the human beta-globin gene cluster: deletion junctions and locations of breakpoints. Genomics 6:226-37.
123. Herrmann, G., T. Lindahl, and P. Schar. 1998. Saccharomyces cerevisiae LIF1: a function involved in DNA double-strand break repair related to mammalian XRCC4. Embo J 17:4188-98.
124. Hesse, J. E., M. R. Lieber, K. Mizuuchi, and M. Gellert. 1989. V(D)J recombination: a functional definition of the joining signals. Genes Dev 3:1053-61.
125. Hopfner, K. P., L. Craig, G. Moncalian, R. A. Zinkel, T. Usui, B. A. Owen, A. Karcher, B. Henderson, J. L. Bodmer, C. T. McMurray, J. P. Carney, J. H. Petrini, and J. A. Tainer. 2002. The Rad50 zinc-hook is a structure joining Mre11 complexes in DNA recombination and repair. Nature 418:562-6.
126. Hudson, J. J., D. W. Hsu, K. Guo, N. Zhukovskaya, P. H. Liu, J. G. Williams, C. J. Pears, and N. D. Lakin. 2005. DNA-PKcs-dependent

signaling of DNA damage in Dictyostelium discoideum. Curr Biol 15:1880-5.
127. Jeggo, P. A. 1997. DNA-PK: at the cross-roads of biochemistry and genetics. Mutat. Res. 384:1-14.
128. Jeggo, P. A., M. Hafezparast, A. F. Thompson, G. P. Kaur, A. K. Sandhu, and R. S. Athwal. 1993. A hamster-human subchromosomal hybrid cell panel for chromosome 2. Somat Cell Mol Genet 19:39-49.
129. Jeggo, P. A., J. Tesmer, and D. J. Chen. 1991. Genetic analysis of ionising radiation sensitive mutants of cultured mammalian cell lines. Mutat Res 254:125-33.
130. Johnson, F. B., H. L. Ozer, and M. D. Hoggan. 1971. Structural proteins of adenovirus-associated virus type 3. J Virol 8:860-63.
131. Johnson, R. D., and M. Jasin. 2000. Sister chromatid gene conversion is a prominent double-strand break repair pathway in mammalian cells. Embo J 19:3398-407.
132. Johnson, R. D., N. Liu, and M. Jasin. 1999. Mammalian XRCC2 promotes the repair of DNA double-strand breaks by homologous recombination. Nature 401:397-9.
133. Kabotyanski, E. B., L. Gomelsky, J. O. Han, T. D. Stamato, and D. B. Roth. 1998. Double-strand break repair in Ku86- and XRCC4-deficient cells. Nucl. Acids Res. 26:5333-5342.
134. Karanjawala, Z. E., N. Adachi, R. A. Irvine, E. K. Oh, D. Shibata, K. Schwarz, C. L. Hsieh, and M. R. Lieber. 2002. The embryonic lethality in DNA ligase IV-deficient mice is rescued by deletion of Ku: implications for unifying the heterogeneous phenotypes of NHEJ mutants. DNA Repair (Amst) 1:1017-26.
135. Karathanasis, E., and T. E. Wilson. 2002. Enhancement of Saccharomyces cerevisiae end-joining efficiency by cell growth stage but not by impairment of recombination. Genetics 161:1015-27.
136. Katsura, Y., S. Sasaki, M. Sato, K. Yamaoka, K. Suzukawa, T. Nagasawa, J. Yokota, and T. Kohno. 2007. Involvement of Ku80 in microhomology-mediated end joining for DNA double-strand breaks in vivo. DNA Repair (Amst) 6:639-48.
137. Kaufmann, W. K., C. B. Campbell, D. A. Simpson, P. B. Deming, L. Filatov, D. A. Galloway, X. J. Zhao, A. M. Creighton, and C. S. Downes. 2002. Degradation of ATM-independent decatenation checkpoint function in human cells is secondary to inactivation of p53 and correlated with chromosomal destabilization. Cell Cycle 1:210-9.
138. Kegel, A., J. O. Sjostrand, and S. U. Astrom. 2001. Nej1p, a cell type-specific regulator of nonhomologous end joining in yeast. Curr. Biol. 11:1611-1167.
139. Knauf, J. A., B. Ouyang, E. S. Knudsen, K. Fukasawa, G. Babcock, and J. A. Fagin. 2006. Oncogenic RAS induces accelerated transition

through G2/M and promotes defects in the G2 DNA damage and mitotic spindle checkpoints. J Biol Chem 281:3800-9.
140. Kogoma, T. 1997. Stable DNA replication: interplay between DNA replication, homologous recombination, and transcription. Microbiol Mol Biol Rev 61:212-38.
141. Kohli, M., C. Rago, C. Lengauer, K. W. Kinzler, and B. Vogelstein. 2004. Facile methods for generating human somatic cell gene knockouts using recombinant adeno-associated viruses. Nucl. Acids Res. 32:e3.
142. Koike, M. 2002. Dimerization, translocation and localization of Ku70 and Ku80 proteins. J Radiat Res (Tokyo) 43:223-36.
143. Kornreich, R., D. F. Bishop, and R. J. Desnick. 1990. Alpha-galactosidase A gene rearrangements causing Fabry disease. Identification of short direct repeats at breakpoints in an Alu-rich gene. J Biol Chem 265:9319-26.
144. Krawczak, M., and D. N. Cooper. 1991. Gene deletions causing human genetic disease: mechanisms of mutagenesis and the role of the local DNA sequence environment. Hum Genet 86:425-41.
145. Kuzminov, A. 1995. Collapse and repair of replication forks in Escherichia coli. Mol Microbiol 16:373-84.
146. Kysela, B., M. Chovanec, and P. A. Jeggo. 2005. Phosphorylation of linker histones by DNA-dependent protein kinase is required for DNA ligase IV-dependent ligation in the presence of histone H1. Proc Natl Acad Sci U S A 102:1877-82.
147. Kysela, B., A. J. Doherty, M. Chovanec, T. Stiff, S. M. Ameer-Beg, B. Vojnovic, P. M. Girard, and P. A. Jeggo. 2003. Ku stimulation of DNA ligase IV-dependent ligation requires inward movement along the DNA molecule. J Biol Chem 278:22466-74.
148. Langston, L. D., and L. S. Symington. 2004. Gene targeting in yeast is initiated by two independent strand invasions. Proc Natl Acad Sci U S A 101:15392-7.
149. Le, S., J. K. Moore, J. E. Haber, and C. W. Greider. 1999. RAD50 and RAD51 define two pathways that collaborate to maintain telomeres in the absence of telomerase. Genetics 152:143-152.
150. Leahy, J. J., B. T. Golding, R. J. Griffin, I. R. Hardcastle, C. Richardson, L. Rigoreau, and G. C. Smith. 2004. Identification of a highly potent and selective DNA-dependent protein kinase (DNA-PK) inhibitor (NU7441) by screening of chromenone libraries. Bioorg Med Chem Lett 14:6083-7.
151. Lee, J. H., and T. T. Paull. 2005. ATM activation by DNA double-strand breaks through the Mre11-Rad50-Nbs1 complex. Science 308:551-4.

152. Lee, K., and S. E. Lee. 2007. Saccharomyces cerevisiae Sae2- and Tel1-dependent single-strand DNA formation at DNA break promotes microhomology-mediated end joining. Genetics 176:2003-14.
153. Lee, S. E., J. K. Moore, A. Holmes, K. Umezu, R. D. Kolodner, and J. E. Haber. 1998. Saccharomyces Ku70, mre11/rad50 and RPA proteins regulate adaptation to G2/M arrest after DNA damage. Cell 94:399-409.
154. Lee, S. E., C. R. Pulaski, D. M. He, D. M. Benjamin, M. J. Voss, J. Um, and E. A. Hendrickson. 1995. Isolation of mammalian cell mutants that are X-ray sensitive, impaired in DNA double-strand break repair and defective for V(D)J recombination. Mutat. Res. 336:279-291.
155. Lees-Miller, S. P. 1996. The DNA-dependent protein kinase, DNA-PK: 10 years and no ends in sight. Biochem Cell Biol 74:503-12.
156. Lees-Miller, S. P., R. Godbout, D. W. Chan, M. Weinfeld, R. S. Day, 3rd, G. M. Barron, and J. Allalunis-Turner. 1995. Absence of p350 subunit of DNA-activated protein kinase from a radiosensitive human cell line. Science 267:1183-1185.
157. Li, B., and L. Comai. 2002. Displacement of DNA-PKcs from DNA ends by the Werner syndrome protein. Nucleic Acids Res 30:3653-61.
158. Li, B., and L. Comai. 2001. Requirements for the nucleolytic processing of DNA ends by the Werner syndrome protein-Ku70/80 complex. J Biol Chem 276:9896-902.
159. Li, B., N. Conway, S. Navarro, L. Comai, and L. Comai. 2005. A conserved and species-specific functional interaction between the Werner syndrome-like exonuclease atWEX and the Ku heterodimer in Arabidopsis. Nucleic Acids Res 33:6861-7.
160. Li, G., F. W. Alt, H. L. Cheng, J. W. Brush, P. H. Goff, M. M. Murphy, S. Franco, Y. Zhang, and S. Zha. 2008. Lymphocyte-specific compensation for XLF/cernunnos end-joining functions in V(D)J recombination. Mol Cell 31:631-40.
161. Li, G., C. Nelsen, and E. A. Hendrickson. 2002. Ku86 is essential in human somatic cells. Proc. Natl. Acad. Sci. U S A 99:832-837.
162. Li, Y., D. Y. Chirgadze, V. M. Bolanos-Garcia, B. L. Sibanda, O. R. Davies, P. Ahnesorg, S. P. Jackson, and T. L. Blundell. 2008. Crystal structure of human XLF/Cernunnos reveals unexpected differences from XRCC4 with implications for NHEJ. Embo J 27:290-300.
163. Li, Z., T. Otevrei, Y. Gao, H.-L. Cheng, B. Seed, T. D. Stamato, G. E. Taccioli, and F. W. Alt. 1995. The XRCC4 gene encodes a novel protein involved in DNA double-strand break repair and V(D)J recombination. Cell 83:1079-1089.
164. Liang, F., and M. Jasin. 1996. Ku80-deficient cells exhibit excess degradation of extrachromosomal DNA. J. Biol. Chem. 271:14405-14411.

165. Liang, L., L. Deng, S. C. Nguyen, X. Zhao, C. D. Maulion, C. Shao, and J. A. Tischfield. 2008. Human DNA ligases I and III, but not ligase IV, are required for microhomology-mediated end joining of DNA double-strand breaks. Nucleic Acids Res 36:3297-310.
166. Lieber, M. R. 2008. The mechanism of human nonhomologous DNA end joining. J Biol Chem 283:1-5.
167. Lieber, M. R., H. Lu, J. Gu, and K. Schwarz. 2008. Flexibility in the order of action and in the enzymology of the nuclease, polymerases, and ligase of vertebrate non-homologous DNA end joining: relevance to cancer, aging, and the immune system. Cell Res 18:125-33.
168. Lieber, M. R., Y. Ma, U. Pannicke, and K. Schwarz. 2003. Mechanism and regulation of human non-homologous DNA end-joining. Nat. Rev. Mol. Cell Biol. 4:712-720.
169. Lieber, M. R., Y. Ma, U. Pannicke, and K. Schwarz. 2004. The mechanism of vertebrate nonhomologous DNA end joining and its role in V(D)J recombination. DNA Repair (Amst) 3:817-26.
170. Lieber, M. R., Y. Ma, Y. Keifu, U. Pannicke, and K. Schwarz. . 2006. The mechanism of vertebrate
nonhomologous DNA end joining and its role in immune system gene rearrangements., p. 609-627. *In* Y. W. K. W. Seide, and P. W. Doetsch (ed.), DNA Damage Recognition. Taylor & Francis
Group, LLC,, New York, NY.
171. Lim, D., and P. Hasty. 1996. A mutation in mouse *rad51* results in an early embryonic lethal phenotype that is suppressed by a mutation in *p53*. Mol. Cell. Biol. 16:7133-7143.
172. Lim, D. S., S. T. Kim, B. Xu, R. S. Maser, J. Lin, J. H. Petrini, and M. B. Kastan. 2000. ATM phosphorylates p95/nbs1 in an S-phase checkpoint pathway. Nature 404:613-7.
173. Lisby, M., J. H. Barlow, R. C. Burgess, and R. Rothstein. 2004. Choreography of the DNA damage response: spatiotemporal relationships among checkpoint and repair proteins. Cell 118:699-713.
174. Liu, N., J. E. Lamerdin, R. S. Tebbs, D. Schild, J. D. Tucker, M. R. Shen, K. W. Brookman, M. J. Siciliano, C. A. Walter, W. Fan, L. S. Narayana, Z. Q. Zhou, A. W. Adamson, K. J. Sorensen, D. J. Chen, N. J. Jones, and L. H. Thompson. 1998. XRCC2 and XRCC3, new human Rad51-family members, promote chromosome stability and protect against DNA cross-links and other damages. Mol Cell 1:783-93.
175. Ljungquist, S., K. Kenne, L. Olsson, and M. Sandstrom. 1994. Altered DNA ligase III activity in the CHO EM9 mutant. Mutat Res 314:177-86.
176. Lobrich, M., and P. A. Jeggo. 2007. The impact of a negligent G2/M checkpoint on genomic instability and cancer induction. Nat Rev Cancer 7:861-9.

177. Lou, Z., B. P. Chen, A. Asaithamby, K. Minter-Dykhouse, D. J. Chen, and J. Chen. 2004. MDC1 regulates DNA-PK autophosphorylation in response to DNA damage. J Biol Chem 279:46359-62.
178. Love, E. M., J. A. Yin, C. J. Harrison, M. N. Narayanan, and M. Bhavnani. 1989. Acute monocytic leukaemia and t(2;6) (p21;q26) translocation. Clin Lab Haematol 11:277-80.
179. Lu, H., U. Pannicke, K. Schwarz, and M. R. Lieber. 2007. Length-dependent binding of human XLF to DNA and stimulation of XRCC4.DNA ligase IV activity. J Biol Chem 282:11155-62.
180. Luo, G., M. S. Yao, C. F. Bender, M. Mills, A. R. Bladl, A. Bradley, and J. H. Petrini. 1999. Disruption of mRad50 causes embryonic stem cell lethality, abnormal embryonic development, and sensitivity to ionizing radiation. Proc Natl Acad Sci U S A 96:7376-81.
181. Lusby, E., K. H. Fife, and K. I. Berns. 1980. Nucleotide sequence of the inverted terminal repetition in adeno-associated virus DNA. J Virol 34:402-9.
182. Ma, J. L., E. M. Kim, J. E. Haber, and S. E. Lee. 2003. Yeast Mre11 and Rad1 proteins define a Ku-independent mechanism to repair double-strand breaks lacking overlapping end sequences. Mol Cell Biol 23:8820-8.
183. Ma, Y., H. Lu, K. Schwarz, and M. R. Lieber. 2005. Repair of double-strand DNA breaks by the human nonhomologous DNA end joining pathway: the iterative processing model. Cell Cycle 4:1193-200.
184. Ma, Y., H. Lu, B. Tippin, M. F. Goodman, N. Shimazaki, O. Koiwai, C. L. Hsieh, K. Schwarz, and M. R. Lieber. 2004. A biochemically defined system for mammalian nonhomologous DNA end joining. Mol Cell 16:701-13.
185. Ma, Y., U. Pannicke, K. Schwarz, and M. R. Lieber. 2002. Hairpin opening and overhang processing by an Artemis/DNA-dependent protein kinase complex in nonhomologous end joining and V(D)J recombination. Cell 108:781-794.
186. Mahajan, K. N., S. A. Nick McElhinny, B. S. Mitchell, and D. A. Ramsden. 2002. Association of DNA polymerase mu (pol mu) with Ku and ligase IV: role for pol mu in end-joining double-strand break repair. Mol Cell Biol 22:5194-202.
187. Manolis, K. G., E. R. Nimmo, E. Hartsuiker, A. M. Carr, P. A. Jeggo, and R. C. Allshire. 2001. Novel functional requirements for non-homologous DNA end joining in *Schizosaccharomyces pombe*. EMBO J. 20:210-221.
188. Martinez, J. J., S. Seveau, E. Veiga, S. Matsuyama, and P. Cossart. 2005. Ku70, a component of DNA-dependent protein kinase, is a mammalian receptor for Rickettsia conorii. Cell 123:1013-23.
189. McBlane, J. F., D. C. van Gent, D. A. Ramsden, C. Romeo, C. A. Cuomo, M. Gellert, and M. A. Oettinger. 1995. Cleavage at a V(D)J

recombination signal requires only RAG1 and RAG2 proteins and occurs in two steps. Cell 83:387-95.
190. McVey, M., and S. E. Lee. 2008. MMEJ repair of double-strand breaks (director's cut): deleted sequences and alternative endings. Trends Genet 24:529-38.
191. McVey, M., D. Radut, and J. J. Sekelsky. 2004. End-joining repair of double-strand breaks in Drosophila melanogaster is largely DNA ligase IV independent. Genetics 168:2067-76.
192. Merkle, D., P. Douglas, G. B. Moorhead, Z. Leonenko, Y. Yu, D. Cramb, D. P. Bazett-Jones, and S. P. Lees-Miller. 2002. The DNA-dependent protein kinase interacts with DNA to form a protein-DNA complex that is disrupted by phosphorylation. Biochemistry 41:12706-14.
193. Mimori, T., M. Akizuki, H. Yamagata, S. Inada, S. Yoshida, and M. Homma. 1981. Characterization of a high molecular weight acidic nuclear protein recognized by autoantibodies in sera from patients with polymyositis-scleroderma overlap. J Clin Invest 68:611-20.
194. Mimori, T., and J. A. Hardin. 1986. Mechanism of interaction between Ku protein and DNA. J. Biol. Chem. 261:10375-10379.
195. Modesti, M., J. E. Hesse, and M. Gellert. 1999. DNA binding of Xrcc4 protein is associated with V(D)J recombination but not with stimulation of DNA ligase IV activity. Embo J 18:2008-18.
196. Montecucco, A., and G. Biamonti. 2007. Cellular response to etoposide treatment. Cancer Lett 252:9-18.
197. Moore, J. K., and J. E. Haber. 1996. Cell cycle and genetic requirements of two pathways of nonhomologous end-joining repair of double-strand breaks in Saccharomyces cerevisiae. Mol Cell Biol 16:2164-73.
198. Morimatsu, M., G. Donoho, and P. Hasty. 1998. Cells deleted for Brca2 COOH terminus exhibit hypersensitivity to gamma-radiation and premature senescence. Cancer Res 58:3441-7.
199. Morra, M., U. Geigenmuller, J. Curran, I. R. Rainville, T. Brennan, J. Curtis, V. Reichert, H. Hovhannisyan, J. Majzoub, and D. T. Miller. 2008. Genetic diagnosis of primary immune deficiencies. Immunol Allergy Clin North Am 28:387-412, x.
200. Morrison, C., E. Sonoda, N. Takao, A. Shinohara, K. Yamamoto, and S. Takeda. 2000. The controlling role of ATM in homologous recombinational repair of DNA damage. Embo J 19:463-71.
201. Moshous, D., I. Callebaut, R. de Chasseval, B. Corneo, M. Cavazzana-Calvo, F. Le Deist, I. Tezcan, O. Sanal, Y. Bertrand, N. Philippe, A. Fischer, and J. P. de Villartay. 2001. Artemis, a novel DNA double-strand break repair/V(D)J recombination protein, is mutated in human severe combined immune deficiency. Cell 105:177-186.

202. Moynahan, M. E., J. W. Chiu, B. H. Koller, and M. Jasin. 1999. Brca1 controls homology-directed DNA repair. Mol. Cell 4:511-518.
203. Moynahan, M. E., A. J. Pierce, and M. Jasin. 2001. BRCA2 is required for homology-directed repair of chromosomal breaks. Mol Cell 7:263-72.
204. Muller, C., J. Paupert, S. Monferran, and B. Salles. 2005. The double life of the Ku protein: facing the DNA breaks and the extracellular environment. Cell Cycle 4:438-41.
205. Muzyczka, N. 1992. Use of adeno-associated virus as a general transduction vector for mammalian cells. Curr Top Microbiol Immunol 158:97-129.
206. Myung, K., G. Ghosh, F. J. Fattah, G. Li, H. Kim, A. Dutia, E. Pak, S. Smith, and E. A. Hendrickson. 2004. Regulation of telomere length and suppression of genomic instability in human somatic cells by Ku86. Mol. Cell. Biol. 24:5050-5059.
207. Myung, K. J., and R. D. Kolodner. 2003. Induction of genome stability by DNA damage in *Saccharomyces cerevisiae*. DNA Repair 2:243-258.
208. Nairz, K., and F. Klein. 1997. mre11S--a yeast mutation that blocks double-strand-break processing and permits nonhomologous synapsis in meiosis. Genes Dev 11:2272-90.
209. Neale, M. J., J. Pan, and S. Keeney. 2005. Endonucleolytic processing of covalent protein-linked DNA double-strand breaks. Nature 436:1053-7.
210. Nick McElhinny, S. A., J. M. Havener, M. Garcia-Diaz, R. Juarez, K. Bebenek, B. L. Kee, L. Blanco, T. A. Kunkel, and D. A. Ramsden. 2005. A gradient of template dependence defines distinct biological roles for family X polymerases in nonhomologous end joining. Mol Cell 19:357-66.
211. Nick McElhinny, S. A., C. M. Snowden, J. McCarville, and D. A. Ramsden. 2000. Ku recruits the XRCC4-ligase IV complex to DNA ends. Mol Cell Biol 20:2996-3003.
212. Nienhuis, A. W., C. E. Dunbar, and B. P. Sorrentino. 2006. Genotoxicity of retroviral integration in hematopoietic cells. Mol Ther 13:1031-49.
213. Nohmi, T., M. Suzuki, K. Masumura, M. Yamada, K. Matsui, O. Ueda, H. Suzuki, M. Katoh, H. Ikeda, and T. Sofuni. 1999. Spi(-) selection: An efficient method to detect gamma-ray-induced deletions in transgenic mice. Environ Mol Mutagen 34:9-15.
214. Noordzij, J. G., N. S. Verkaik, M. van der Burg, L. R. van Veelen, S. de Bruin-Versteeg, W. Wiegant, J. M. Vossen, C. M. Weemaes, R. de Groot, M. Z. Zdzienicka, D. C. van Gent, and J. J. van Dongen. 2003. Radiosensitive SCID patients with Artemis gene mutations show a

complete B-cell differentiation arrest at the pre-B-cell receptor checkpoint in bone marrow. Blood 101:1446-52.
215. Nussenzweig, A., and M. C. Nussenzweig. 2007. A backup DNA repair pathway moves to the forefront. Cell 131:223-5.
216. O'Driscoll, M., K. M. Cerosaletti, P. M. Girard, Y. Dai, M. Stumm, B. Kysela, B. Hirsch, A. Gennery, S. E. Palmer, J. Seidel, R. A. Gatti, R. Varon, M. A. Oettinger, H. Neitzel, P. A. Jeggo, and P. Concannon. 2001. DNA ligase IV mutations identified in patients exhibiting developmental delay and immunodeficiency. Mol. Cell 8:1175-1185.
217. Oettinger, M. A., D. G. Schatz, C. Gorka, and D. Baltimore. 1990. RAG-1 and RAG-2, adjacent genes that synergistically activate V(D)J recombination. Science 248:1517-23.
218. Palmbos, P. L., J. M. Daley, and T. E. Wilson. 2005. Mutations of the Yku80 C terminus and Xrs2 FHA domain specifically block yeast nonhomologous end joining. Mol Cell Biol 25:10782-90.
219. Pang, D., S. Yoo, W. S. Dynan, M. Jung, and A. Dritschilo. 1997. Ku proteins join DNA fragments as shown by atomic force microscopy. Cancer Res. 57:1412-1415.
220. Park, E. J., D. W. Chan, J. H. Park, M. A. Oettinger, and J. Kwon. 2003. DNA-PK is activated by nucleosomes and phosphorylates H2AX within the nucleosomes in an acetylation-dependent manner. Nucleic Acids Res 31:6819-27.
221. Patel, K. J., V. P. Yu, H. Lee, A. Corcoran, F. C. Thistlethwaite, M. J. Evans, W. H. Colledge, L. S. Friedman, B. A. Ponder, and A. R. Venkitaraman. 1998. Involvement of Brca2 in DNA repair. Mol Cell 1:347-57.
222. Paull, T. T., and M. Gellert. 2000. A mechanistic basis for Mre11-directed DNA joining at microhomologies. Proc. Natl. Acad. Sci. U S A 97:6409-6414.
223. Perlot, T., G. Li, and F. W. Alt. 2008. Antisense transcripts from immunoglobulin heavy-chain locus V(D)J and switch regions. Proc Natl Acad Sci U S A 105:3843-8.
224. Perrault, R., H. Wang, M. Wang, B. Rosidi, and G. Iliakis. 2004. Backup pathways of NHEJ are suppressed by DNA-PK. J Cell Biochem 92:781-94.
225. Petrini, J. H. J. 2000. The Mre11 complex and ATM: collaborating to navigate S phase. Curr. Opin. Cell Biol. 12:293-296.
226. Pierce, A. J., R. D. Johnson, L. H. Thompson, and M. Jasin. 1999. XRCC3 promotes homology-directed repair of DNA damage in mammalian cells. Genes Dev 13:2633-8.
227. Pluth, J. M., L. M. Fried, and C. U. Kirchgessner. 2001. Severe combined immunodeficient cells expressing mutant hRAD54 exhibit a marked DNA double-strand break repair and error-prone chromosome repair defect. Cancer Res 61:2649-55.

228. Pospiech, H., A. K. Rytkonen, and J. E. Syvaoja. 2001. The role of DNA polymerase activity in human non-homologous end joining. Nucleic Acids Res 29:3277-88.
229. Postow, L., C. Ghenoiu, E. M. Woo, A. N. Krutchinsky, B. T. Chait, and H. Funabiki. 2008. Ku80 removal from DNA through double strand break-induced ubiquitylation. J Cell Biol 182:467-79.
230. Puebla-Osorio, N., D. B. Lacey, F. W. Alt, and C. Zhu. 2006. Early embryonic lethality due to targeted inactivation of DNA ligase III. Mol Cell Biol 26:3935-41.
231. Ramsden, D. A., and M. Gellert. 1998. Ku protein stimulates DNA end joining by mammalian DNA ligases: a direct role for Ku in repair of DNA double-strand breaks. Embo J 17:609-14.
232. Rassool, F. V. 2003. DNA double strand breaks (DSB) and non-homologous end joining (NHEJ) pathways in human leukemia. Cancer Lett 193:1-9.
233. Reddy, Y. V., Q. Ding, S. P. Lees-Miller, K. Meek, and D. A. Ramsden. 2004. Non-homologous end joining requires that the DNA-PK complex undergo an autophosphorylation-dependent rearrangement at DNA ends. J Biol Chem 279:39408-13.
234. Riballo, E., S. E. Critchlow, S.-H. Teo, A. J. Doherty, A. Priestley, B. Broughton, B. Kysela, H. Beamish, N. Plowman, C. F. Arlett, A. R. Lehmann, S. J. Jackson, and P. A. Jeggo. 1999. Identification of a defect in DNA ligase IV in a radiosensitive leukemia patient. Current Biol. 9:699-702.
235. Riballo, E., M. Kuhne, N. Rief, A. Doherty, G. C. Smith, M. J. Recio, C. Reis, K. Dahm, A. Fricke, A. Krempler, A. R. Parker, S. P. Jackson, A. Gennery, P. A. Jeggo, and M. Lobrich. 2004. A pathway of double-strand break rejoining dependent upon ATM, Artemis, and proteins locating to gamma-H2AX foci. Mol Cell 16:715-24.
236. Richardson, C., and M. Jasin. 2000. Coupled homologous and nonhomologous repair of a double-strand break preserves genomic integrity in mammalian cells. Mol Cell Biol 20:9068-75.
237. Rivera-Calzada, A., J. D. Maman, L. Spagnolo, L. H. Pearl, and O. Llorca. 2005. Three-dimensional structure and regulation of the DNA-dependent protein kinase catalytic subunit (DNA-PKcs). Structure 13:243-55.
238. Robins, P., and T. Lindahl. 1996. DNA ligase IV from HeLa cell nuclei. J Biol Chem 271:24257-61.
239. Rooney, S., F. W. Alt, D. Lombard, S. Whitlow, M. Eckersdorff, J. Fleming, S. Fugmann, D. O. Ferguson, D. G. Schatz, and J. Sekiguchi. 2003. Defective DNA repair and increased genomic instability in Artemis-deficient murine cells. J. Exp. Med. 197:553-565.
240. Rooney, S., J. Sekiguchi, C. Zhu, H. L. Cheng, J. Manis, S. Whitlow, J. DeVido, D. Foy, J. Chaudhuri, D. Lombard, and F. W. Alt. 2002. Leaky

scid phenotype associated with defective V(D)J coding end processing in Artemis-deficient mice. Mol. Cell 10:1379-1390.
241. Rose, J. A., K. I. Berns, M. D. Hoggan, and F. J. Koczot. 1969. Evidence for a single-stranded adenovirus-associated virus genome: formation of a DNA density hybrid on release of viral DNA. Proc Natl Acad Sci U S A 64:863-9.
242. Roth, D. B., J. P. Menetski, P. B. Nakajima, M. J. Bosma, and M. Gellert. 1992. V(D)J recombination: broken DNA molecules with covalently sealed (hairpin) coding ends in scid mouse thymocytes. Cell 70:983-991.
243. Roth, D. B., and J. H. Wilson. 1986. Nonhomologous recombination in mammalian cells: role for short sequence homologies in the joining reaction. Mol Cell Biol 6:4295-304.
244. Rothkamm, K., I. Kruger, L. H. Thompson, and M. Lobrich. 2003. Pathways of DNA double-strand break repair during the mammalian cell cycle. Mol Cell Biol 23:5706-15.
245. Ruis, B. L., K. R. Fattah, and E. A. Hendrickson. 2008. The catalytic subunit of DNA-dependent protein kinase regulates proliferation, telomere length, and genomic stability in human somatic cells. Mol Cell Biol 28:6182-95.
246. Russell, D. W., and R. K. Hirata. 1998. Human gene targeting by viral vectors. Nat Genet 18:325-30.
247. Saintigny, Y., A. Dumay, S. Lambert, and B. S. Lopez. 2001. A novel role for the Bcl-2 protein family: specific suppression of the RAD51 recombination pathway. Embo J 20:2596-607.
248. Sale, J. E., and M. S. Neuberger. 1998. TdT-accessible breaks are scattered over the immunoglobulin V domain in a constitutively hypermutating B cell line. Immunity 9:859-69.
249. Samulski, R. J., X. Zhu, X. Xiao, J. D. Brook, D. E. Housman, N. Epstein, and L. A. Hunter. 1991. Targeted integration of adeno-associated virus (AAV) into human chromosome 19. Embo J 10:3941-50.
250. Sawada, M., W. Sun, P. Hayes, K. Leskov, D. A. Boothman, and S. Matsuyama. 2003. Ku70 suppresses the apoptotic translocation of Bax to mitochondria. Nat. Cell Biol. 5:320-329.
251. Schar, P., G. Herrmann, G. Daly, and T. Lindahl. 1997. A newly identified DNA ligase of Saccharomyces cerevisiae involved in RAD52-independent repair of DNA double-strand breaks. Genes Dev 11:1912-24.
252. Schatz, D. G., M. A. Oettinger, and D. Baltimore. 1989. The V(D)J recombination activating gene, RAG-1. Cell 59:1035-48.
253. Schlissel, M., A. Constantinescu, T. Morrow, M. Baxter, and A. Peng. 1993. Double-strand signal sequence breaks in V(D)J recombination

are blunt, 5'-phosphorylated, RAG-dependent, and cell-cycle regulated. Genes Dev. 7:2520-2532.
254. Schuler, W., N. R. Ruetsch, M. Amsler, and M. J. Bosma. 1991. Coding joint formation of endogenous T cell receptor genes in lymphoid cells from scid mice: unusual P-nucleotide additions in VJ-coding joints. Eur J Immunol 21:589-96.
255. Schulte-Uentrop, L., R. A. El-Awady, L. Schliecker, H. Willers, and J. Dahm-Daphi. 2008. Distinct roles of XRCC4 and Ku80 in non-homologous end-joining of endonuclease- and ionizing radiation-induced DNA double-strand breaks. Nucleic Acids Res 36:2561-9.
256. Scully, R., S. F. Anderson, D. M. Chao, W. Wei, L. Ye, R. A. Young, D. M. Livingston, and J. D. Parvin. 1997. BRCA1 is a component of the RNA polymerase II holoenzyme. Proc Natl Acad Sci U S A 94:5605-10.
257. Scully, R., and D. M. Livingston. 2000. In search of the tumour-suppressor functions of BRCA1 and BRCA2. Nature 408:429-32.
258. Sekiguchi, J. M., and D. O. Ferguson. 2006. DNA double-strand break repair: a relentless hunt uncovers new prey. Cell 124:260-2.
259. Seluanov, A., D. Mittelman, O. M. Pereira-Smith, J. H. Wilson, and V. Gorbunova. 2004. DNA end joining becomes less efficient and more error-prone during cellular senescence. Proc Natl Acad Sci U S A 101:7624-9.
260. Sharan, S. K., M. Morimatsu, U. Albrecht, D. S. Lim, E. Regel, C. Dinh, A. Sands, G. Eichele, P. Hasty, and A. Bradley. 1997. Embryonic lethality and radiation hypersensitivity mediated by Rad51 in mice lacking Brca2. Nature 386:804-10.
261. Shiomi, N., M. Mori, H. Tsuji, T. Imai, H. Inoue, S. Tateishi, M. Yamaizumi, and T. Shiomi. 2007. Human RAD18 is involved in S phase-specific single-strand break repair without PCNA monoubiquitination. Nucleic Acids Res 35:e9.
262. Shroff, R., A. Arbel-Eden, D. Pilch, G. Ira, W. M. Bonner, J. H. Petrini, J. E. Haber, and M. Lichten. 2004. Distribution and dynamics of chromatin modification induced by a defined DNA double-strand break. Curr Biol 14:1703-11.
263. Sibanda, B. L., S. E. Critchlow, J. Begun, X. Y. Pei, S. P. Jackson, T. L. Blundell, and L. Pellegrini. 2001. Crystal structure of an Xrcc4-DNA ligase IV complex. Nat Struct Biol 8:1015-9.
264. Smanik, P. A., T. L. Furminger, E. L. Mazzaferri, and S. M. Jhiang. 1995. Breakpoint characterization of the ret/PTC oncogene in human papillary thyroid carcinoma. Hum Mol Genet 4:2313-8.
265. Smith, J., E. Riballo, B. Kysela, C. Baldeyron, K. Manolis, C. Masson, M. R. Lieber, D. Papadopoulo, and P. Jeggo. 2003. Impact of DNA ligase IV on the fidelity of end joining in human cells. Nucleic Acids Res 31:2157-67.

266. Snouwaert, J. N., L. C. Gowen, A. M. Latour, A. R. Mohn, A. Xiao, L. DiBiase, and B. H. Koller. 1999. BRCA1 deficient embryonic stem cells display a decreased homologous recombination frequency and an increased frequency of non-homologous recombination that is corrected by expression of a *Brca1* transgene. Oncogene 18:7900-7907.

267. Sonoda, E., M. S. Sasaki, J. M. Buerstedde, O. Bezzubova, A. Shinohara, H. Ogawa, M. Takata, Y. Yamaguchi-Iwai, and S. Takeda. 1998. Rad51-deficient vertebrate cells accumulate chromosomal breaks prior to cell death. Embo J 17:598-608.

268. Soulas-Sprauel, P., G. Le Guyader, P. Rivera-Munoz, V. Abramowski, C. Olivier-Martin, C. Goujet-Zalc, P. Charneau, and J. P. de Villartay. 2007. Role for DNA repair factor XRCC4 in immunoglobulin class switch recombination. J Exp Med 204:1717-27.

269. Soulas-Sprauel, P., P. Rivera-Munoz, L. Malivert, G. Le Guyader, V. Abramowski, P. Revy, and J. P. de Villartay. 2007. V(D)J and immunoglobulin class switch recombinations: a paradigm to study the regulation of DNA end-joining. Oncogene 26:7780-91.

270. Staunton, J. E., and D. T. Weaver. 1994. *Scid* cells efficiently integrate hairpin and linear DNA substrates. Mol. Cell. Biol. 14:3876-3883.

271. Stephanou, N. C., F. Gao, P. Bongiorno, S. Ehrt, D. Schnappinger, S. Shuman, and M. S. Glickman. 2007. Mycobacterial nonhomologous end joining mediates mutagenic repair of chromosomal double-strand DNA breaks. J Bacteriol 189:5237-46.

272. Stewart, G. S., R. S. Maser, T. Stankovic, D. A. Bressan, M. I. Kaplan, N. G. J. Jaspers, A. Raams, P. J. Byrd, J. H. J. Petrini, and A. M. R. Taylor. 1999. The DNA double-strand break repair gene *hMRE11* is mutated in individuals with an Ataxia Telangiectasia-like disorder. Cell 99:577-587.

273. Stiff, T., C. Reis, G. K. Alderton, L. Woodbine, M. O'Driscoll, and P. A. Jeggo. 2005. Nbs1 is required for ATR-dependent phosphorylation events. Embo J 24:199-208.

274. Suwa, A., M. Hirakata, Y. Takeda, S. A. Jesch, T. Mimori, and J. A. Hardin. 1994. DNA-dependent protein kinase (Ku protein-p350 complex) assembles on double-stranded DNA. Proc. Natl. Acad. Sci. USA 91:6904-6908.

275. Takata, M., M. S. Sasaki, E. Sonoda, T. Fukushima, C. Morrison, J. S. Albala, S. M. Swagemakers, R. Kanaar, L. H. Thompson, and S. Takeda. 2000. The Rad51 paralog Rad51B promotes homologous recombinational repair. Mol Cell Biol 20:6476-82.

276. Takata, M., M. S. Sasaki, E. Sonoda, C. Morrison, M. Hashimoto, H. Utsumi, Y. Yamaguchi-Iwai, A. Shinohara, and S. Takeda. 1998. Homologous recombination and non-homologous end-joining pathways of DNA double-strand break repair have overlapping roles

in the maintenance of chromosomal integrity in vertebrate cells. EMBO J. 17:5497-5508.
277. Takata, M., M. S. Sasaki, S. Tachiiri, T. Fukushima, E. Sonoda, D. Schild, L. H. Thompson, and S. Takeda. 2001. Chromosome instability and defective recombinational repair in knockout mutants of the five Rad51 paralogs. Mol Cell Biol 21:2858-66.
278. Tebbs, R. S., M. L. Flannery, J. J. Meneses, A. Hartmann, J. D. Tucker, L. H. Thompson, J. E. Cleaver, and R. A. Pedersen. 1999. Requirement for the Xrcc1 DNA base excision repair gene during early mouse development. Dev Biol 208:513-29.
279. Teo, S. H., and S. P. Jackson. 1997. Identification of Saccharomyces cerevisiae DNA ligase IV: involvement in DNA double-strand break repair. Embo J 16:4788-95.
280. Thacker, J., J. Chalk, A. Ganesh, and P. North. 1992. A mechanism for deletion formation in DNA by human cell extracts: the involvement of short sequence repeats. Nucleic Acids Res 20:6183-8.
281. Tong, W. M., M. P. Hande, P. M. Lansdorp, and Z. Q. Wang. 2001. DNA strand break-sensing molecule poly(ADP-Ribose) polymerase cooperates with p53 in telomere function, chromosome stability, and tumor suppression. Mol Cell Biol 21:4046-54.
282. Tsai, C. J., S. A. Kim, and G. Chu. 2007. Cernunnos/XLF promotes the ligation of mismatched and noncohesive DNA ends. Proc Natl Acad Sci U S A 104:7851-6.
283. Tseng, H. M., and A. E. Tomkinson. 2002. A physical and functional interaction between yeast Pol4 and Dnl4-Lif1 links DNA synthesis and ligation in nonhomologous end joining. J Biol Chem 277:45630-7.
284. Tseng, H. M., and A. E. Tomkinson. 2004. Processing and joining of DNA ends coordinated by interactions among Dnl4/Lif1, Pol4, and FEN-1. J Biol Chem 279:47580-8.
285. Tsuji, H., H. Ishii-Ohba, T. Katsube, H. Ukai, S. Aizawa, M. Doi, K. Hioki, and T. Ogiu. 2004. Involvement of illegitimate V(D)J recombination or microhomology-mediated nonhomologous end-joining in the formation of intragenic deletions of the Notch1 gene in mouse thymic lymphomas. Cancer Res 64:8882-90.
286. Tsuzuki, T., Y. Fujii, K. Sakumi, Y. Tominga, K. Nakao, M. Sekiguchi, A. Matsushiro, Y. Yoshimura, and T. Morita. 1996. Targeted disruption of the *Rad51* gene leads to lethality in embryonic mice. Proc. Natl. Acad. Sci. USA 93:6236-6240.
287. Tutt, A., D. Bertwistle, J. Valentine, A. Gabriel, S. Swift, G. Ross, C. Griffin, J. Thacker, and A. Ashworth. 2001. Mutation in Brca2 stimulates error-prone homology-directed repair of DNA double-strand breaks occurring between repeated sequences. Embo J 20:4704-16.

288. Uchiyama, Y., S. Kimura, T. Yamamoto, T. Ishibashi, and K. Sakaguchi. 2004. Plant DNA polymerase lambda, a DNA repair enzyme that functions in plant meristematic and meiotic tissues. Eur J Biochem 271:2799-807.
289. Usui, T., H. Ogawa, and J. H. Petrini. 2001. A DNA damage response pathway controlled by Tel1 and the Mre11 complex. Mol Cell 7:1255-66.
290. Valencia, M., M. Bentele, M. B. Vaze, G. Herrmann, E. Kraus, S. E. Lee, P. Schar, and J. E. Haber. 2001. *NEJ1* controls non-homologous end joining in *Saccharomyces cerevisiae*. Nature 414:666-669.
291. van Attikum, H., P. Bundock, R. M. Overmeer, L. Y. Lee, S. B. Gelvin, and P. J. Hooykaas. 2003. The Arabidopsis AtLIG4 gene is required for the repair of DNA damage, but not for the integration of Agrobacterium T-DNA. Nucleic Acids Res 31:4247-55.
292. van den Bosch, M., P. H. Lohman, and A. Pastink. 2002. DNA double-strand break repair by homologous recombination. Biol Chem 383:873-92.
293. van der Burg, M., H. Ijspeert, N. S. Verkaik, T. Turul, W. W. Wiegant, K. Morotomi-Yano, P. O. Mari, I. Tezcan, D. J. Chen, M. Z. Zdzienicka, J. J. van Dongen, and D. C. van Gent. 2009. A DNA-PKcs mutation in a radiosensitive T-B- SCID patient inhibits Artemis activation and nonhomologous end-joining. J Clin Invest 119:91-8.
294. Van Dyck, E., A. Z. Stasiak, A. Stasiak, and S. C. West. 1999. Binding of double-strand breaks in DNA by human Rad52 protein. Nature 398:728-731.
295. van Gent, D. C., J. H. Hoeijmakers, and R. Kanaar. 2001. Chromosomal stability and the DNA double-stranded break connection. Nat. Rev. Genet. 2:196-206.
296. van Veelen, L., J. Wesoly, and R. Kanaar. 2006. Biochemical and cellular aspects of homologous recombination., p. 581-607. *In* W. Seide, Y. W. Kow, and P. Doetsch (ed.), DNA Damage Recognition. Taylor and Francis Group, New York.
297. Varon, R., C. Vissinga, M. Platzer, K. M. Cerosaletti, K. H. Chrzanowska, K. Saar, G. Beckmann, E. Seemanova, P. R. Cooper, N. J. Nowak, M. Stumm, C. M. Weemaes, R. A. Gatti, R. K. Wilson, M. Digweed, A. Rosenthal, K. Sperling, P. Concannon, and A. Reis. 1998. Nibrin, a novel DNA double-strand break repair protein, is mutated in Nijmegen breakage syndrome. Cell 93:467-76.
298. Vasileva, A., and R. Jessberger. 2005. Precise hit: adeno-associated virus in gene targeting. Nat Rev Microbiol 3:837-47.
299. Verkaik, N. S., R. E. Esveldt-van Lange, D. van Heemst, H. T. Bruggenwirth, J. H. Hoeijmakers, M. Z. Zdzienicka, and D. C. van Gent. 2002. Different types of V(D)J recombination and end-joining

defects in DNA double-strand break repair mutant mammalian cells. Eur. J. Immunol. 32:701-709.
300. Walker, J. R., R. A. Corpina, and J. Goldberg. 2001. Structure of the Ku heterodimer bound to DNA and its implications for double-strand break repair. Nature 412:607-614.
301. Wang, H., A. R. Perrault, Y. Takeda, W. Qin, H. Wang, and G. Iliakis. 2003. Biochemical evidence for Ku-independent backup pathways of NHEJ. Nucleic Acids Res 31:5377-88.
302. Wang, M., W. Wu, W. Wu, B. Rosidi, L. Zhang, H. Wang, and G. Iliakis. 2006. PARP-1 and Ku compete for repair of DNA double strand breaks by distinct NHEJ pathways. Nucleic Acids Res 34:6170-82.
303. Wang, Z. Q., L. Stingl, C. Morrison, M. Jantsch, M. Los, K. Schulze-Osthoff, and E. F. Wagner. 1997. PARP is important for genomic stability but dispensable in apoptosis. Genes Dev 11:2347-58.
304. Weller, G. R., B. Kysela, R. Roy, L. M. Tonkin, E. Scanlan, M. Della, S. K. Devine, J. P. Day, A. Wilkinson, F. di Fagagna, K. M. Devine, R. P. Bowater, P. A. Jeggo, S. P. Jackson, and A. J. Doherty. 2002. Identification of a DNA nonhomologous end-joining complex in bacteria. Science 297:1686-1689.
305. West, S. C. 2003. Molecular views of recombination proteins and their control. Nat Rev Mol Cell Biol 4:435-45.
306. Weterings, E., and D. C. van Gent. 2004. The mechanism of non-homologous end-joining: a synopsis of synapsis. DNA Repair (Amst) 3:1425-35.
307. Wilson, T. E., U. Grawunder, and M. R. Lieber. 1997. Yeast DNA ligase IV mediates non-homologous DNA end joining. Nature 388:495-8.
308. Wilson, T. E., and M. R. Lieber. 1999. Efficient processing of DNA ends during yeast nonhomologous end joining. Evidence for a DNA polymerase beta (Pol4)-dependent pathway. J Biol Chem 274:23599-609.
309. Windhofer, F., W. Wu, and G. Iliakis. 2007. Low levels of DNA ligases III and IV sufficient for effective NHEJ. J Cell Physiol 213:475-83.
310. Windhofer, F., W. Wu, M. Wang, S. K. Singh, J. Saha, B. Rosidi, and G. Iliakis. 2007. Marked dependence on growth state of backup pathways of NHEJ. Int J Radiat Oncol Biol Phys 68:1462-70.
311. Wood, R. D., M. Mitchell, J. Sgouros, and T. Lindahl. 2001. Human DNA repair genes. Science 291:1284-9.
312. Woodhouse, B. C., and G. L. Dianov. 2008. Poly ADP-ribose polymerase-1: an international molecule of mystery. DNA Repair (Amst) 7:1077-86.
313. Woods-Samuels, P., H. H. Kazazian, Jr., and S. E. Antonarakis. 1991. Nonhomologous recombination in the human genome: deletions in the human factor VIII gene. Genomics 10:94-101.

314. Wu, W., M. Wang, T. Mussfeldt, and G. Iliakis. 2008. Enhanced use of backup pathways of NHEJ in G2 in Chinese hamster mutant cells with defects in the classical pathway of NHEJ. Radiat Res 170:512-20.
315. Wu, X., V. Ranganathan, D. S. Weisman, W. F. Heine, D. N. Ciccone, T. B. O'Neill, K. E. Crick, K. A. Pierce, W. S. Lane, G. Rathbun, D. M. Livingston, and D. T. Weaver. 2000. ATM phosphorylation of Nijmegen breakage syndrome protein is required in a DNA damage response. Nature 405:477-82.
316. Wu, X., T. E. Wilson, and M. R. Lieber. 1999. A role for FEN-1 in nonhomologous DNA end joining: the order of strand annealing and nucleolytic processing events. Proc Natl Acad Sci U S A 96:1303-8.
317. Wyman, C., D. Ristic, and R. Kanaar. 2004. Homologous recombination-mediated double-strand break repair. DNA Repair 3:827-833.
318. Xia, F., D. G. Taghian, J. S. DeFrank, Z. C. Zeng, H. Willers, G. Iliakis, and S. N. Powell. 2001. Deficiency of human BRCA2 leads to impaired homologous recombination but maintains normal nonhomologous end joining. Proc Natl Acad Sci U S A 98:8644-9.
319. Xiao, Y., and D. T. Weaver. 1997. Conditional gene targeted deletion by Cre recombinase demonstrates the requirement for the double-strand break repair Mre11 protein in murine embryonic stem cells. Nucl. Acids Res. 25:2985-2991.
320. Yamaguchi-Iwai, Y., E. Sonoda, M. S. Sasaki, C. Morrison, T. Haraguchi, Y. Hiraoka, Y. M. Yamashita, T. Yagi, M. Takata, C. Price, N. Kakazu, and S. Takeda. 1999. Mre11 is essential for the maintenance of chromosomal DNA in vertebrate cells. Embo J 18:6619-29.
321. Yan, C. T., C. Boboila, E. K. Souza, S. Franco, T. R. Hickernell, M. Murphy, S. Gumaste, M. Geyer, A. A. Zarrin, J. P. Manis, K. Rajewsky, and F. W. Alt. 2007. IgH class switching and translocations use a robust non-classical end-joining pathway. Nature 449:478-82.
322. Yaneva, M., T. Kowalewski, and M. R. Lieber. 1997. Interaction of DNA-dependent protein kinase with DNA and with Ku: biochemical and atomic-force microscopy studies. Embo J 16:5098-112.
323. Yannone, S. M., S. Roy, D. W. Chan, M. B. Murphy, S. Huang, J. Campisi, and D. J. Chen. 2001. Werner syndrome protein is regulated and phosphorylated by DNA-dependent protein kinase. J Biol Chem 276:38242-8.
324. Yano, K., K. Morotomi-Yano, S. Y. Wang, N. Uematsu, K. J. Lee, A. Asaithamby, E. Weterings, and D. J. Chen. 2008. Ku recruits XLF to DNA double-strand breaks. EMBO Rep 9:91-6.
325. Young, S. M., Jr., and R. J. Samulski. 2001. Adeno-associated virus (AAV) site-specific recombination does not require a Rep-dependent

origin of replication within the AAV terminal repeat. Proc Natl Acad Sci U S A 98:13525-30.
326. Yu, V. P., M. Koehler, C. Steinlein, M. Schmid, L. A. Hanakahi, A. J. van Gool, S. C. West, and A. R. Venkitaraman. 2000. Gross chromosomal rearrangements and genetic exchange between nonhomologous chromosomes following BRCA2 inactivation. Genes Dev 14:1400-6.
327. Yu, X., and A. Gabriel. 2003. Ku-dependent and Ku-independent end-joining pathways lead to chromosomal rearrangements during double-strand break repair in Saccharomyces cerevisiae. Genetics 163:843-56.
328. Yu, Y., B. L. Mahaney, K. Yano, R. Ye, S. Fang, P. Douglas, D. J. Chen, and S. P. Lees-Miller. 2008. DNA-PK and ATM phosphorylation sites in XLF/Cernunnos are not required for repair of DNA double strand breaks. DNA Repair (Amst) 7:1680-92.
329. Yuan, S. S., S. Y. Lee, G. Chen, M. Song, G. E. Tomlinson, and E. Y. Lee. 1999. BRCA2 is required for ionizing radiation-induced assembly of Rad51 complex in vivo. Cancer Res 59:3547-51.
330. Zdzienicka, M. Z. 1995. Mammalian mutants defective in the response to ionizing radiation-induced DNA damage. Mutat. Res. 336:203-213.
331. Zha, S., F. W. Alt, H. L. Cheng, J. W. Brush, and G. Li. 2007. Defective DNA repair and increased genomic instability in Cernunnos-XLF-deficient murine ES cells. Proc Natl Acad Sci U S A 104:4518-23.
332. Zhang, X., and T. T. Paull. 2005. The Mre11/Rad50/Xrs2 complex and non-homologous end-joining of incompatible ends in S. cerevisiae. DNA Repair (Amst) 4:1281-94.
333. Zhao, S., Y. C. Weng, S. S. Yuan, Y. T. Lin, H. C. Hsu, S. C. Lin, E. Gerbino, M. H. Song, M. Z. Zdzienicka, R. A. Gatti, J. W. Shay, Y. Ziv, Y. Shiloh, and E. Y. Lee. 2000. Functional link between ataxia-telangiectasia and Nijmegen breakage syndrome gene products. Nature 405:473-7.
334. Zhong, Q., C. F. Chen, P. L. Chen, and W. H. Lee. 2002. BRCA1 facilitates microhomology-mediated end joining of DNA double strand breaks. J Biol Chem 277:28641-7.
335. Zhou, B. B., and S. J. Elledge. 2000. The DNA damage response: putting checkpoints in perspective. Nature 408:433-9.
336. Zhu, J., S. Petersen, L. Tessarollo, and A. Nussenzweig. 2001. Targeted disruption of the Nijmegen breakage syndrome gene NBS1 leads to early embryonic lethality in mice. Curr Biol 11:105-9.